Prediction of Clean Air Turbulence

By
Harry P. Foltz

Principal Investigator: Elmar. R. Reiter

Technical Paper No. 106
Department of Atmospheric Science
Colorado State University
Fort Collins, Colorado

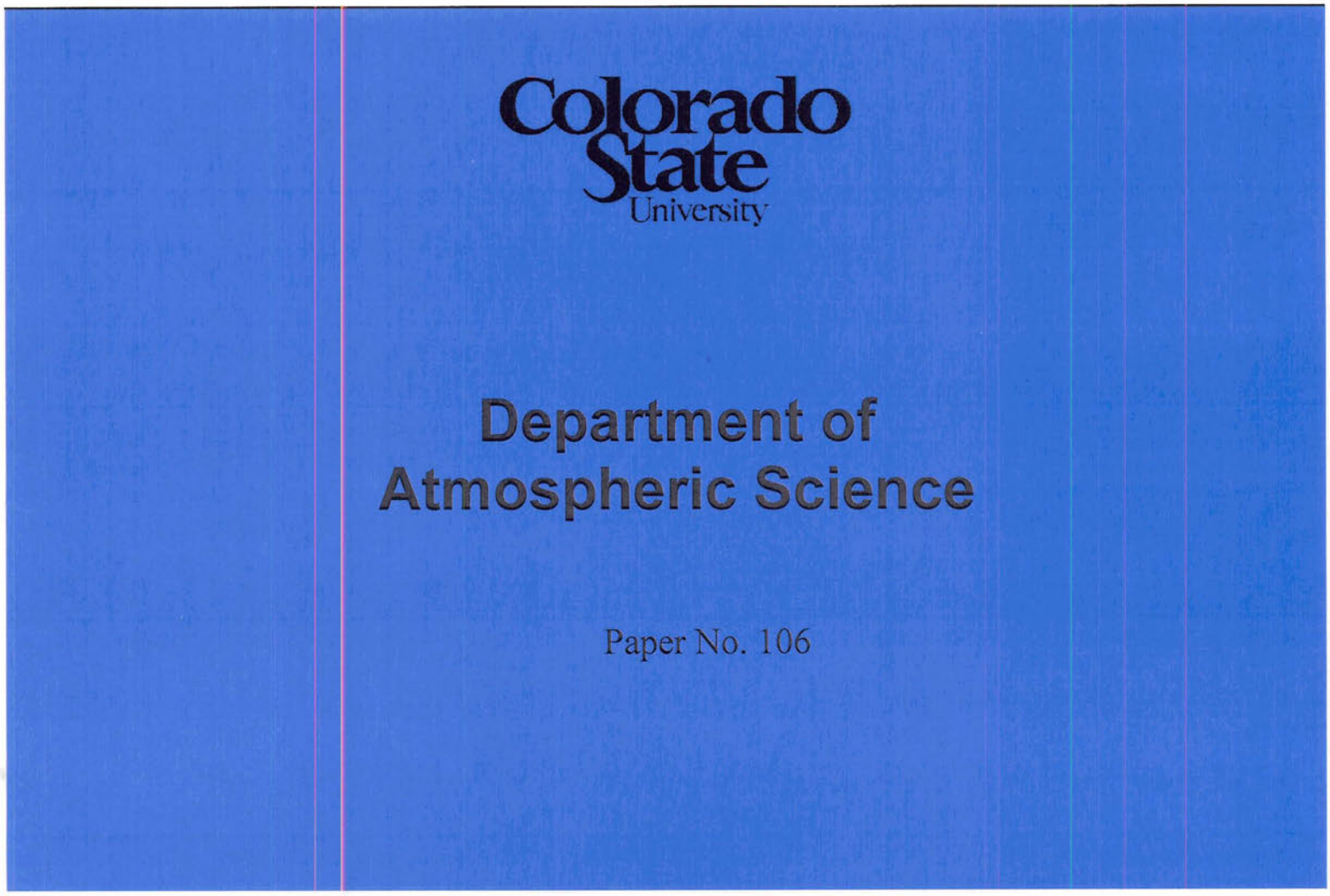

PREDICTION OF

CLEAR AIR TURBULENCE

By
Harry P. Foltz
Colorado State University

This Report was prepared with support under
Grant WBG-59 from the
National Environmental Satellite Center, ESSA.

Department of Atmospheric Science
Colorado State University
Fort Collins, Colorado

January 1967

Atmospheric Science Paper No. 106

ABSTRACT

Prediction of Clear Air Turbulence

A climatological study of three years of aircraft turbulence reports covering the western United States shows a possible connection between lee waves and such turbulence. Maxima of turbulence frequency are found just to the lee of all major mountain ridges. The frequency maxima of the various degrees of turbulence display a well organized pattern with the highest intensity maxima closest to the mountain range. The frequency maxima of less intense turbulence are located further downwind from the ridge. This is explainable on the basis of energy levels contained in lee waves and their potential to cause clear air turbulence.

The relationship between mountain lee waves and clear air turbulence is investigated using the theoretical results of Scorer, Corby, and Wallington and the power spectra of atmospheric turbulence determined from recent aircraft measurements. The theoretically computed vertical velocities in the mountain lee waves are consistent with power spectrum measurements observed by aircraft while experiencing clear air turbulence. By using the "-5/3" spectral density slope, the energy per cycle in the mesoscale obtained theoretically is related to that observed in the microscale and also to the degree of clear air turbulence. The intensity of turbulence expected on

using this method agrees quite well with actual reports of aircraft turbulence. The pilot reports of turbulence generally come from lee wave areas where the atmospheric and terrain parameters allow sufficient theoretically computed input energy into the mesoscale to result in clear air turbulence as the energy is passed into the microscale. Energy decay times based upon computed dissipation rates using the "-5/3 law" are consistent with observed clear air turbulence patterns. The wavelengths of mountain lee waves observed by satellite are found to be close to those derived from theory.

Numerous graphical and computational aids are developed which allow forecasting of clear air turbulence by the use of rawinsonde and satellite information. Verification of the forecasting methods is accomplished by the use of evidence collected in seven mountain lee wave cases observed principally by satellite, and in five cases observed during a field measurement program utilizing constant level balloon trajectories, cloud photogrammetry, and satellite photography.

Harry P. Foltz
Department of Atmospheric Science
Colorado State University
January 1967

ACKNOWLEDGMENTS

The author wishes to express gratitude to Professor Elmar R. Reiter for his many helpful suggestions made while the manuscript was being prepared, to Mr. Vincent J. Oliver of the National Environmental Satellite Center, ESSA, who planned the mountain wave pilot report program and who was instrumental in providing the pilot reports and satellite pictures; to Dr. Ignaz Vergeiner for his many stimulating discussions and for his computer programming; to Mr. Gene Wooldridge, who processed the photogrammetric data; to Mr. James White, who drafted the figures; and finally to my wife, Betty, for her constant help and encouragement.

Much of the data used for analysis were made available by the National Environmental Satellite Center, ESSA, Suitland, Maryland; The National Weather Records Center, ESSA, Asheville, North Carolina; and the Weather Bureau Offices, ESSA, in Salt Lake City, Utah; Denver, Colorado; New York, New York; Washington, D. C.; and Suitland, Maryland. The computer facility of the National Center of Atmospheric Research made available free computer time for the present research program.

This material is based upon a dissertation submitted as partial fulfillment of the requirements for the Doctor of Philosophy Degree at Colorado State University.

TABLE OF CONTENTS

TABLE OF CONTENTS (Continued)

LIST OF TABLES

LIST OF FIGURES

LIST OF FIGURES (Continued)

LIST OF FIGURES (Continued)

CHAPTER I

INTRODUCTION

Introductory Remarks

Clear air turbulence (henceforth denoted as CAT), which seems to consist of random three dimensional eddies that occur in certain confined regions of the atmosphere, is the special interest of many groups and organizations. It is of prime importance to the aviation industry because it affects the safety and comfort of passengers and crew, as well as operational costs. Aircraft manufacturers and the airlines are interested in CAT in order to determine to what strength airframes must be built to withstand all degrees of turbulence. They also realize that CAT may be even a greater operational problem in the era of the supersonic jet transport. CAT is of interest to certain government and civilian agencies responsible for the safety of aircraft operations. Military agencies must understand CAT more fully so that they may take it into account operationally in all areas of the world. Finally, scientists are concerned with CAT because it is a phenomenon of our environment that is not clearly understood. A better comprehension of CAT may result in determining the processes whereby mesoscale wave-energy is transformed into microscale turbulent energy.

CAT is usually less intense than turbulence encountered in thunderstorms (Beckwith 1964, Colson 1966), but it can cause passenger discomfort and, infrequently, passenger injuries and loss of aircraft control. In rare instances it can cause damage to the airframe. CAT may at times be more dangerous than "in cloud" turbulence, as it usually occurs with no visible warning.

The Problem Under Consideration

The nature of clear air turbulence and its meteorology are still not completely understood. More mesoscale (2 km to 100 km horizontal distance) and microscale (<2 km) studies must be made concerning the causes and generation of CAT. The operational forecasting of CAT is based upon synoptic scale data (>100 km) and, although it has some skill, it must be considered as inadequate for present and future needs. Any improvement in forecasting skill that we hope to bring about by this study will probably result from increased mesoscale input into the forecast problem. The only mesoscale measurements available operationally at this time which concern the problem are rawinsonde data that give a nearly continuous measurement in the vertical of wind, pressure, temperature, and humidity from the surface to above 30 km in altitude, and satellite cloud pictures that delineate cloud structures down to a scale of about 3 km.

Purpose of This Study

This investigation concerns itself principally with the relationship between CAT and mountain lee waves. Statistical evidence shows that CAT has a maximum frequency to the lee of major mountain ridges (Clodman et al. 1960). This suggests that CAT has a physical connection with lee waves. Computations of lee wavelengths and of vertical velocities contained in lee waves, based upon atmospheric wind and temperature structures and the work of Scorer, Corby, and Wallington, yield perturbation energy values at lee wavelengths which can be correlated with various degrees of CAT when this energy is passed into the microscale while obeying the "-5/3 law" of turbulence.

A better understanding of the processes leading to CAT over mountainous terrain results in the development of several aids and procedures for CAT prediction. These make use of the routinely available rawinsonde and satellite data.

A field measurement program to study lee waves using constant level balloon trajectories, cloud photogrammetry, satellite photography, pilot turbulence reports, and rawinsonde data was carried out near Fort Collins, Colorado in the spring of 1966. The results are included in this report and some of them are used to verify the CAT forecasting procedures. Mountain lee wave cases observed principally by satellite are also used to evaluate the CAT forecasting methods.

CAPTER II

THE PHENOMENON OF CLEAR AIR TURBULENCE

Discussion of CAT Pilot Reports

The usual definition of CAT is "atmospheric turbulence which is not in or near convective clouds, including thunderstorms, and is not below 15,000 ft. in altitude." Thus, mechanical turbulence induced by rough terrain is not considered. It is realized that this is an extremely arbitrary definition resulting from a desire to simplify pilot reporting procedures.

Turbulence intensities are, at present, designated as light, moderate, severe, and extreme. There are few quantitative measurements of atmospheric turbulence at any scale. The bulk of the aircraft turbulence data available is based upon the four categories above, and, consequently is highly subjective and qualitative in nature (Beckwith 1964). Included in the factors that affect the subjective decision of the pilot when reporting turbulence are the wing loading, the aircraft's speed and attitude, the pilot's training, experience, and his psychological reactions (Beckwith 1964).

When studying subjective pilot reports, the aircraft's design or response function must also be considered by use of the relationship

$$E_o(\omega) = E_i(\omega) \left| T(\omega) \right|^2 \qquad 1)$$

where $E_o(\omega)$ is the output spectrum function in terms of frequency

and represents the degree of turbulence "felt" by the aircraft. $E_i(\omega)$ is the input spectrum function representing the turbulence which exists in the surrounding atmosphere, and $T(\omega)$ is the frequency response function of the aircraft describing the oscillation modes of the aircraft in response to periodic gusts of various frequencies.

In recent years several definitions of the four categories of turbulence have been proposed. The current definitions in official use, which were developed by the NACA Subcommittee on Meteorological Problems (1957), are listed in Table 1.

Table 1. AIRCRAFT TURBULENCE CRITERIA

CATEGORY	DEFINITION
Light	A turbulent condition during which occupants may be required to use seat belts, but objects in the aircraft remain at rest.
Moderate	A turbulent condition in which occupants require seat belts and occasionally are thrown against the belt. Unsecured objects in the aircraft move about.
Severe	A turbulent condition in which the aircraft momentarily may be out of control. Occupants are thrown violently against the belt and back into the seat. Objects not secured in the aircraft are tossed about.
Extreme	A rarely encountered turbulent condition in which the aircraft is violently tossed about, and is practically impossible to control. May cause structural damage.

Objective criteria for the reporting of turbulence must wait until more measurements are made of the conditions existing in the turbulent eddies, and until cockpit instrumentation includes a gust load or turbulence indicator.

Observational Techniques

Much time, effort, and financial support have been expended in this country by the government, the aircraft industry, and private and public research facilities to investigate the problem of CAT and to find promising avenues leading to a solution of this problem. This research has gone forward in three broad categories: first, research concerning the correlation of CAT with macroscale, mesoscale, and/or microscale atmospheric measurements; second, research into instrumentation for the detection of CAT sufficiently in advance of the aircraft to allow evasive measures; and third, research by military and airline organizations concerning the operational aspects of CAT.

As pointed out earlier, the meteorologist has few direct measurements of turbulence intensities and must depend upon the accuracy of the intensities reported by pilots. He has attempted to find correlations between these reports and synoptic patterns and large scale data such as smoothed wind shears, jet stream configuration and upper fronts. These data are taken at six to twelve hour intervals with a grid scale of about 300 km. It can

be seen that any attempt to find an accurate and objective technique to forecast CAT, a phenomenon of the microscale (about 100 meters), by use of synoptic scale data would lead to disappointment. This has largely been the case.

There have been a few measurements of the mesoscale structure of atmospheric turbulence using Doppler radar navigation systems on aircraft (Reiter 1961b, Panofsky and McLean 1964).

Measurements of the microstructure, which contains the perturbations of CAT dimensions (100-500 m wavelength), have been taken by specially instrumented aircraft (Shur 1962, Reiter and Burns 1965). Until recently the aircraft itself was used as a sensor to measure atmospheric gusts from the aircraft acceleration data. A full knowledge of the aircraft's response to turbulence over a wide range of wavelengths [$T(\omega)$ in Eq. (1)] is required for meaningful interpretation of such data. This procedure usually gives reliable results at short wavelengths up to a few hundred meters. At long wavelengths, this instrumentation becomes less sensitive. Accelerations in longer waves are usually small and can be masked by pilot induced aircraft motions. Recent measurements of turbulence (Reiter and Burns, 1965, 1966) involved the use of instrumentation carried aloft by an aircraft, but the airplane served only as an inertial platform for the instruments.

It is this second system that offers hope for direct measurement throughout most of the microscale and part of the mesoscale of the atmosphere (Crooks 1965, Loving 1966). At the present time, this system is not perfected for turbulent eddies of wavelengths above six kilometers and we continue to have no quantitative measurements from aircraft over much of the mesoscale range.

There are some measurements in the mesoscale region obtained by tracking constant level balloons with radar, but at great distances there is a lack of definition of small-scale fluctuations due to the width of the radar beam. In order to get long enough trajectories to give meaningful results in strong wind situations, several radar sets must be placed strategically along the track. Experimental use of optical radar and microwave radar to observe atmospheric turbulence has been made and under certain conditions this may offer a possibility for measurement of turbulence in the microscale range (Hardy et al. 1966).

With the advent of meteorological satellites in 1960, a new observational tool became available with which one could study the turbulence problem on the mesoscale. There have been attempts to correlate satellite cloud pictures with turbulence reports (Serebreny and Wiegman 1964, Wiegman 1965) but results were not conclusive. Satellite pictures have been used in the

study of mountain waves (Döös 1962, Fritz and Lindsay 1964, Fritz 1965), but not specifically in connection with the CAT problem.

Results of Research to Date

CAT has been found to be statistically related to terrain (Clodman et al. 1960, Colson 1963), to the jet stream and its configuration (Bannon 1952, Endlich and McLean 1957, Reiter 1963a, Kadlec 1963, 1964, Reiter and Nania 1964), and to horizontal and/or vertical wind shear (Colson 1963, Endlich 1963, Reiter 1963a, Colson and Panofsky 1965). Some degree of turbulence occurs about fifteen per cent of all flight time over the United States during the winter months. Three per cent of the time turbulence is moderate or of greater intensity (Endlich et al. 1966). CAT has a frequency maximum near the tropopause. It is less frequent during the summer months and seems to be an order of magnitude less over oceans than over land (Clodman et al. 1960).

Studies have been made of the energy spectral density in the macroscale and in the long-wave end of the mesoscale (Kao and Woods 1964). There seem to be perturbation kinetic energy input regions at wavelengths of about 1,000 km due to planetary waves and at about 100 km due to gravity-inertial waves.

It has been found that during cases of moderate to severe CAT the kinetic energy contained in the wavelengths of two kilometers or less is appreciably greater than during cases of light or no turbulence (Reiter and Burns 1965, 1966). The energy distribution of

the u and v wind components approximately obeys the "-5/3 law" at wavelengths less than the input wavelength indicated by a "hump" in the spectral curve (Reiter et al. 1965, Reiter and Burns 1965, 1966).

As mentioned earlier, there is a data gap in the range of turbulence with wavelengths between six and sixty kilometers. This may be a region of perturbation kinetic energy input into the atmosphere since, as will be shown later, it covers most of the range of mountain lee waves. This possible input is presumed to be of varying degree because aircraft measurements of energy levels contained in perturbations with wavelengths of six kilometers or less differ greatly with the various degrees of CAT experienced by the aircraft.

From previous investigations we thus find that among the important parameters to be considered when studying CAT are terrain features, the jet stream, wind shears, and the tropopause location.

Turbulence Theory

In his original work, Kolmogorov (1941) presented his similarity hypothesis for the structure function, D, which is defined as the variance of the velocity difference between two points

$$D_{(11)} = \overline{\left| u(x) - u(x + r) \right|^2} \qquad 2)$$

where r is a distance measured along the direction of flow. It was assumed that for some range of values of r, called the inertial subrange, three dimensional turbulence was isotropic and the structure functions were functions only of energy dissipation. By

dimensional analysis they must be of the form $D \propto (\epsilon r)^{2/3}$, where ϵ is the rate of dissipation of energy. This function can be transformed (Batchelor 1953) by a Fourier transformation to the spectral density function, E (k),

$$E(k) = a \epsilon^{2/3} k^{-5/3} \qquad 3)$$

where a is a universal constant and k is the wave number.

It has been found from aircraft measurements that the kinetic energy contained in atmospheric turbulence of wavelengths less than one-half kilometer obeys the "-5/3 law" of turbulence (Reiter and Burns 1965, 1966, Loving 1966). Observations have shown that at times this spectral decay law holds for the horizontal wind components to much longer mesoscale wavelengths. In these cases sources and sinks of turbulent energy are in balance with each other.

In time space, the autocorrelation function, $R_w(\tau)$, describes the velocity fluctuations by determining the average correlation between the vertical gust velocity at time t and a later time $t + \tau$

$$R_w(\tau) = \lim_{T \to \infty} \frac{1}{2T} \int_{-T}^{T} w(t)\, w(t+\tau)\, dt \, . \qquad 4)$$

The average distribution of energy in the gusts as a function of wave number is obtained from the characteristics of the random gust time record which shows the rate of change of random gusts. The power spectral density E (k) (Blackman and Tukey 1959) is

related to the autocorrelation function through the Fourier cosine transformation

$$E(k) = \frac{2}{\pi} \int_0^{\infty} R_w(\tau) \cos \omega \tau \, d\tau. \qquad 5)$$

$E(k)$ and $R_w(\tau)$ are equivalent and are just two different methods of expressing the rate of change of the vertical gust time record.

In order to easily compare the energy levels of observed spectral measurements with each other, the spectral density curves must be transformed into a coordinate system with ln k as abscissa and k E(k) as ordinate. This system is energy conservative, since

$$\int_{k_1}^{k_2} k \, E(k) \, d(\ln k) = \int_{k_1}^{k_2} E(k) \, dk \qquad 6)$$

and the area under the curve between k_1 and k_2 represents the turbulent energy in that wave band.

Spectral measurements taken by aircraft and --although less reliable--subjective pilot reports indicate the value of $E_o(\omega)$ in Eq.(1). If $T(\omega)$, the frequency response function, is known, these objective measurements and subjective reports may be compared with each other. A study by Beckwith (1964) has verified that commercial pilot reports of CAT are highly correlated with measured spectral densities.

The -5/3 slope of E(k) with k, as shown in Eq.(3), holds in the inertial subrange of turbulence wherein viscosity and buoyancy have no effect. Within this inertial subrange the energy is passed on from the larger eddies to smaller ones by the process of inertial transfer. Slopes less steep than -5/3 in the lower

microscale wavelength range would indicate an energy input into the system and this has been observed during some occurrences of CAT (Reiter and Burns 1965, 1966).

Steeper slopes represent an energy loss similar to that observed in the buoyant subrange (at wavelengths just above the inertial subrange) wherein there is an additional dissipation of energy mainly in the w component of the velocity, due to buoyant forces in a stable environment. Bolgiano (1959, 1962), in his theoretical treatment of the "buoyant subrange", arrived at the proportionality

$$E(k) \propto k^{-11/5}. \qquad 7)$$

CAT Pilot Reports Used in This Study

With the satellite coverage described earlier in this chapter, it was possible to initiate a comprehensive study of mountain waves as photographed by satellites, and their correlation with reports of CAT made by pilots in the mountain wave region. A CAT data collection program, making such a correlated study possible, has been carried out by the National Environmental Satellite Center (NESC).

When mountain waves were observed by the satellites, the NESC notified the U.S. Weather Bureau Regional Office nearest to the mountain wave regions. That office, in turn, requested the responsible Air Route Traffic Control Center of the Federal Aviation Agency to elicit pilot reports concerning turbulence and clouds from aircraft flying in the mountain wave area.

The pilot reports used in this study consist of two types. The first type contains the special reports which were requested of all aircraft in the lee wave area, regardless of their altitude, whenever the satellites observed wave clouds. These reports include cases of light and no turbulence as well as higher degrees of turbulence. They also include observations of cloud coverage and cloud heights all of which were made within four hours of the time at which the satellite pictures were taken. The second type of pilot reports, which also were used in the climatological study to follow, are the normal aircraft CAT report of light to moderate or higher intensity turbulence above altitudes of 18,000 ft msl. These reports include no cloud information. The second type of report would usually be the only one available in areas where there was no satellite coverage or where satellites did not observe a lee wave cloud structure.

Climatological Study of CAT Over the Western United States

The clear air turbulence reported by pilots over the western United States during eighteen months when there was a high probability of lee waves was investigated. The months considered were November, December, January, February, March and April of 1962, 1963 and 1964. Over 9000 pilot-reports were used in this study. These reports were furnished by the U.S. Weather Bureau, and included all observations above 18,000 ft msl. that were not in cloudy areas. The reported turbulence should therefore be

attributed to causes other than convection and mechanical inducement within the turbulent boundary layer.

The data were plotted in 1/4 degree latitude-longitude "squares" for each category of turbulence reported. They consisted of reports by military and private pilots who are not bound to air traffic corridors, and reports by the scheduled air carriers who follow established air routes between major cities. The data density sharply reflects the air route patterns since the majority of the reports came from the scheduled carriers.

The plotted data were weighted to correct for the latitudinal difference of the area of the "square". This procedure yielded the "number of turbulence occurrences during an eighteen month period over an area of 3600 sq nm". This number in each "square" was averaged with the numbers from adjacent "squares".

The mean values of occurrences thus obtained were analyzed. The final results are shown in Figs. 1 through 5. This process decreased the sharp gradients in CAT frequency resulting from a tendency for pilots to report over certain check points. However, it also suppressed the sharpness of the gradients on the lee side of mountain ridges.

The maxima near Denver, shown in Figs. 1 through 5, were probably enhanced by the fact that many of the aircraft reporting turbulence in the lee of the Rockies in this area were at a lower altitude than in most other lee areas. This is because most aircraft

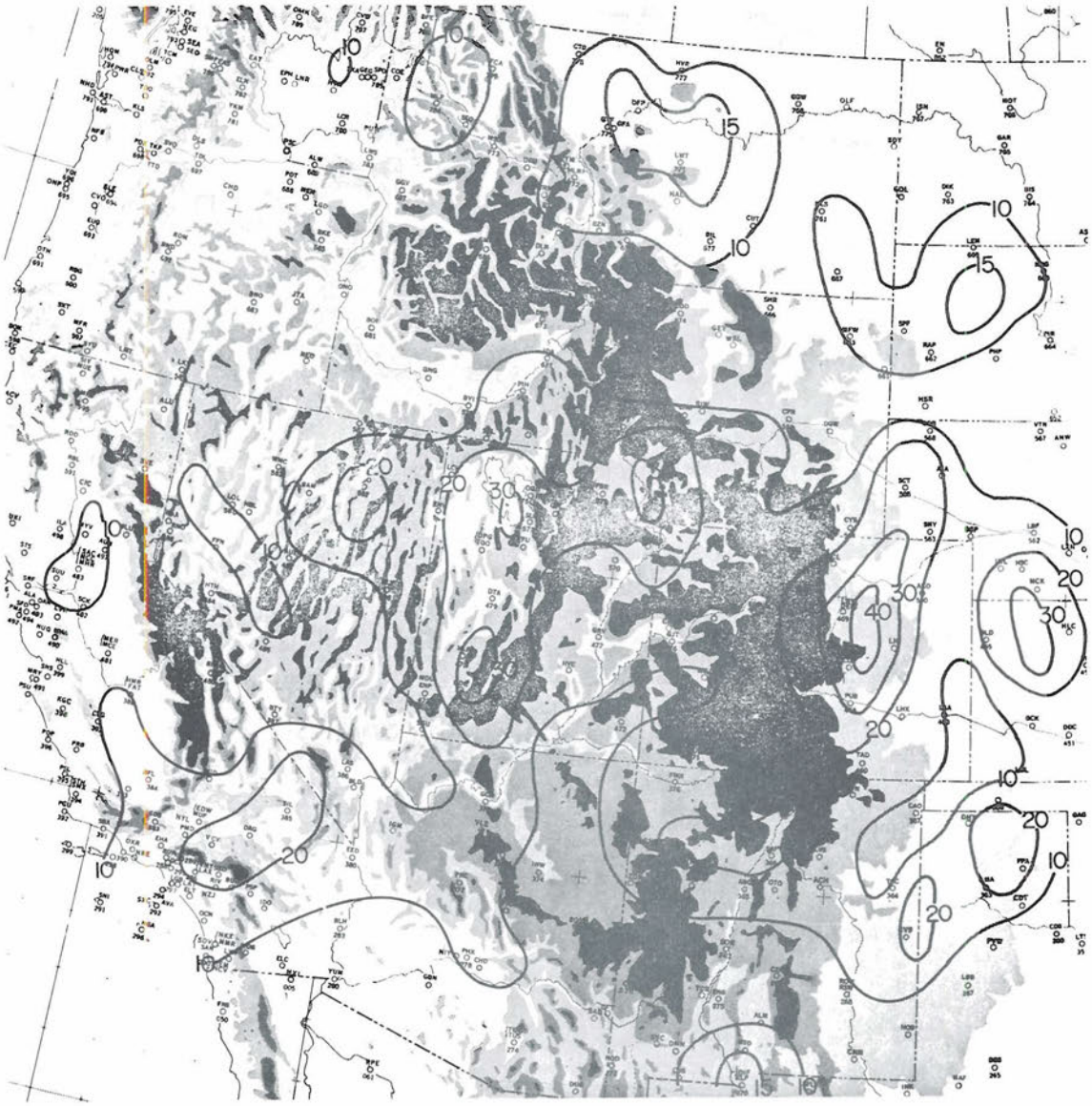

FIG. 1. Mean value of light to moderate CAT frequency over the western United States during 18 months per 3600 nm^2.

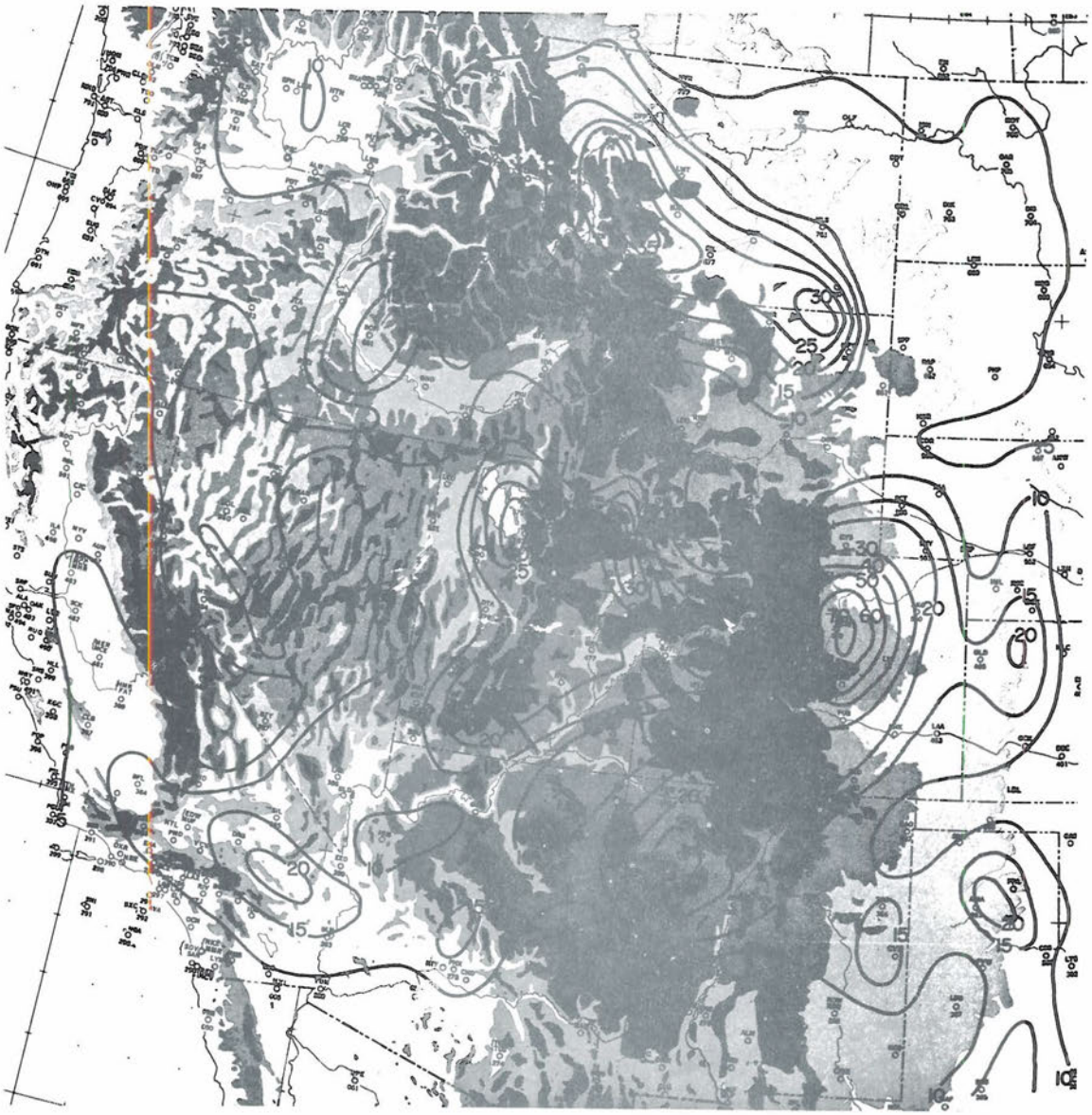

FIG. 2. Mean value of moderate CAT frequency over the western United States during 18 months per 3600 nm^2.

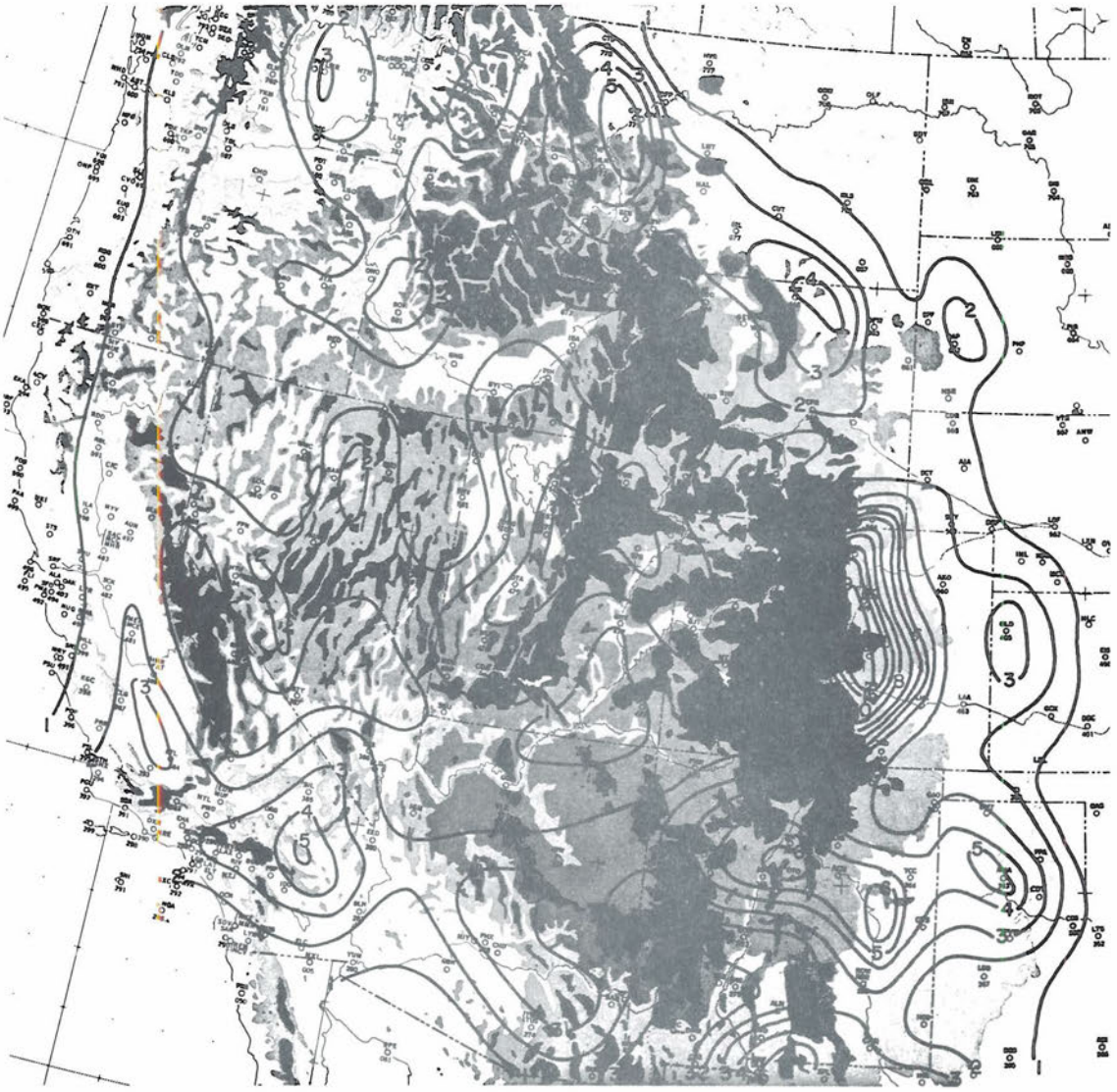

FIG. 3. Mean value of moderate to severe CAT frequency over the western United States during 18 months per 3600 nm^2 .

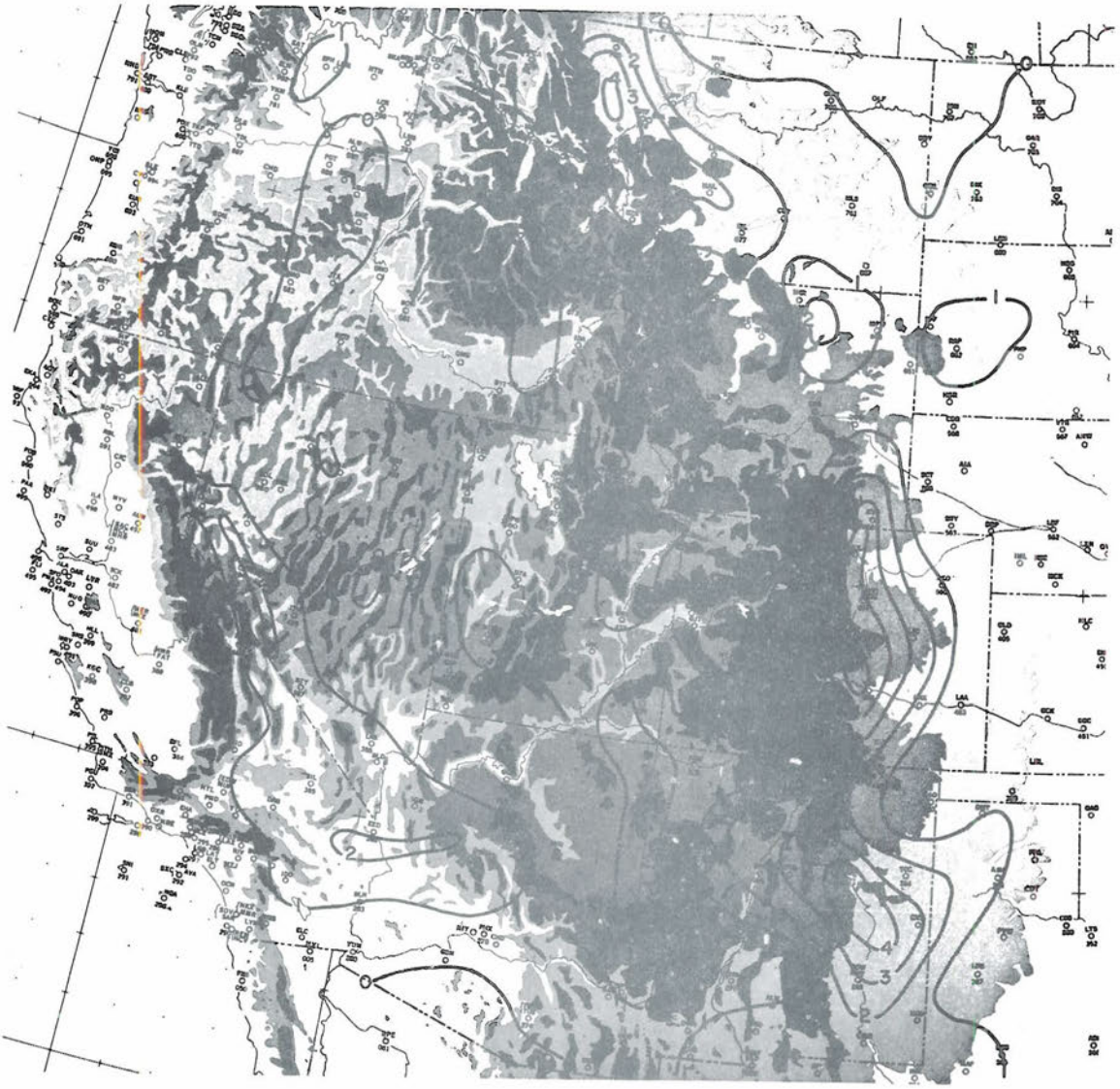

FIG. 4. Mean value of severe CAT frequency over the western United States during 18 months per 3600 nm^2.

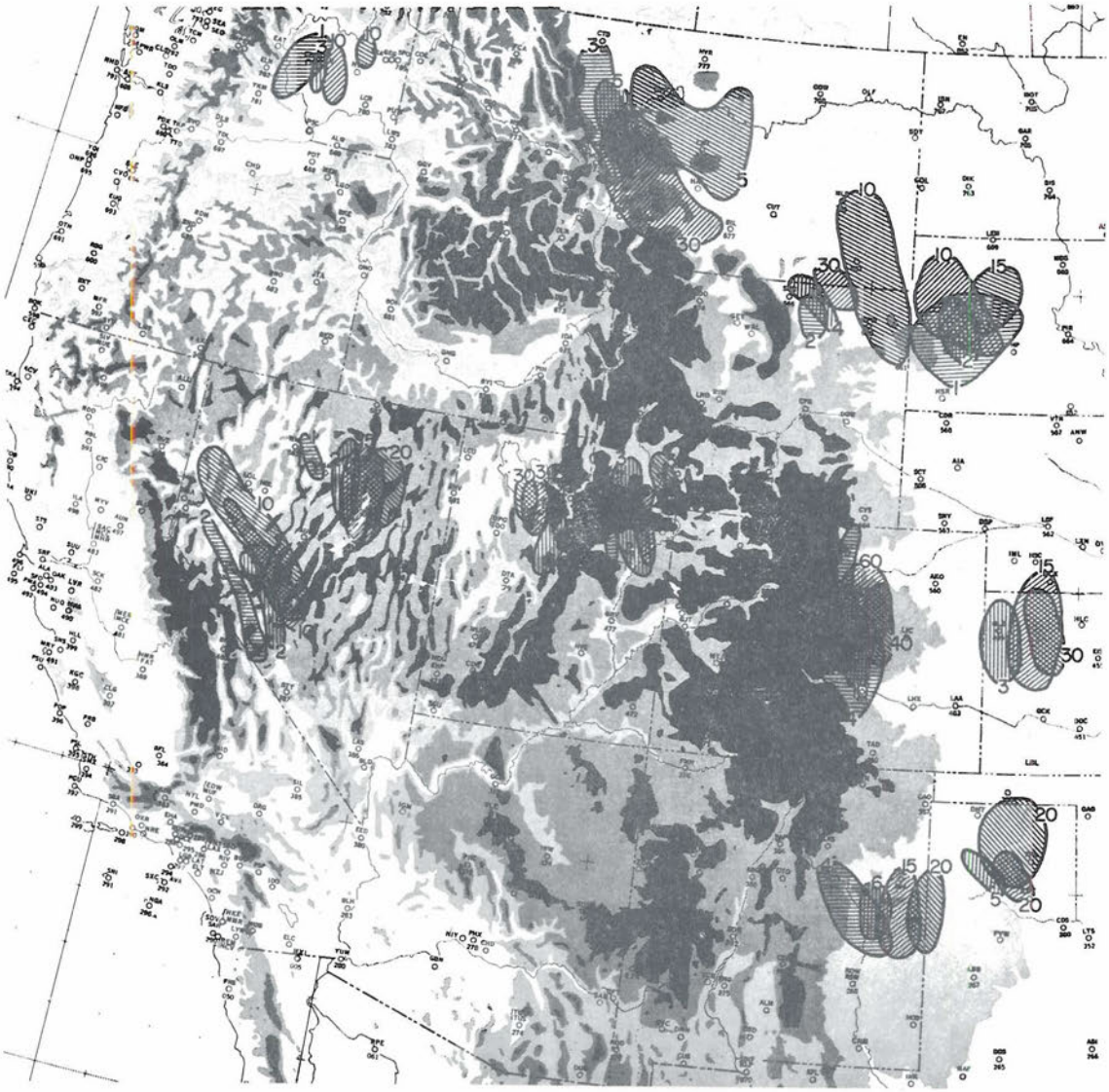

FIG. 5. Patterns of CAT over the western United States. The maximum isopleths (mean frequency during 18 months per 3600 nm^2) were chosen from Figs. 1 through 4, with the condition that these isopleths had to cover enough area to show the orientation of the maxima with respect to the mountains.

in this region had probably descended or ascended in transit to or from the Denver air terminal while experiencing the turbulence. Their attitude and altitude should tend, on the average, to increase the degree of turbulence experienced over that of level flying aircraft at higher altitudes.

A further consideration, indicating a certain bias in the analyzed CAT distributions, is the unequal volume of air traffic normally experienced over each "square" in the western United States. Exact figures for a two year period in 1961 and 1962 (Harrison and Sowa 1966) show that for every flight over the northern sections of the western United States there were four over the central sections and six over the southern routes.

Even though all these factors indicate an uneven distribution of the data sample, certain points were brought out clearly. The effect of the mountain ridges oriented normal to the mean flow during these months was apparent. However, the turbulence maxima did not occur over the major mountain ridges but downstream following the direction of the prevailing upper winds.

The maximum values of severe turbulence usually occurred within 120 km of all major ridges. The isopleths of the highest number of occurrences for each degree of turbulence were oriented parallel to the ridge configurations in most cases. The maximum frequency of all categories of turbulence that were less than severe also occurred downwind from the ridge, but each was located

successively further downwind from the severe turbulence maxima in decreasing order of severity (see Fig. 5).

TABLE 2. Values of Turbulence Maxima (number of occurrences in 18 months per 3600 sq nm).

Mountain Range	S	M/S	M	L/M
Cascades	1	3	12	12
Montana Rockies	4	5	35	18
Sierras	2	2	11	12
Ruby Range	1	2	18	20
Wasatch	2	4	30	30
Big Horn	2	4	30	12
Black Hills	1	2	10	17
Colorado Rockies	5	19	70	40
Sangre de Cristo	4	6	15	20

Table 2 shows the values of the maximum isopleths of turbulence occurrences during 18 months over an area of 3600 sq nm for each category of turbulence in the lee of all major ridges. In these regions, on the average, there were twice as many moderate to severe cases as there were severe cases. There were about ten cases of moderate turbulence for every case of severe turbulence. The fact that there was at times less light to moderate than moderate turbulence reported might be attributed to a possible tendency of some pilots to categorize turbulence only as "light", "moderate" or "severe" (compare with Table 1). Allowing for the relative density of air traffic, it appears that the greatest probability of turbulence in any category could be expected in the lee of the Montana and Colorado Rockies.

An explanation of these patterns of CAT frequency distribution will be given in Chapter IV. It should be pointed out, however, that the location of the CAT maxima suggests a strong connection between CAT and mountain lee wave formation. Therefore, the physical processes leading to orographic wave disturbances will be considered first.

CHAPTER III

OROGRAPHIC WAVE DISTRUBANCES

Orographic Effects

Whether investigated theoretically or by use of field measurements, the problem of air flow over mountains is very complex. If eddies and disturbances produced by air flow over rough terrain were completely random, studies would have to be made entirely along statistical lines However, disturbances often show up in organized patterns such as seen in mountain lee waves It is this type of flow that may be described by mathematical techniques. Before taking a theoretical approach a few words might be said about conditions observed in mountain lee waves and about the broader influences which the mountains might have on the general circulation.

The largest mountain barriers, such as the Rockies, seem to impose disturbances of all scales on the atmospheric air flow from the scale of long waves (> 1000 km) in the westerlies through that of lee depressions and gravity-inertia waves (about 100 km) to smaller scale turbulent eddies (about 10 km or less). The present study will concern itself mainly with the quasi-stationary gravity waves originated by the mountains and we will investigate if they might be the sources of CAT over and near mountainous terrain. This is a reasonable possibility since we have found that CAT maxima are located just downwind from mountain ridges, and larger

orographic disturbances of wavelengths of 100 km or more therefore, could not have a direct effect. The wavelengths of mountain lee waves normally range from 1 to 25 km, and at times are accompanied by aircraft turbulence (Holmboe and Klieforth, 1957). Vertical currents in lee waves may reach substantial values and at times have carried gliders as high as the lower stratosphere (Alaka, 1960). These large vertical currents are found on the lee side of the mountains.

Any realistic theoretical treatment of lee waves must satisfy the above observations concerning lee wavelengths and vertical velocities in lee waves. The problem is to determine the nature of stably stratified air flow over a mountain ridge. In the wave formation process, the temperature stratification of the undisturbed current plays an important role. If the undisturbed flow is unstably stratified, an air parcel forced from its initial level will, upon moving over the ridge, continue in the direction of the impulse for some time. During its ascent the parcel temperature will drop adiabatically with height until it reaches the temperature of the surrounding air and the lifting force vanishes. In this case there is no restoring force to return the parcel to its initial position, and it fails to undergo periodic oscillatory motion in the vertical. If an air parcel in stably stratified undisturbed flow is given a vertical displacement due to flow over a ridge, it seeks its equilibrium level, and then continues its oscillatory motion by inertia. Gravity-buoyant

forces then tend to cause the parcel to oscillate about its equilibrium position according to

$$\frac{d^2\delta}{dt^2} + \frac{g}{\theta}\frac{\partial\theta}{\partial z}\,\delta = 0 \qquad 8)$$

where δ is the vertical displacement of a particle from its original level, θ is potential temperature and g is the acceleration of gravity. The oscillating parcels move downstream to the lee of the ridge forming lee waves in the process. Due to frictional forces in the atmosphere the energy of the oscillating motion is gradually dissipated and these motions slowly damp out. The wavelengths of the oscillatory motions are also obtained from the solution to Eq. (8), which constitutes the Brunt-Väisälä frequency:

$$\lambda = 2\pi U\sqrt{\theta/g\,\frac{\partial\theta}{\partial z}} \qquad 9)$$

where U is the mean horizontal wind speed. Eqs. 8 and 9 result from a very simple atmospheric model wherein the atmosphere is stably stratified at all levels being considered and the effect of moisture on stability is neglected. The atmosphere does not normally respond in this simple way and more sophisticated models may give more realistic results.

The vertical displacement of air parcels could be caused by effects other than mountains. For example, air parcels flowing over a wedge of cold air would be forced upward. A mountain ridge would have a greater effect than a single mountain because

flow downstream from a ridge is complicated by disturbances which arise from other ridges or hills in the area, either upstream or downstream from the ridge under consideration.

Thus we find that the important parameters which should be considered when studying lee waves are the wind velocity and vertical wind shear of the undisturbed air current, the thermal stability of the atmosphere, and mountain dimensions, configurations, and locations.

Theory of Lee Waves

In order to solve for the streamline configuration of flow over a mountain range the set of basic hydrodynamic equations must be used. This set consists of the equation of motion

$$\frac{\partial \tilde{V}}{\partial t} + \tilde{V} \cdot \nabla \tilde{V} = -\frac{1}{\rho} \nabla p - 2\tilde{\Omega} \times \tilde{V} - \tilde{g} + \tilde{F} \qquad 10)$$

the equation of continuity

$$\frac{\partial \rho}{\partial t} + \tilde{V} \cdot \nabla \rho + \rho \nabla \cdot \tilde{V} = 0 \qquad 11)$$

and the physical equation

$$\frac{\partial \rho}{\partial t} + \tilde{V} \cdot \nabla \rho - \gamma \left(\frac{\partial p}{\partial t} + \tilde{V} \cdot \nabla p \right) = 0 \quad . \qquad 12)$$

In addition, the gas law, $p = \rho RT$ must be used. In these expressions $\tilde{V}$ is the vector wind, p is the atmospheric pressure, g is the acceleration of gravity, $\tilde{\Omega}$ is the earth's angular velocity vector, $\tilde{F}$ is the frictional force vector, γ is the coefficient of piezotropy, R is the universal meteorological gas constant, and

T is the absolute temperature. In order to simplify the problem, friction is neglected by assuming an inviscid fluid, and the effects of conduction, radiation, and condensation are neglected by assuming adiabatic motion. The scale of motion is such that the effect of the earth's rotation may also be neglected.

The set of equations is linearized by perturbation theory techniques. The motion is considered to be in a steady state and two dimensional in the xz plane. The undisturbed flow quantities are all a function of z only (except $\overline{W} = 0$) and the perturbation quantities are all a function of x and z. Investigators (Queney 1947, Scorer 1949, 1954, Corby and Wallington 1956, Musaelyan 1964), using such techniques, have been successful in describing mathematically the essential features of flow over mountains.

Scorer (1949), using this approach with a model in which the Scorer parameter, $(\ell^*)^2 = \frac{g\beta}{U^2} - \frac{1}{U}\frac{\partial^2 U}{\partial^2 z}$, was constant in each of two layers, obtained the following simplified equation for ψ, the streamfunction, over a wave-like configuration of the ground of wavelength $2\pi/k$

$$\frac{\partial^2\psi}{\partial z^2} - \left(\frac{g}{c_s^2} + \beta\right)\frac{\partial\psi}{\partial z} + \left(\frac{g\beta}{U^2} - k^2 - \frac{1}{U}\frac{\partial^2 U}{\partial z^2}\right)\psi = 0 \qquad 13)$$

where c_s is the speed of sound, $\beta = \frac{g}{\theta}\frac{\partial\theta}{\partial z}$, U is the mean horizontal wind speed normal to the mountains, and k is the horizontal wave number.

Corby and Wallington (1956) elaborated upon Scorer's work and determined that the vertical displacement of an air parcel traversing a lee wave is given by

$$\zeta_z = -2\pi hbe^{-kb}(U_1/U_z)\,\psi_{zk}(\partial\psi_{1k}/\partial k)^{-1}\sin kx \qquad 14)$$

where ζ_z is the vertical displacement of a streamline from its undisturbed height z, U_1 is the horizontal gradient level wind component normal to the mountains, U is the horizontal wind component normal to the mountains at level z, ψ_{zk} is the streamfunction at level z for wave number k, ψ_{1k} is the streamfunction at gradient wind level for wave number k, x is the horizontal distance from the mountain, h is the height of the mountain, and b is the half-width of the mountain given by

$$z = \frac{hb^2}{b^2 + x^2} \qquad 15)$$

where z in this case is the mountain height anywhere along its profile.

The maximum vertical velocity w_o is given at the inflection points of ζ_z

$$w_o = \left[U_z \frac{\partial \zeta_z}{\partial x}\right]_{max} = -2\pi hbe^{-kb}\,U_1 a_n k \qquad 16)$$

where a_n, the amplitude factor is

$$a_n = \psi_{zk}\,(\partial\psi_{1k}/\partial k)^{-1} \quad . \qquad 17)$$

In Eqs. (14) and (17), ψ satisfies the equation

$$\frac{\partial^2 \psi}{\partial z^2} + [(\ell *)^2 - k^2]\psi = 0 \qquad 18)$$

which is equivalent to Eq. (13) after scale considerations and where

$$(\ell *)^2 = \frac{g\beta}{U^2} - \frac{1}{U}\frac{\partial^2 U}{\partial z^2} \qquad 19)$$

is the Scorer parameter. The second term on the right involving the curvature of the vertical wind profile is generally only important in the surface boundary layer and at times near the jet stream. For these reasons it was not considered in any lee wave computations in this report. The resulting expression, which is known as Lyra's parameter (Lyra 1940), was used instead.

$$\ell^2 = \frac{g\beta}{U^2} \qquad 20)$$

Scorer (1949) imposed the boundary conditions that lee waves die away at great height, that at the interface separating the layers wherein ℓ is constant, ψ and its first derivative are continuous, and that the earth's surface is a streamline. This permitted a periodic solution of Eq. (13) in the lower layer but the solution for the upper layer had to be negative exponential. From this he determined an expression for k, the horizontal wave number. In order for it to be possible to have a solution he found that the atmosphere must be structured according to

$$L = \ell_1^2 - \ell_2^2 > \frac{\pi}{4h_1^2} \qquad 21)$$

where h_1 is the height of the interface and suffixes 1 and 2 refer to the lower and upper layers, respectively.

Corby and Wallington (1956) introduced another parameter α for k

$$k^2 = \ell_2^2 + L^2 \cos^2 \alpha \qquad 22)$$

and developed the expression that determines α (k)

$$Lh_1 = (n\pi - \alpha)/\sin \alpha \quad . \qquad 23)$$

The amplitude factor in Eq. (17) may then be expressed as

$$a_n = L^2 \sin^2 \alpha \, (\ell^2 + L^2 \cos^2 \alpha)^{-\frac{1}{2}} \, (n\pi - \alpha + \tan \alpha)^{-1} \qquad 24)$$

and Eq. (16) becomes

$$w_o = -2\pi hbe^{-kb} U_1 L^2 \sin^2 \alpha \, (n\pi - \alpha + \tan \alpha)^{-1} \quad . \qquad 25)$$

Their study revealed how sensitive lee wave amplitudes were to the stability of the air and to the relationship between wavelengths of the lee wave oscillations and the mountain range scale. They found that the largest amplitude waves occur when the air stream satisfies the conditions (see Eq. (21)) for waves by only a small margin, and, in this region, large changes in the amplitude of lee waves result from small changes in air stream characteristics. It can also be seen from Eq. (25) that high narrow mountains and a strong gradient level wind are conducive to large amplitude waves.

Computational techniques leading to lee wave length and lee wave energy values based upon the above lee wave theory are outlined in Appendix B.

Observations of Lee Waves

In this paper two series of case studies will be used to investigate the characteristics of mountain lee waves. The first series will be referred to as "lee waves observed principally by satellite" and the second as "lee waves observed during a Colorado field measurement program". Although observation by satellite was also used together with the field program, it was not the major method employed, as was the case in the first series. The special pilot reports described in Chapter II were available for the cases observed principally by satellite. Routine pilot reports were the only reports of that kind used in the field program cases.

The satellite pictures used in connection with mountain wave cased over the eastern United States were taken by TIROS X launched in July 1965. This satellite has a perigee of 467 statute miles and an apogee of 521 statute miles. In February 1966, two satellites, ESSA I and ESSA II, were launched to allow for morning and afternoon coverage over the entire globe. These satellites are in nearly polar, sun-synchronous orbits and view cloud patterns all over the world. They photograph a given area at about the same time each day. The satellites rotate like a cartwheel in their orbits at approximately 10 rpm, with each of their two cameras pointing straight downward towards earth once during each rotation. Photographs of mountain waves over the western United States are available from these satellites. ESSA I has an orbit

with an apogee of 521 statute miles and a perigee of 432 miles while ESSA II has an apogee of 654 miles and a perigee of 625 miles. Their orbital periods are 100 and 113 minutes, respectively.

ESSA I carries two identical one-half inch vidicon type cameras. They have a resolution of about two miles at the picture center. Each camera has a wide-angle (104 degrees) lens. Onboard triggering systems program the cameras on both ESSA spacecraft to take pictures only when looking directly downward at the earth. ESSA II's camera subsystem consists of two one inch APT vidicons with wide-angle (90 degree) lenses which take more than 140 two-thousand statute mile-square pictures daily with a resolution of about two miles at the picture center.

Eastern Colorado is particularly suitable as a region for the study of orographically-induced wave formations. Climatologically, the Colorado Rockies have conditions conducive to the relatively frequent formation of mountain lee waves. In many instances these waves are accompanied by a spectacular display of cloud formations. At times clouds of vastly different wavelengths, ranging from mesoscale to microscale, can be seen simultaneously (Reiter 1962).

During the spring of 1966 a field program was carried out near Fort Collins, Colorado, with the purpose of examining lee waves by several independent methods. Radar tracking of constant

level balloons, cloud photogrammetry, satellite cloud photography, and more conventional information, such as surface weather observations, rawinsonde observations and pilot reports of turbulence were employed to make the study as comprehensive as possible. This program was in the nature of a pilot project to determine the feasibility of combining these methods in a comprehensive field study.

Surface weather observations were available from Denver and Fort Collins, Colorado, and Cheyenne, Wyoming. Rawinsonde measurements were taken at Denver each day at 1200Z. Rawinsonde observations were made at about 1400Z on April 1 and May 11, 13, and 14, 1966 as well as at 1900Z on April 1, 1966, at Fort Collins. These measurements provided an opportunity to compare lee wavelengths and lee wave energies computed by using smoothed upper air information from Denver and the more detailed data from Fort Collins (see Appendix B for the computational methods). Upper air wind information at Fort Collins was obtained by radar tracking of rawinsonde or pibal balloons. The Fort Collins upper air temperature data were very detailed since the rawinsonde instrument circuitry normally devoted to humidity measurement was rendered inoperative. Thus the continuous measurement of temperature with height was interrupted only at every fifth instrument contact when pressure data were recorded.

The constant level balloon data were obtained from a series of superpressure balloon flights on April 1 and May 13 and 14, 1966. The superpressure balloons were constructed of 0. 2 mil clear Mylar, a non-expandable material, which allowed the balloon volume to remain essentially constant. The balloons were in the shape of pillows, having a volume of approximately 0. 17 cubic meter (if set for 15, 000 ft msl) and 0. 73 cubic meter (if set for 20, 000 ft msl). Superpressure is necessary to insure that the balloon will remain completely expanded for sufficiently long periods in spite of any slow seepage of helium through the balloon skin (Angell and Pack 1960).

These balloons will seek a density level at which the height of the air displaced by them will be exactly equal to the weight of the balloon, helium, and all attachments, according to

$$V_b(\rho_a - \rho_h) - W_b = 0 \qquad 26)$$

where V_b is the volume of the balloon, W_b is the weight of the balloon and its attachments and ρ_a and ρ_h are the densities of air and helium, respectively. If the balloon is displaced above (below) this density level, it becomes negatively (positively) buoyant and seeks to return to its original level. Thus, it is in stable equilibrium and it will be displaced from this equilibrium level only by vertical air motion.

The balloon ballast is attached in such a way as to insure that the pillow balloon floats with its greatest surface area in horizontal planes. This attitude presents the greatest drag in the direction of vertical air currents, causing the balloon to respond sensitively to vertical disturbances in the air stream.

The balloons are towed aloft by neoprene launch balloons with a rate of ascent of about 2.5 m sec^{-1} (the balloons used on April 1, 1966, had a rate of ascent of 4.0 m sec^{-1}). The Mylar "pillows" are separated from the launch balloons at the desired altitude by means of a fuse that burns through the tow line. A twelve inch aluminum foil reflector which efficiently returns the radar signal and the necessary ballast are attached to each constant-level balloon.

Several of the flights at the beginning of the program were equipped with transponders, but the modified M-33 radar set used in the operation of the field program failed to track by this method. These transponder-carrying flights were launched far upwind in the hope of having long tracks at designated altitudes. The launch of the reflector carrying constant-level balloons had to be made within five miles of the Colorado State University M-33 radar site (12 miles east of Fort Collins at an elevation of 5000 ft msl) in order to allow tracking from launch. Without transponder capability the constant-level balloon was usually far downwind before

separation from the launch balloon, and thus, only relatively short tracks were possible at designated altitudes.

The burn rate of the fuse rope employed to separate the launch balloon proved to be not entirely predictable in rarefied atmosphere. Many flights did not separate until well above designated flight level, and some did not separate at all.

Photogrammetric methods were used to investigate lee wave clouds The principal instrumentation employed in these methods consisted of two K-24 aerial reconnaissance cameras equipped with 178 mm Aerer-Ektar lenses. These cameras were mounted on permanent stands located 3.2 miles apart. The camera sites were located in an area about twelve miles east northeast of Fort Collins where the terrain was quite level. The coordinates of the two sites, in the Colorado State Plane Coordinate System, Northern Zone, are:

Station Name	South	Foundation
X(E-W) Coordinate	2,159,408.8	2,175,074.8
Y(N-S) Coordinate	469,831.4	476,785.3
Z(Elevation above MSL)	5,245.9	5,302.3

The bases of the cameras were fitted with dials from which the azimuth and elevation angles of the camera axes at the time of each photograph could be read. The cameras were fired manually. The pictures at the two sites were taken simultaneously at two minute intervals by use of predetermined times observed on previously synchronized watches.

Stereo pairs of photographs were taken between 1700Z and 1900Z on April 16 and between 1830Z and 2000Z on May 13, 1966. The image positions of the lee wave cloud features were precisely measured and recorded by means of a standard precision comparator. This study concentrates upon mesoscale lee wave cloud formations. The same methods employed here have been used by Reiter (Reiter and Hayman 1962) to investigate microscale lee wave clouds.

The orientation of the cameras, the time at which the photographs were taken, the cloud image measurements, the base line data of the camera positions, as well as camera information concerning lens distortion and film shrinkage, were all included in a numerical computer program utilizing geometrical triangulation methods to locate the proper position in space of cloud features observed in stereo pairs of photographs. For the complete program and more detailed information see Reiter and Hayman (1962) and Hayman and Peterka (1963).

Satellite photographs taken on the days of field program operation were made available by the National Environmental Satellite Center.

The first seven cases described below (January 7 and 24; February 14; March 1, 7, and 9; and April 26, 1966) were observed principally by satellite. The last five cases (April 1

and 16 and May 11, 13 and 14, 1966) were observed during the field measurement program.

Scorer's theoretical development was used to determine lee wavelengths from rawinsonde data on all days (see Appendix B). The computed lee wavelengths and those observed by satellite for the first series of cases are given in Table 12 (Chapter V). The pressure altitude of all density interfaces existing on field program days and the computed lee wavelengths are shown in Table 10 (Chapter V).

Four lee wave cases over the Appalachian Range were observed by satellite. They occurred at 1616Z on January 7, 1966, 1608Z on January 24, 1966, 1720Z on February 14, 1966, and at 1834Z on March 1, 1966. Only the February 14th case with southwesterly flow will be described in full. On the other three days the flow aloft was west to northwesterly with cross mountain components ranging from 25 knots (January 24) to 75 knots (March 2) at 700 mb and from 35 knots (January 24) to 100 knots (March 2) at 500 mb.

The lee wavelengths and maximum vertical motions on these interfaces, computed from the rawinsonde information by methods outlined in Appendix B are included in Tables 12 and 13 (Chapter V).

The best display of lee wave clouds over the eastern United States as observed by satellite occurred between 1700 and 1900Z on February 14, 1966 (Figure 6). The wavelengths in the photograph were between 10 and 14 km which agreed quite well with the theoretical value of 10 km obtained over New England and 12 km over Washington D. C. The lee wave cloud regions are shown as shaded areas in Figure 7.

The surface chart for 0000Z, February 15, 1966 (Figure 7) shows a weak low center over the Ohio River Valley with a flat pressure gradient over much of the eastern United States. A deep low system over Nova Scotia resulted in strong northerly to northwesterly flow over the New England States. The warm front through Pennsylvania was very weak. Cross sections depicted in Figure 37 are projected on this surface chart. Winds aloft were westerly and more than 50 knots at 700 mb and greater than 100 knots at 500 mb (see Figure 8) over the lee wave cloud areas.

The satellite picture, shown in Figure 9, taken at 2003Z on March 7, 1966 shows an unusually well developed display of mountain wave clouds extending inland from the Sierra Nevadas for over 400 miles (see Figure 10 for lee wave area). The wavelengths of these clouds are, on the average, about 13 km. The orientation of the lee wave clouds is parallel to that of the Sierras but the orientation changes from north northwest to south

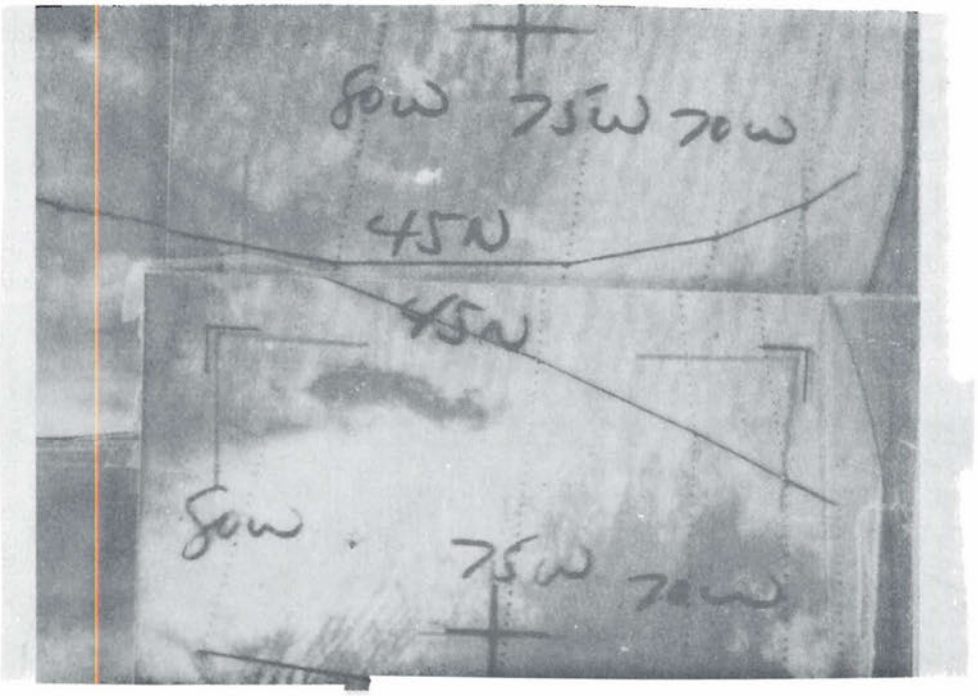

FIG. 6. Satellite photograph taken at 1720Z on February 14, 1966.

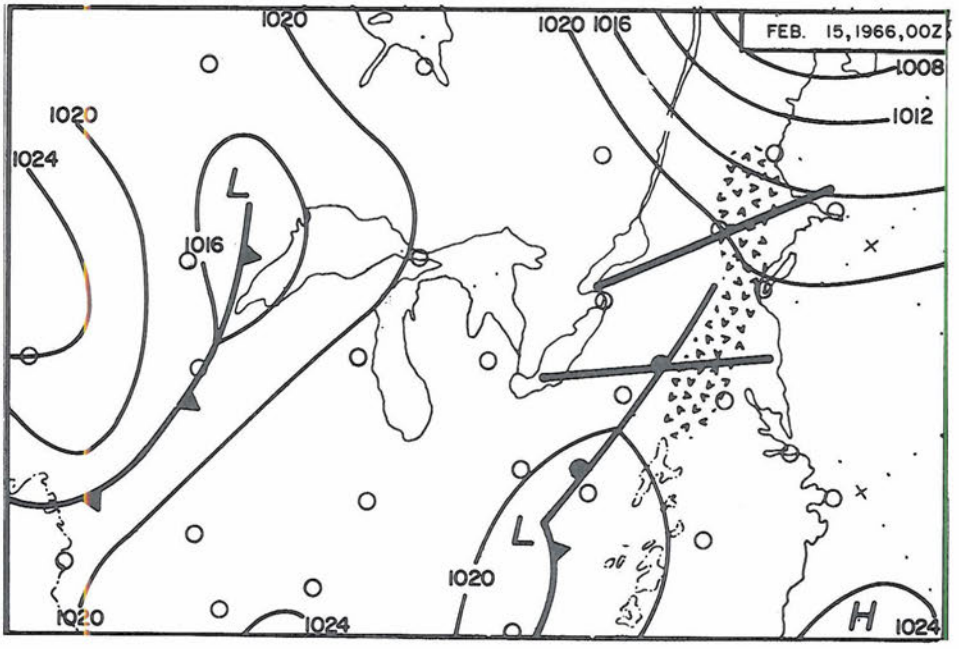

FIG. 7. Surface chart for 00Z, February 15, 1966. The heavy straight lines are surface projections of the cross sections shown in Fig. 37. The shaded area is the lee wave cloud region shown in Fig. 6.

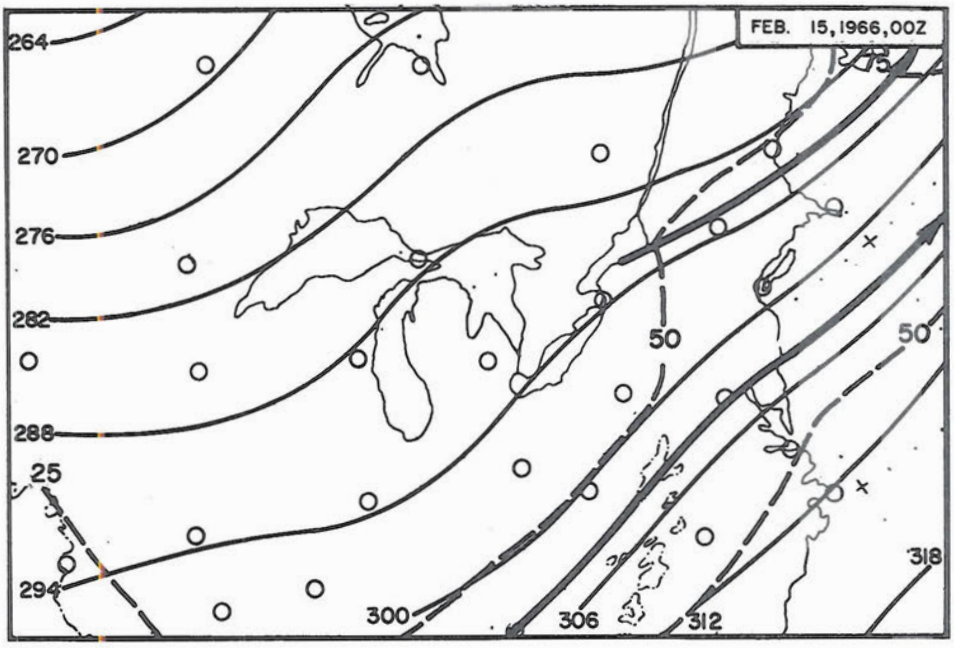

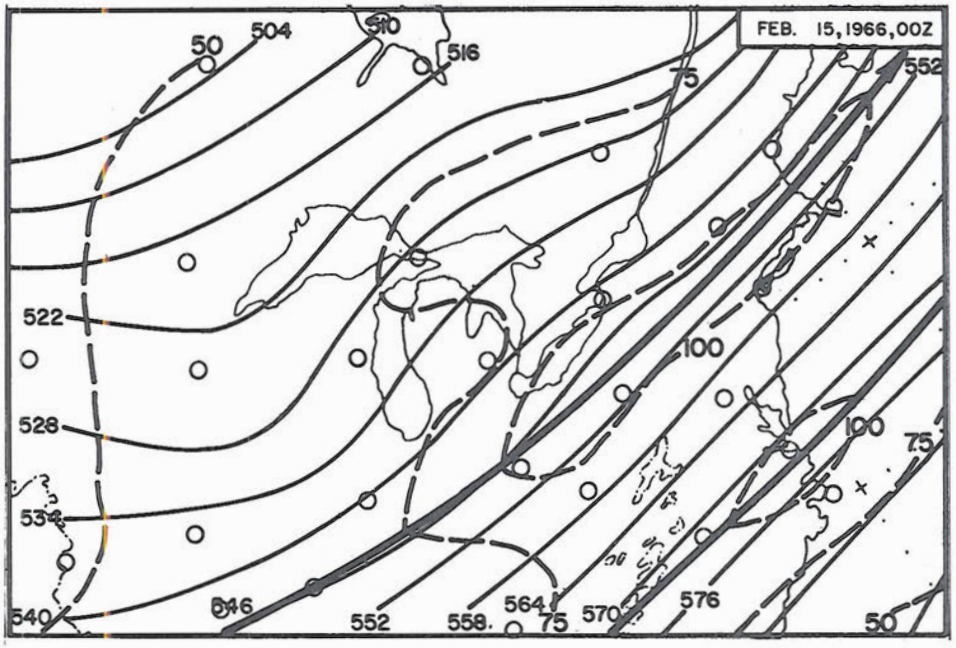

FIG. 8. 700 mb (upper) and 500 mb (lower) charts for 00Z, February 15, 1966.

southeast in the area just to the lee of the Sierras to approximately north northeast to south southwest further inland. This is the orientation of the lesser mountain ridges over Nevada and western Utah.

It appears that the lee wavelength does not change appreciably throughout the mountain wave area. Scorer's lee wave theory states that the lee wavelength is determined entirely by atmospheric physical parameters and not by the dimensions of the disturbing obstacles, such as the mountains. The dimensions of the mountains and hills located in the lee wave area of Fig. 9 vary widely, but the cloud wavelengths are consistent with the theory interpreted above.

Figs. 10 and 11 show the surface, 500 mb, and 300 mb charts for 0000Z, March 8, 1966. A high pressure area was located just offshore from southern California and a Pacific front had pushed inland into eastern Montana, central Wyoming, northern Utah and northern Nevada. The flow aloft over the cloud area was west southwesterly at about 50 knots at 500 mb and 75 knots at 300 mb. This flow velocity has a large cross-mountain component in the lee wave areas, as required by lee wave theory.

Three typical rawinsonde ascents including temperature, wind, and $(l)^2$ parameter profiles are shown in Figure 12. The sounding and $(l)^2$ profiles for Winnemucca, Nevada; Ely, Nevada; Boise, Idaho; Salt Lake City, Utah; Lander, Wyoming; Grand Junction, Colorado; and Denver, Colorado, all showed a very stable layer

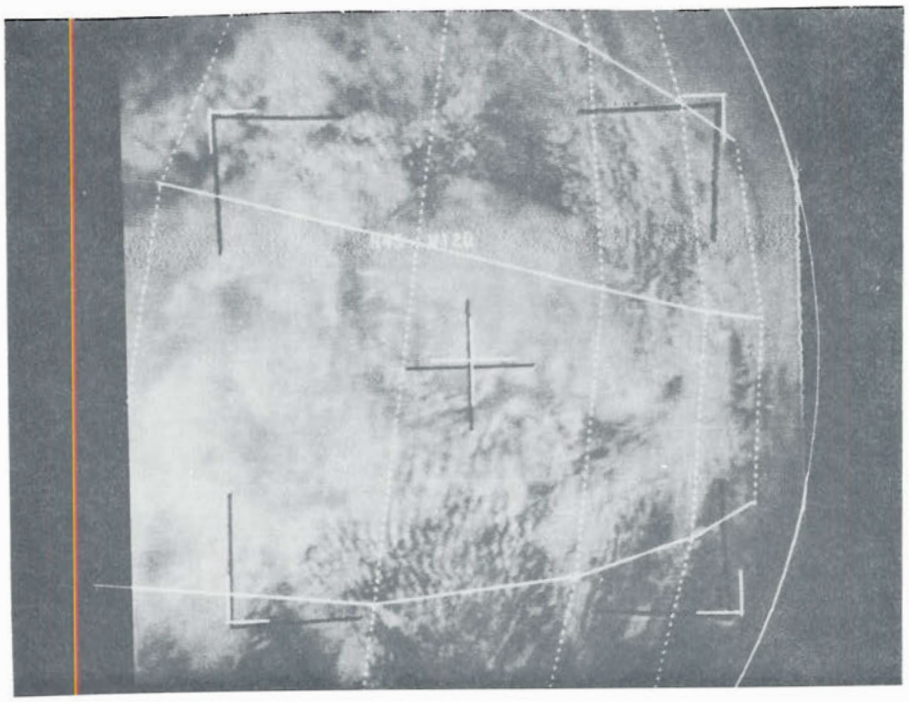

FIG. 9. Satellite photograph taken at 2003Z, March 7, 1966. This unusual cloud display is over the western U.S.

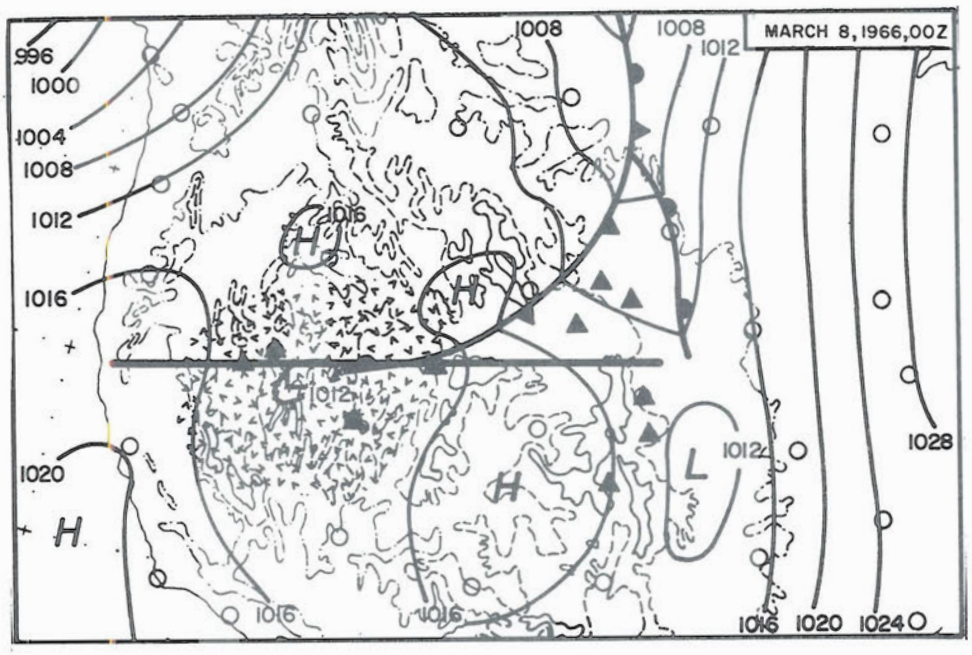

FIG. 10. Surface chart for 00Z, March 8, 1966. Heavy line depicts the surface projection of the cross section in Fig. 38. The triangles are the locations observing lee wave clouds from the ground. The shaded area is the lee wave region shown in Fig. 9.

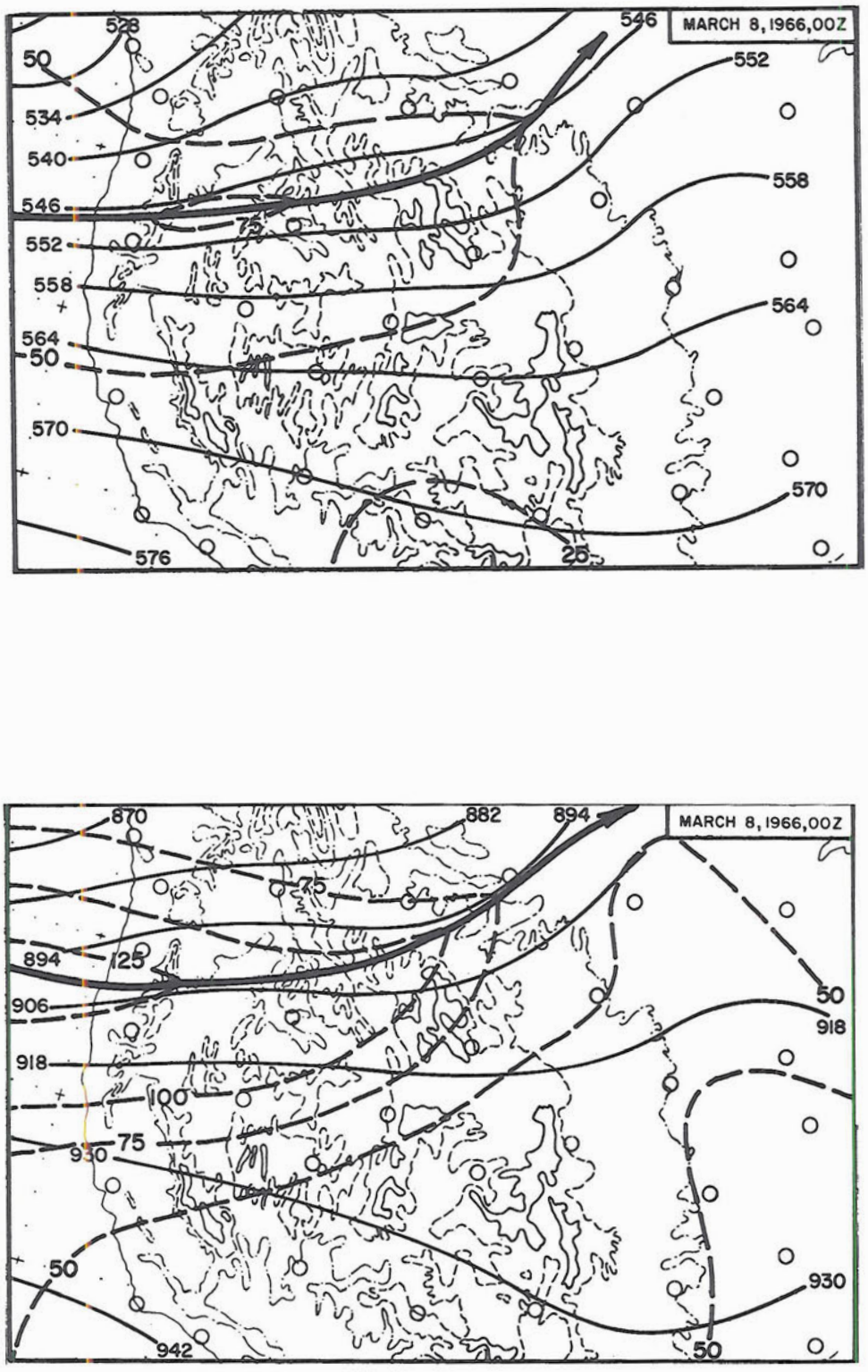

FIG. 11. 500 mb (upper) and 300 mb (lower) charts for 00Z, March 8, 1966.

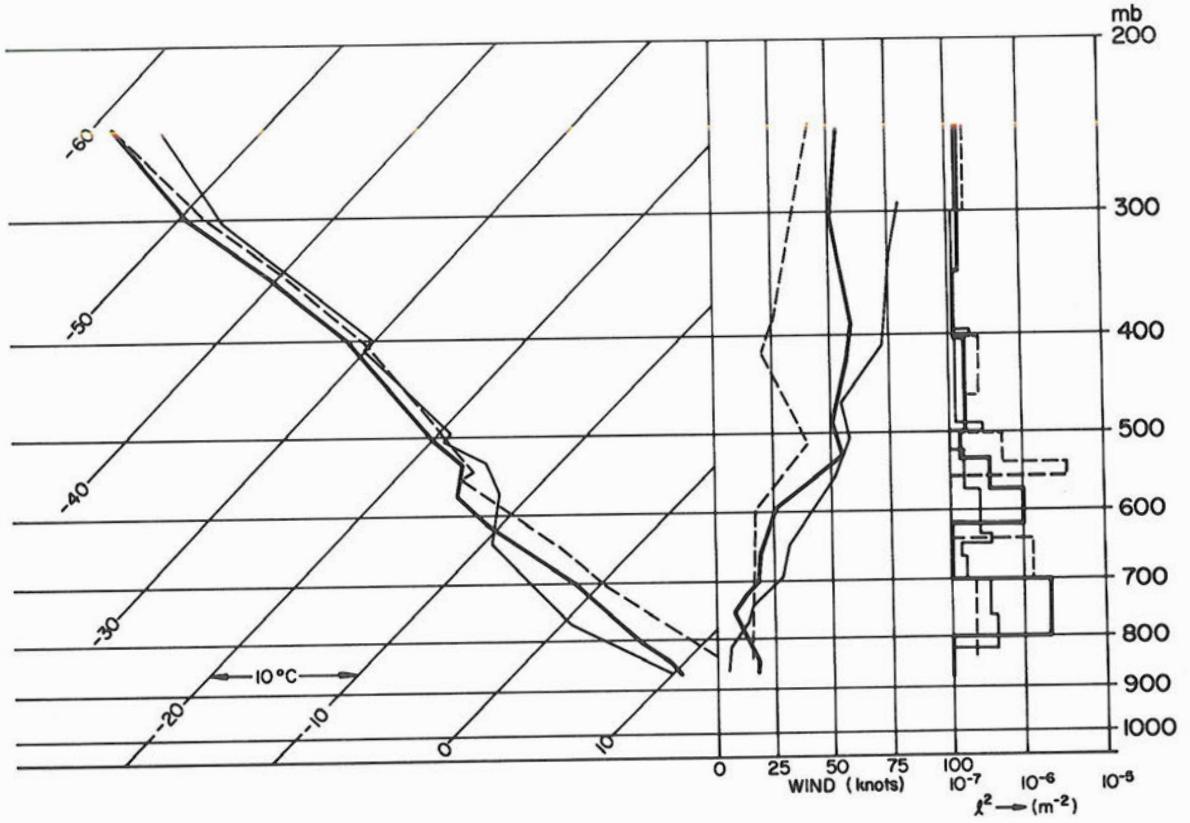

FIG. 12. Rawinsonde information for Winnemucca (light solid), Salt Lake City (dark solid), and Denver (dashed) at 00Z, March 8, 1966. The temperature (Centigrade), winds (knots), and Lyra parameter are plotted against pressure.

located between 500 and 600 mb upon which lee waves could form. The moisture in the air permitted clouds to form over northeastern California, most of Nevada, southern Idaho, and western Utah when air ascended in each lee wave crest. The air was too dry aloft over eastern Utah and most of western Colorado and western Wyoming for lee wave clouds to form (none were observed from the ground or by satellite). Lee waves were probably in these regions, since further east, over eastern Wyoming and Colorado, lee wave clouds were observed again from the ground (see Fig. 10). The satellite camera angle was such that any lee waves over eastern Wyoming and Colorado were not discernible in the satellite photographs.

Some lee wave clouds that seem to show up better than others in Fig. 9 appear to be accompanied by lower level cumulus. This is true of the area just to the lee of the Sierras. The lee wave structure observed by satellite over western Montana appears to be composed mainly of towering cumulus since all surface observations in that area report only that type of cloud.

The lee wavelength was computed from theory to be nearly 9 km at Denver, 8 km at Salt Lake City and 11 km at Winnemucca. The value of 11 km is fairly close to that observed by the satellite in the Winnemucca area, but we have no satellite comparison further east.

Numerous stations (denoted in Fig. 10 by triangles) observed the wave cloud phenomenon and reported altocumulus lenticularis frequently in their 0000Z March 8, 1966 weather observations. Hence, these clouds still existed at rawinsonde time over northern Nevada, western Utah, eastern Wyoming and Colorado.

Fig. 13 is a satellite photograph taken at 2033Z on March 9, 1966. Mountain lee wave clouds existed in two areas, one over northwestern Wyoming, and one over eastern Colorado. The observed lee wavelengths appear to be about 10 km over Wyoming and about 15 km over Colorado. The computed wavelengths were 7 km over Wyoming and 4.5 km over Colorado. Each of the lee cloud regions is much smaller than in the March 7 case. The clouds are oriented along the direction of the mountains and do not change their orientation appreciably downstream from the ridges. Surface, 500 mb and 300 mb charts for 0000Z, March 10, 1966 are given in Figs. 14 and 15. Both cloud areas (entered in Fig. 14) were well ahead of a Pacific front that had pushed inland into Oregon and Washington. The flow aloft at 500 mb and 300 mb was approximately at right angles to the mountains upwind from the lee wave clouds and the wind speeds were around 40 knots at both levels.

Fig. 17 is the surface chart for 0000Z, April 27, 1966. It shows a complex low pressure system over eastern Wyoming and Colorado and a large high cell off the west coast of the United States.

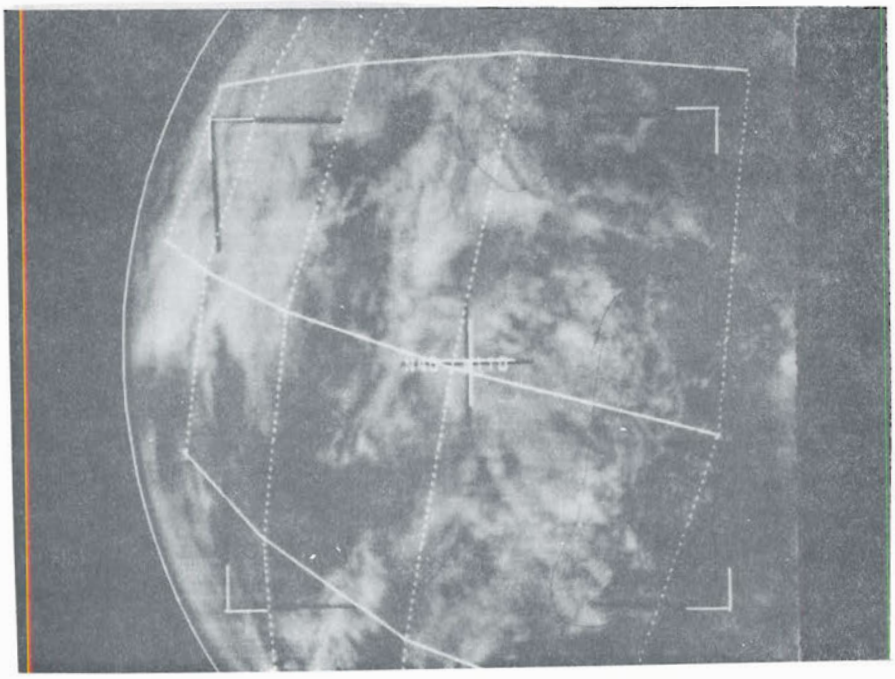

FIG. 13. Satellite photograph of lee wave clouds over the western U.S. taken at 2030Z, March 9. 1966.

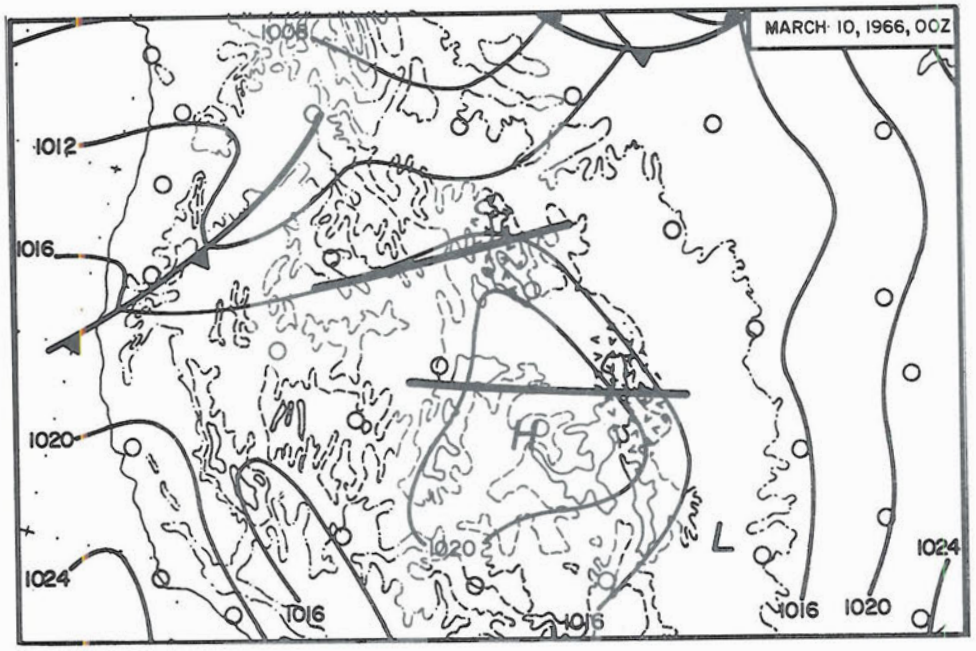

FIG. 14. Surface chart for 00Z, March 10, 1966. Heavy lines are the surface projections of the cross sections shown in Fig. 39. The shaded areas are the lee wave cloud regions shown in Fig. 13.

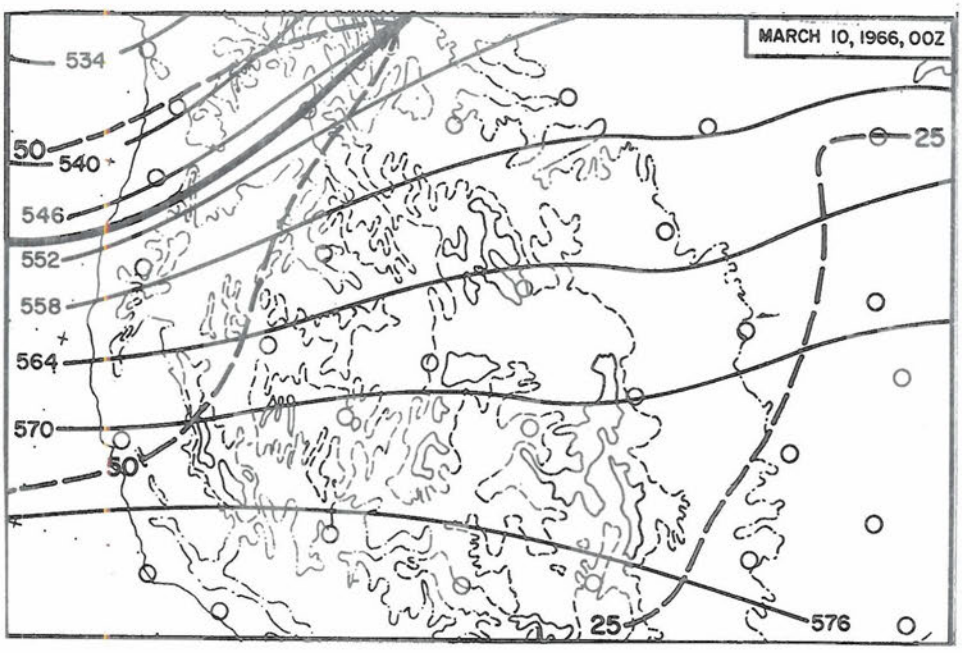

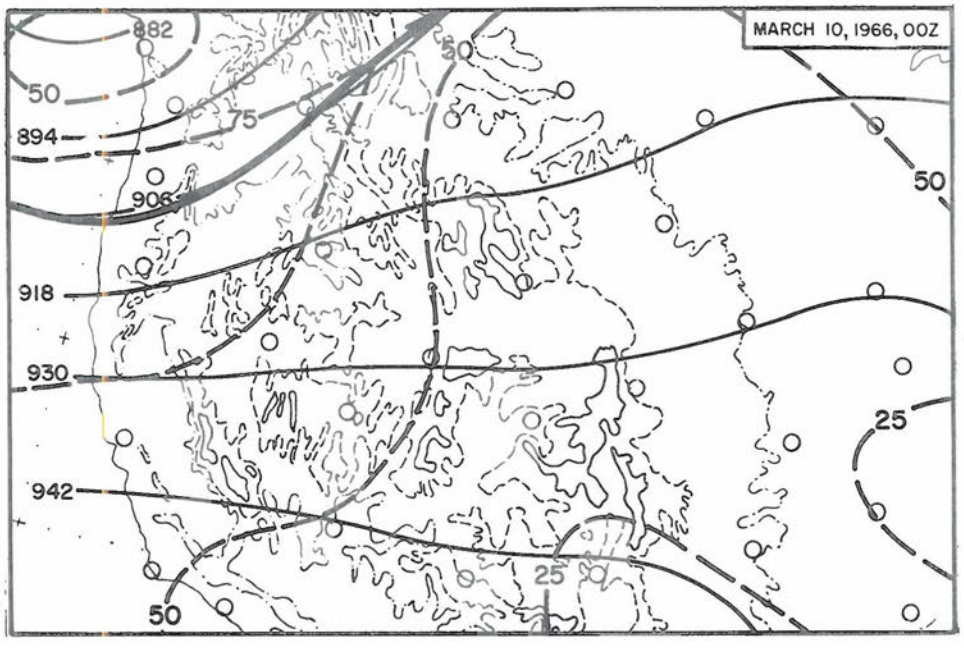

FIG. 15. 500 mb (upper) and 300 mb (lower) charts for 00Z, March 10, 1966.

A stationary front was located along the eastern slopes of the Rockies in Montana and northwestern Wyoming and along an east-west line through central Wyoming. A cold front oriented northeast-southwest through western Colorado was moving eastward over the Colorado Rockies. The two lines shown on this chart depicting the surface projection of the cross sections in Fig. 40 were in areas of west to northwest flow of 35 knots at 700 mb and west to southwest flow of 70 knots at 500 mb. At both of these upper levels there were closed lows over central Montana. Fig. 18 shows the 700 mb and 500 mb charts for 0000Z, April 27, 1966.

Fig. 16 is the satellite photograph taken at 2045Z on April 26, 1966. The lee wavelength in the photograph is about 10 km near Salt Lake City, Utah, and Lander, Wyoming, and about 20 km near Ely, Nevada, while the computed wavelength was 8 km over Salt Lake City and 21 km over Ely and Lander. On April 1, 1966, a large high pressure system was located over northern Wyoming (Fig. 20) with a ridge of high pressure extending southeastward over eastern Colorado. The winds aloft over northeastern Colorado were northwesterly at about 25 knots at 700 mb and 50 knots at 500 mb (Fig. 21). The sky was generally cloudless in the Denver-Fort Collins area during the day but there were some cumuli near 14,000 ft msl over the mountains and a

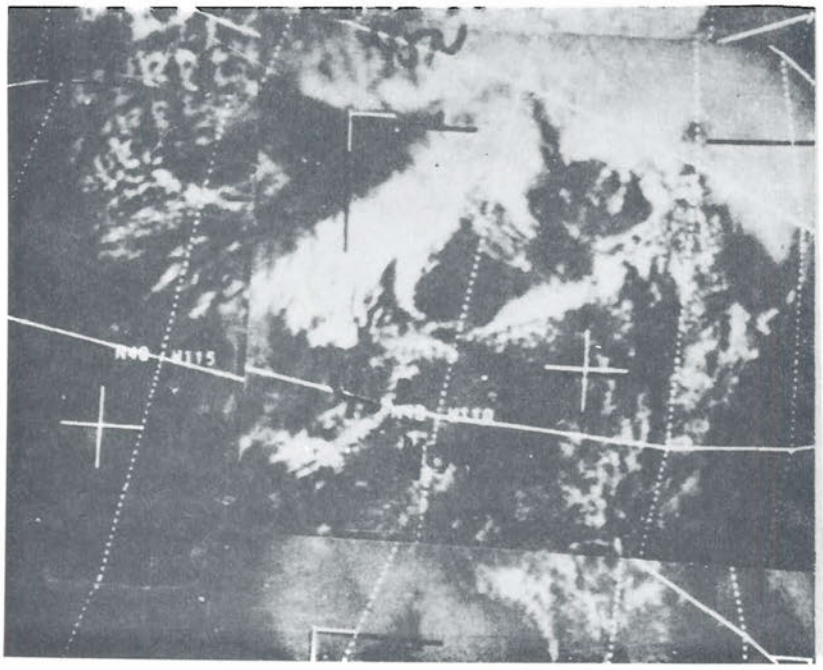

FIG. 16. Satellite photograph taken at 2045Z on April 26, 1966 over the western U.S.

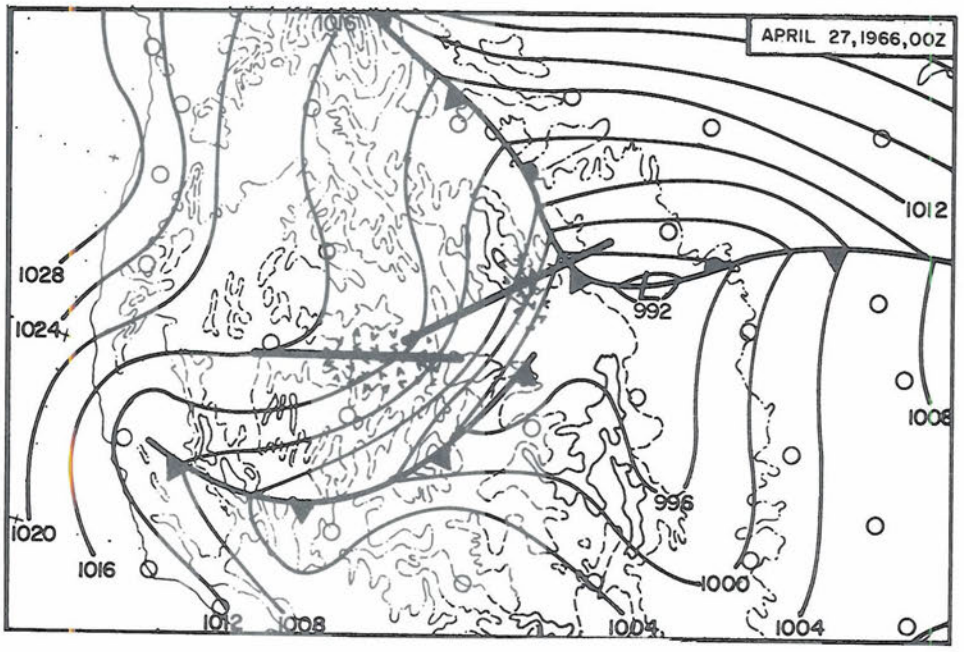

FIG. 17. Surface chart for 00Z, April 27, 1966. Heavy lines depict the surface projections of the cross sections shown in Fig. 40. The shaded areas are the lee wave cloud regions shown in Fig. 16.

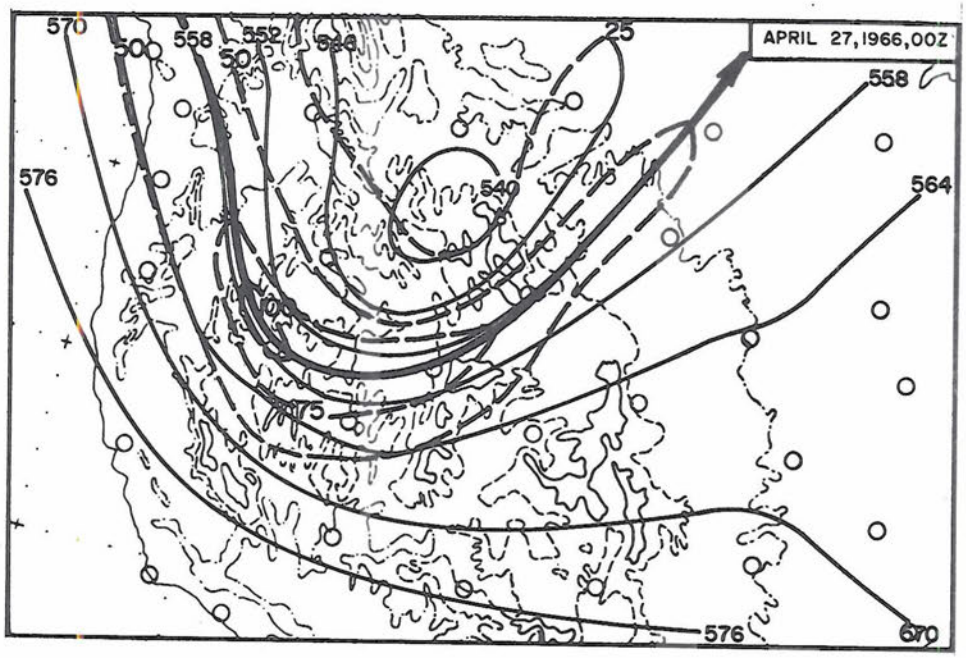

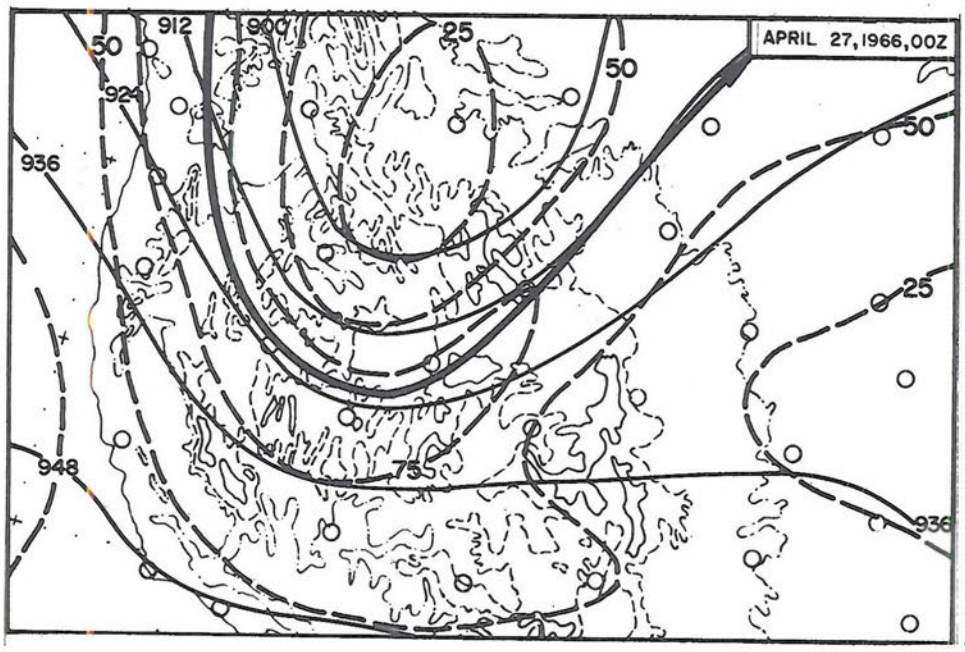

FIG. 18. 500 mb (upper) and 300 mb (lower) charts for 00Z, April 27, 1966.

few lee wave cirrus clouds above 20,000 ft msl. The surface winds were light and variable.

No cloud photogrammetric data were taken on this date due to camera malfunction. Three constant level balloons (all constant level balloon data are depicted graphically in Appendix D) were released, one of which failed to separate from its launch balloon and another ruptured. The second release at 2025Z was set for separation at 20,000 ft msl altitude. The balloon traveled 60,000 ft downwind from the radar site before reaching altitude and traversed a half lee wavelength before moving out of range. The lee wavelength was 33 km at 20,000 ft msl which agrees with the computed wavelength of 34 km at 489 mb at 1400Z (Table 10, Chapter V). The wavelength for this level could not be computed from the 1900Z sounding due to the termination of the wind data at that time at a lower level.

Besides the aforementioned lee wavelength of 33 km observed in run two, there were indications of a 10 km wavelength in the vertical velocity profiles of run one and two. This also was noticeable during the ascending portions of the flights, before separation occurred. When comparing vertical velocities before and after separation, the ascent rate of the launch balloons must be subtracted from the w component measured before separation.

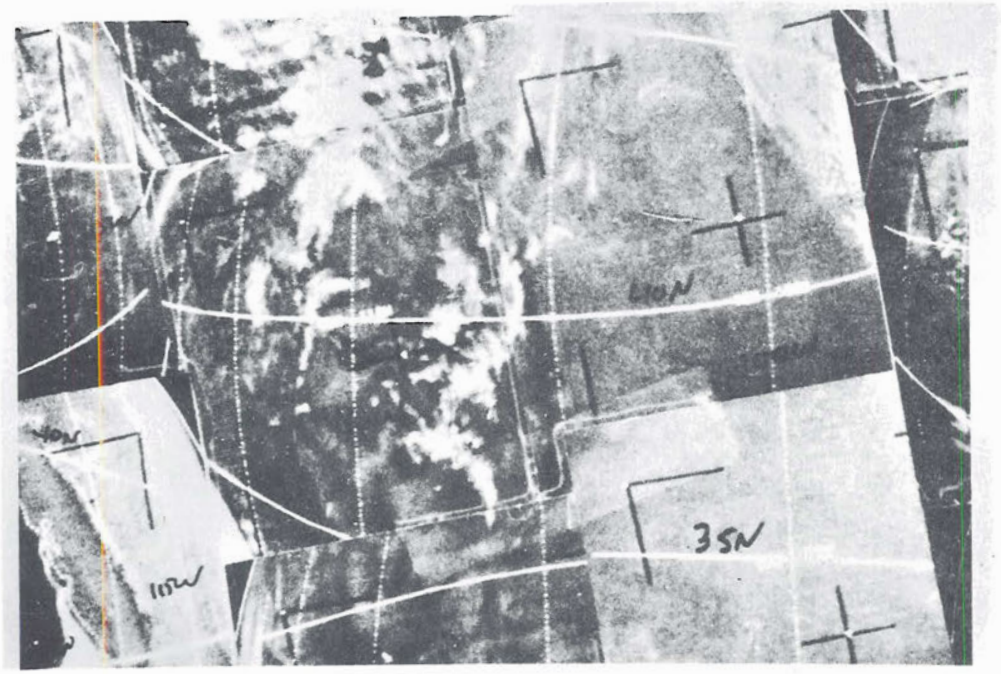

FIG. 19. Satellite photograph taken at 2026Z, April 1, 1966 over the western U.S.

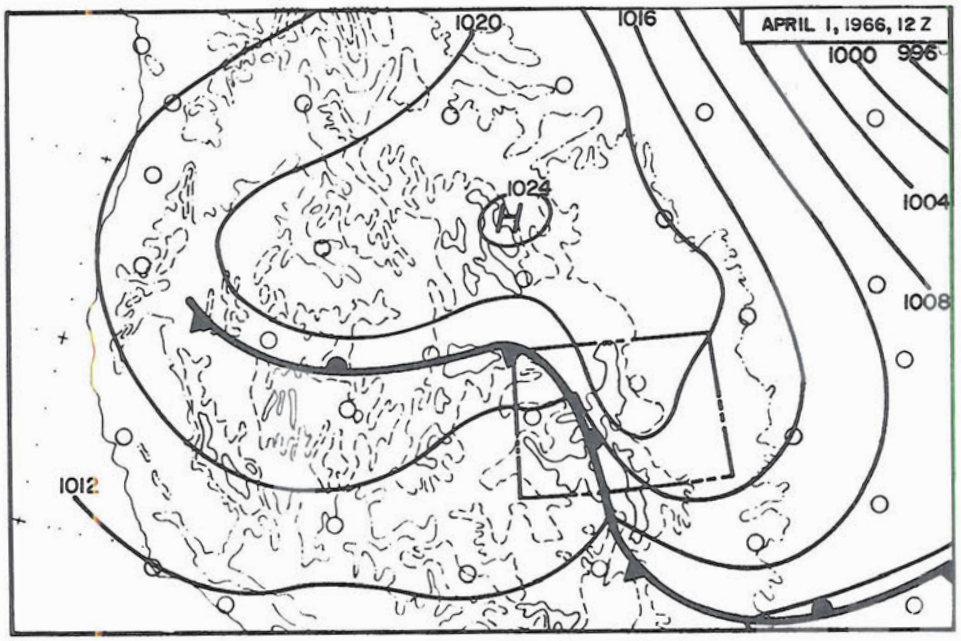

FIG. 20. Surface chart for 12Z, April 1, 1966.

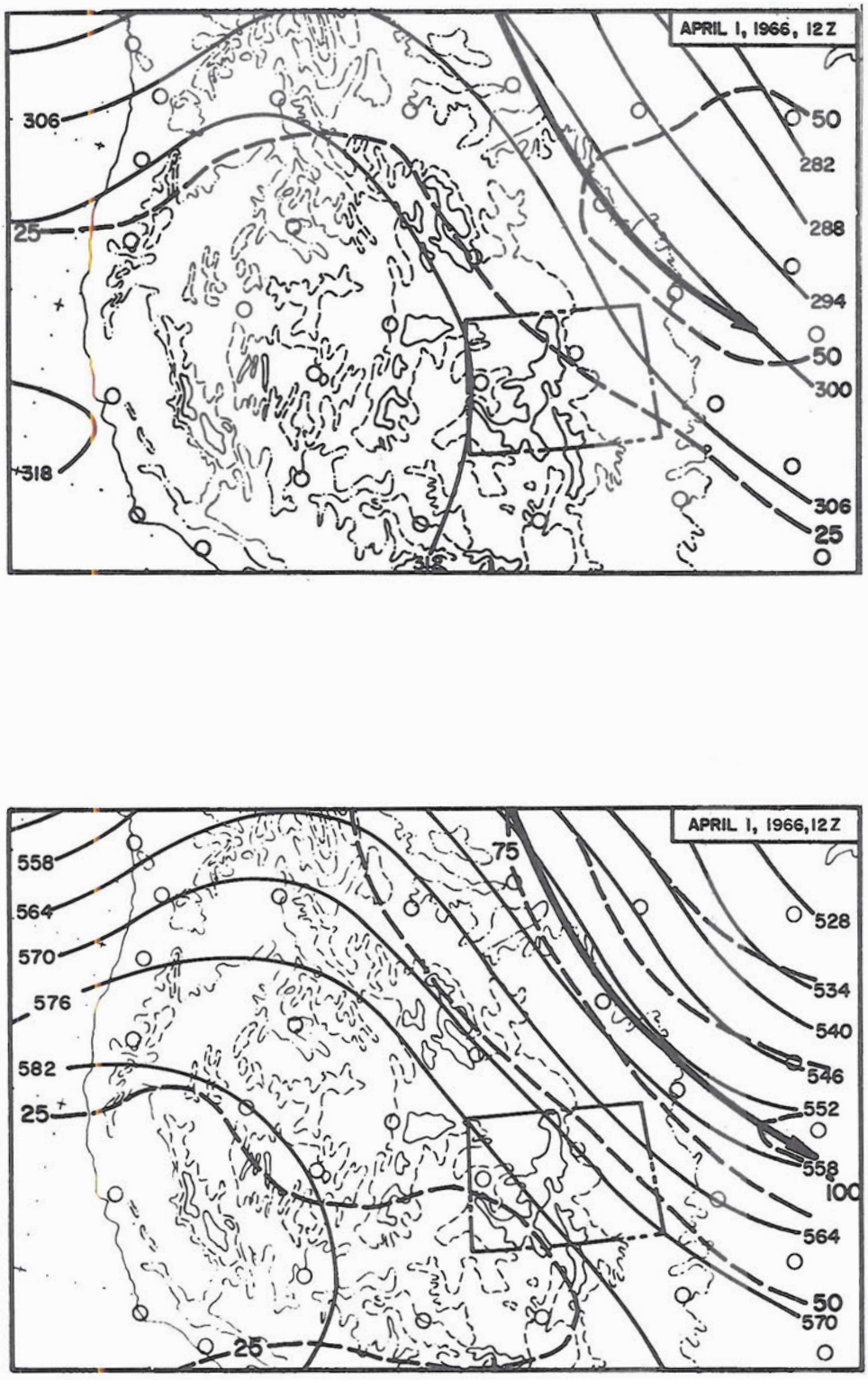

FIG. 21. 700 mb (upper) and 500 mb (lower) charts for 12Z, April 1, 1966.

Most of the cirrus clouds were too thin to show up well in the satellite photograph taken at 2026Z and shown in Fig. 19. The denser cloud formations over Fort Collins and 100 miles to the north seem to have a wavelength of about 35 km which is in agreement with the constant level balloon trajectory and the wavelength computations for the 489 mb interface shown in Table 10 (Chapter V).

A broad complex surface low pressure system covered the Rocky Mountain Region on April 16, 1966. The deepest low center of 1009 mb was near Fort Collins and a nearly stationary front was located just to the north of the Fort Collins area. There was a ridge of high pressure over the eastern Pacific. The winds aloft over eastern Colorado were west northwesterly 20 to 25 knots at 700 and 500 mb (see Figs. 23 and 24) while the surface winds were light and variable. There was a scattered to broken cumulus cloud layer at about 11000 ft msl and scattered to broken lee wave clouds at 18000 ft msl with higher cirrus above.

There were no rawinsonde or constant level balloon observations taken at Fort Collins on this date but the 1200Z Denver sounding indicated was a very stable layer at 515 mb on which lee waves of 5.6 km wavelengths could form (see Table 10, Chapter V).

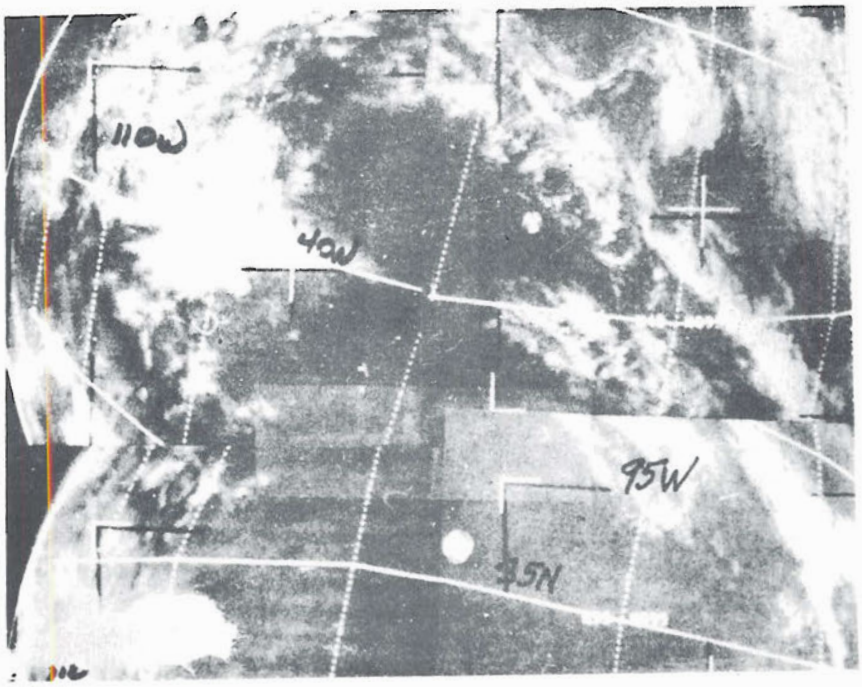

FIG. 22. Satellite photograph taken at 1959Z, April 16, 1966 over the western U.S.

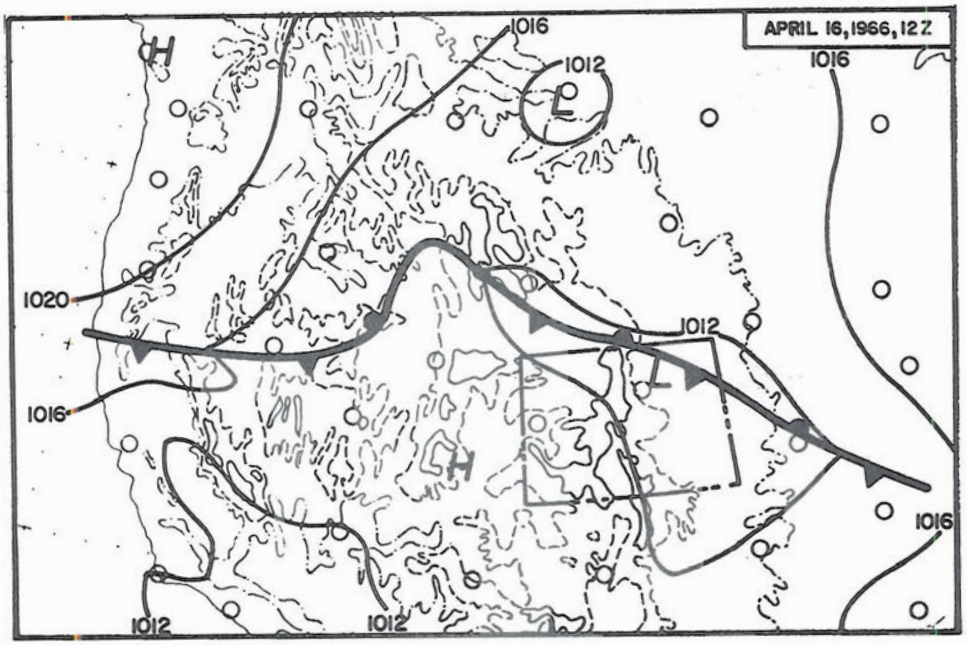

FIG. 23. Surface chart for 12Z, April 16, 1966.

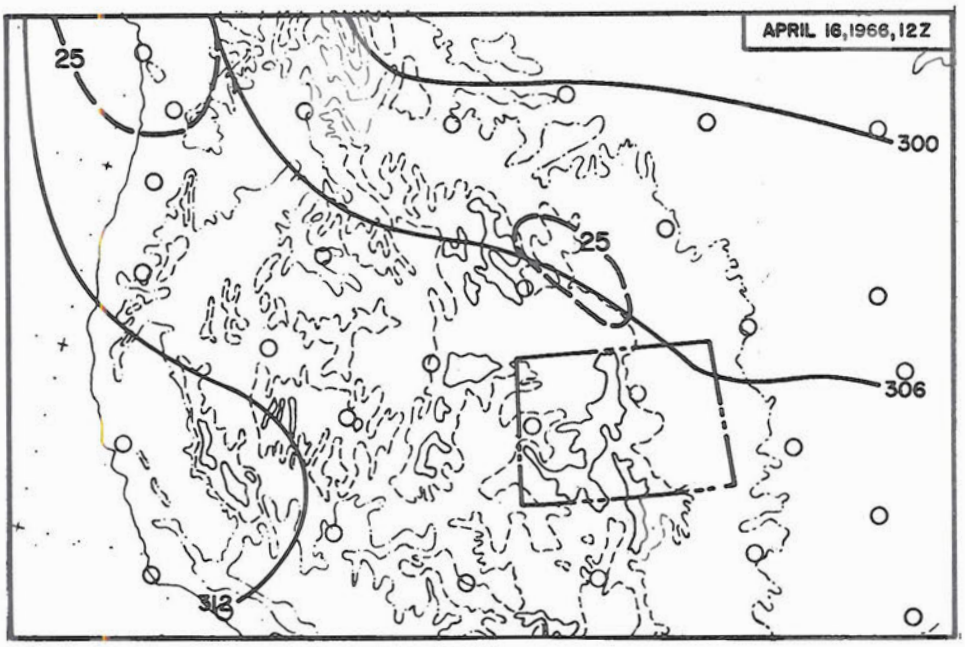

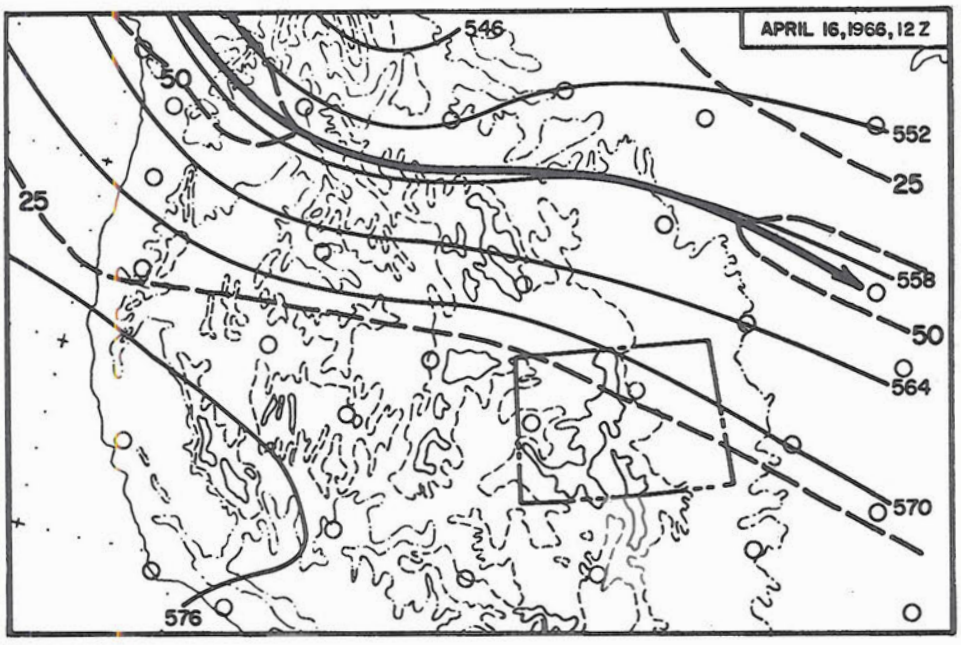

FIG. 24. 700 mb (upper) and 500 mb (lower) charts for 12Z, April 16, 1966.

The various broken cloud layers appeared as a solid sheet of cloudiness over northeastern Colorado when photographed by satellite at 1959Z (see Fig. 22). Therefore, it was not possible to determine the lee wavelengths from clouds observed in this photograph.

Photogrammetric cloud measurements between 1718Z and 1726Z showed that there were several lenticular cloud layers 20 km to the north northwest of the camera sites which were oriented north northeast to south southwest and were normal to the flow aloft at their levels. In one of the waves there were two layers of lenticulars ranging from 19,000 ft msl to 31,000 ft msl in altitude. The dimensions of the largest clouds were 3.5 km along the direction of flow and 9 km normal to it.

Upstream to the west northwest of these clouds, other lenticulars of smaller dimensions were observed at a single level. The lee wavelength, as determined from the lenticular pattern in the photographs, was 4.5 km, which was reasonably close to the computed theoretical lee wavelength of 5.6 km for the very strong interface at 516 mb in the 1200Z Denver rawinsonde, the only upper air data available on this day. These clouds remained nearly stationary during the period of observation. It was not possible to deduce vertical motions in these clouds since the observed cloud pattern displayed little, if any,

movement, and the vertical dimensions of the clouds could not be determined with certainty.

Other lenticular clouds located 26 km to the west of the camera sites were photographed at 1810Z. They were also oriented north northeast to south southwest and appeared to be in the same wave crest as the clouds to the north northwest of the camera sites. Lower level cumulus had formed in the intervening hour between cloud pictures and at 1810Z it was not possible to observe the clouds to the north northwest. Moments later the second set of lenticular clouds to the west was obscured by developing cumulus.

The lee wave clouds to the west were in two layers, similar to those to the north northwest. The base of the lower layer was 16,000 ft msl and the tops of the upper cloud layer were 26,000 ft msl. They were 25 km to the south southwest of the lenticulars that were observed at 1726Z. The cloud dimensions were 4.5 km along the direction of flow and 25 km normal to the flow. No other lee wave clouds were observed to the west, so no wavelength calculation in that region was possible.

Fig. 25 shows the picture frames taken at 1726Z, with a view towards the northwest. Fig. 26 shows the coordinate positions in the xz plane of the cloud features in these photographs. This plane is oriented very nearly along the direction

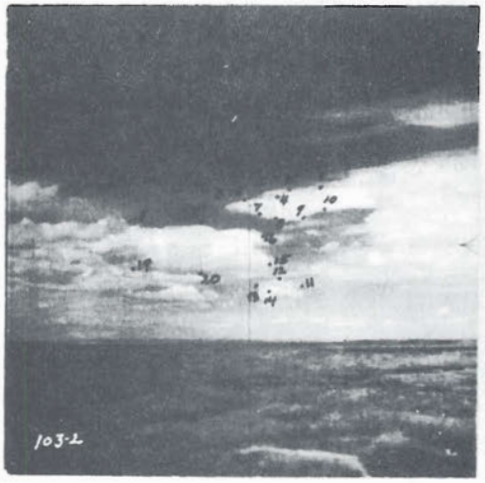

FIG. 25. Cloud photographs taken at 1726Z on April 16, 1966 with a view towards the northwest. The camera sites were located 12 miles east northeast of Fort Collins, Colorado.

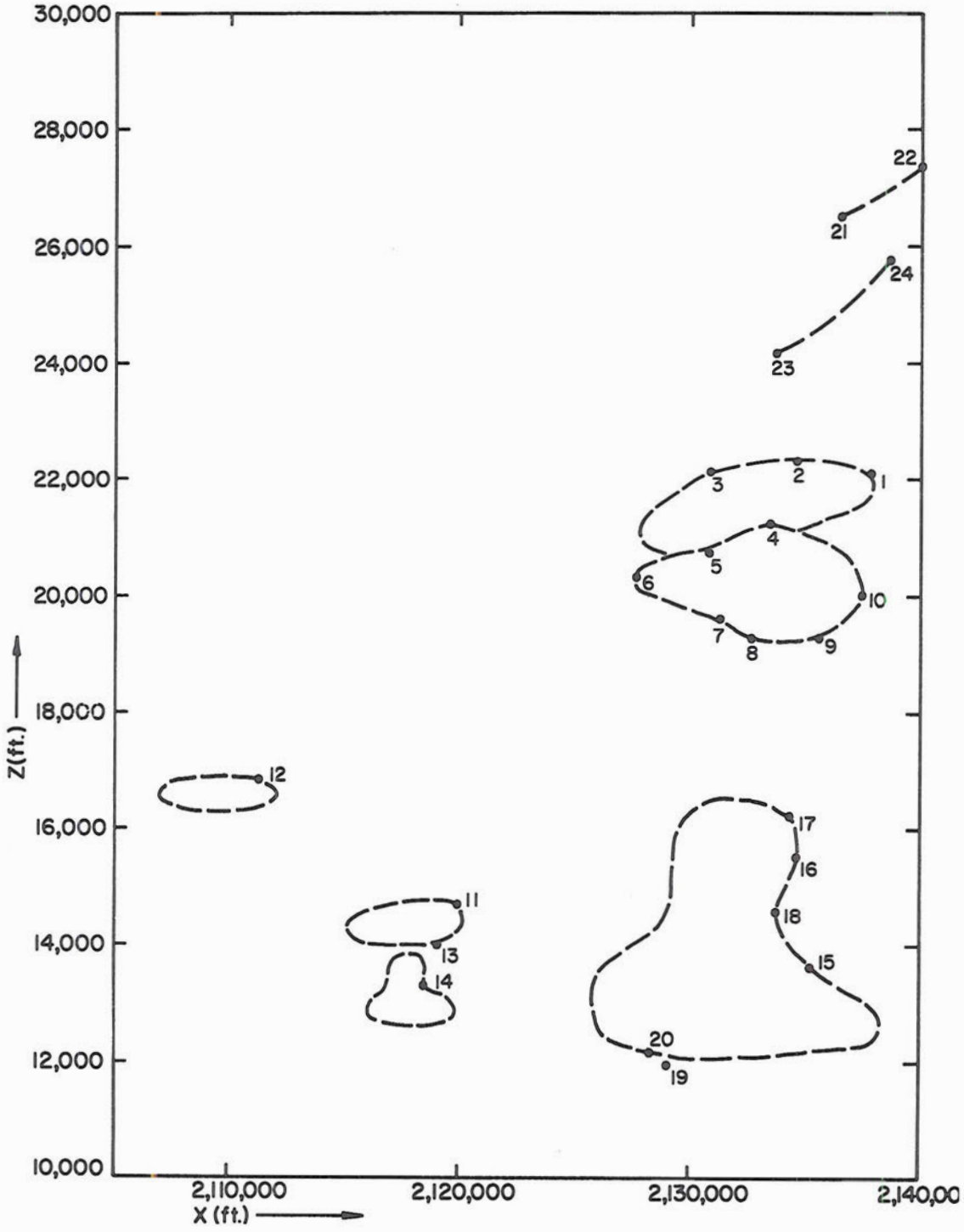

FIG 26. The coordinate positions in the xz plane of the cloud features numbered in Fig. 25 (Photograph taken at 1726Z, April 16, 1966). The probable shapes of the clouds are indicated by dashed lines. The vertical scale is exaggerated by a factor of 2.5.

of flow aloft. Note that the cumuli seem to form under the lee wave crests.

A very intense high pressure cell was located over south central Canada on May 11, 1966, while a deepening low system over the Central Plains was moving slowly east northeastward. In addition there was a strong cold front through northern New Mexico and the Texas Panhandle, pushing slowly southward, while low level flow was easterly and very strong over eastern Colorado. There were westerly winds near 25 knots at 700 mb and 500 mb (see Figs. 28 and 29) over northeastern Colorado. Surface winds in the Fort Collins area were northeasterly 35 knots with gusts to 60 knots during the late morning hours.

Scattered to broken cloud layers prevailed near 10,000 ft msl and 20,000 ft msl, with higher broken to overcast cirrus layers above. Photogrammetry measurements of the clouds were not taken on this date and high surface winds which developed during the late morning forced the cancellation of radar balloon tracking because the resulting antenna movement caused target loss. However, a Fort Collins rawinsonde was obtained at 1400Z, before the winds increased to high values.

The numerous cloud layers in the Fort Collins-Denver area made it difficult to define the lee wave clouds in the satellite photograph shown in Fig. 27 taken at 2021Z. However, there is an indication of waves with a wavelength of about 10 km

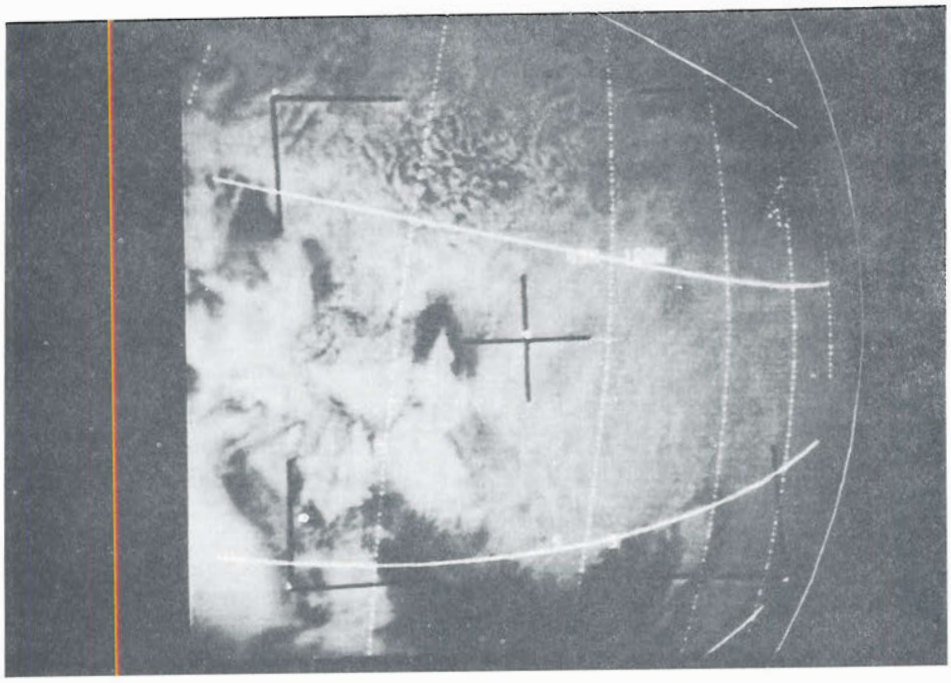

FIG. 27. Satellite photograph taken at 2021Z, May 11, 1966.

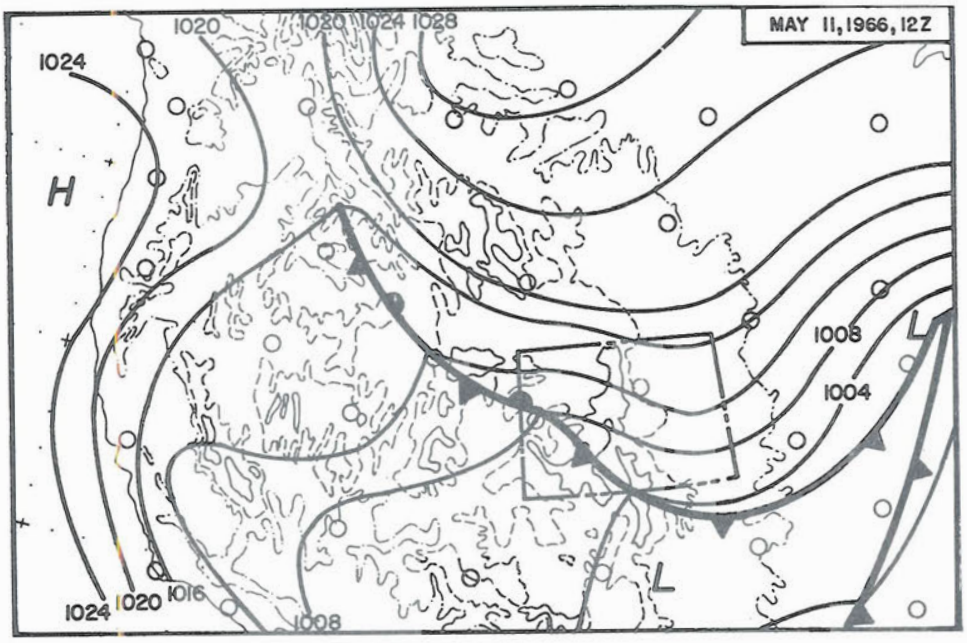

FIG. 28. Surface chart for 12Z, May 11, 1966.

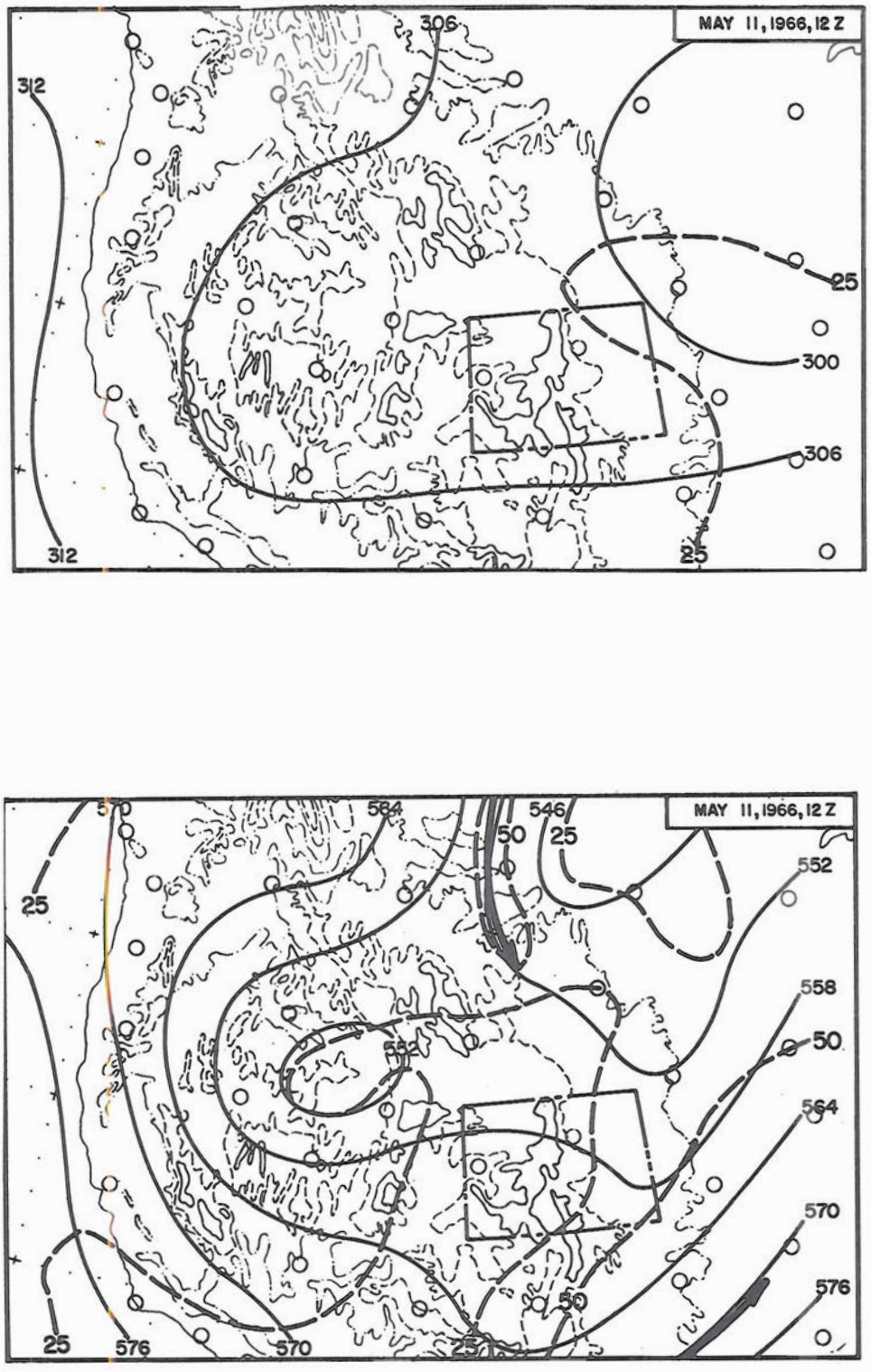

FIG. 29. 700 mb (upper) and 500 mb (lower) charts for 12Z May 11, 1966.

on the northern edge of a large break in the cloudiness to the east of Fort Collins. This agrees reasonably well with the computed wavelength of 8.4 km at 554 mb over Fort Collins shown in Table 10.

On May 13, 1966, the surface weather pattern over the Rockies was very complex with small high pressure cells over Colorado and Arizona and low pressure centers over Utah and near the Montana-Wyoming border. The flow aloft was westerly 25 knots at 700 mb and 40 knots at 500 mb (see Figs. 31 and 32). Surface winds were west to southwest 5 to 10 knots with scattered to broken cloud layers at 12,000 ft msl and 22,000 ft msl. Altocumulus lenticularis were visible from all reporting stations in the area.

Two of the constant level balloons released during the morning were lost in cumulus and the third failed to separate properly from the launch balloon. Rapid cumulus development during the late morning, accompanied by virga, forced the abandonment of any further constant-level balloon measurements.

Run one at 1532Z as well as the run at 1715Z show perturbations in the $\underline{w}$ component of the wind of wavelengths of about 5 km. This agrees quite well with the dominant wavelength computed to be 4.8 km from the Fort Collins rawinsonde data (shown in Table 10).

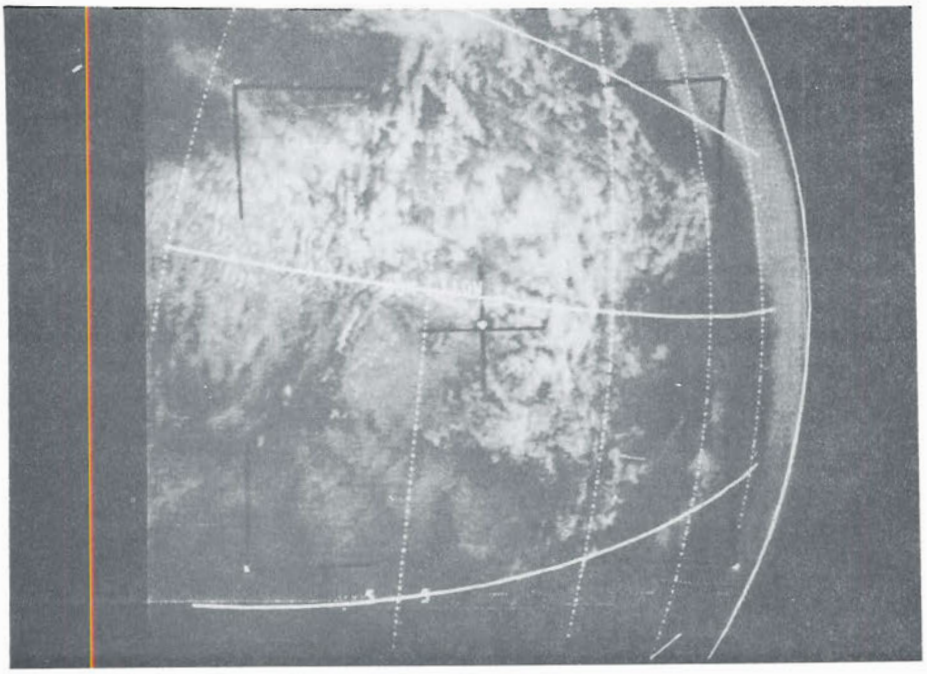

FIG. 30. Satellite photograph taken at 2051Z, May 13, 1966.

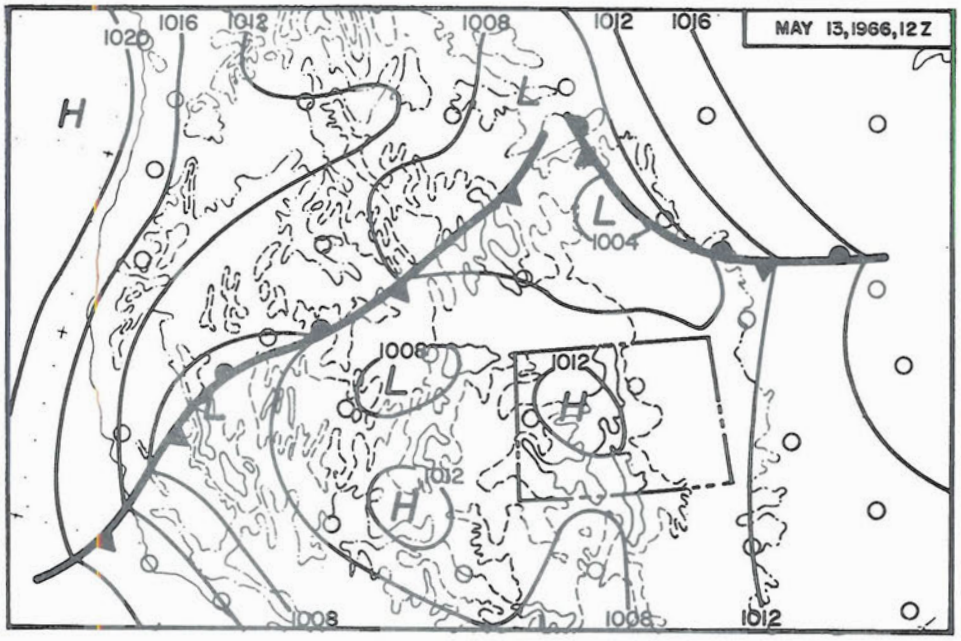

FIG. 31. Surface chart for 12Z, May 13, 1966.

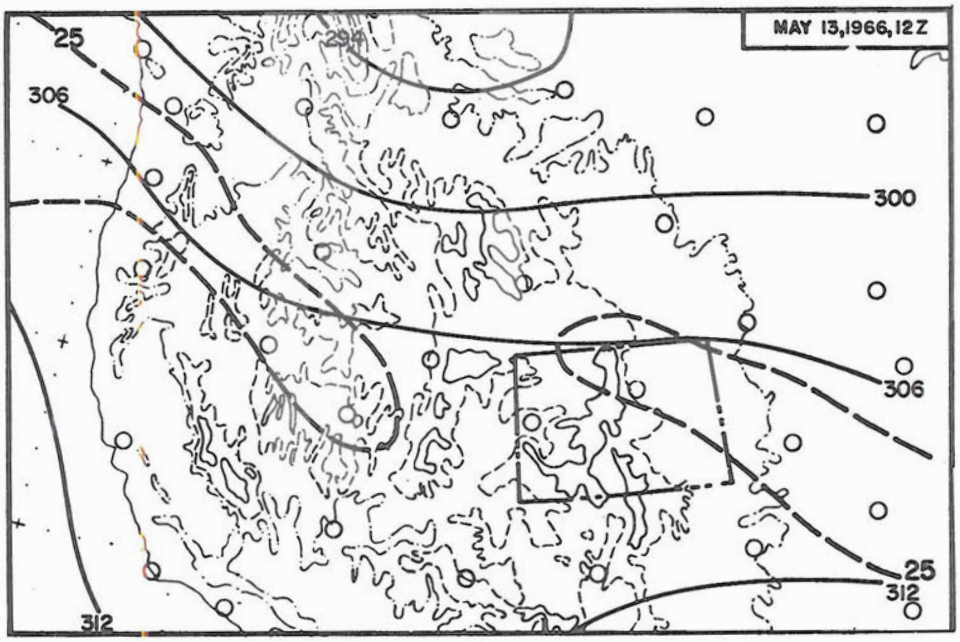

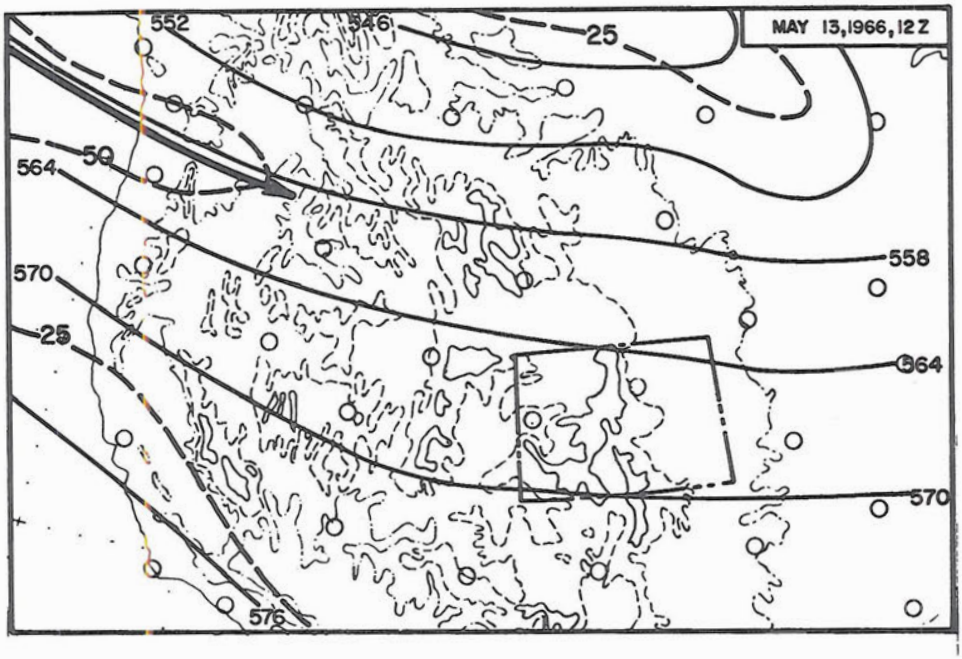

FIG. 32. 700 mb (upper) and 500 mb (lower) charts for 12Z, May 13, 1966.

The angle at which the satellite picture (2051Z) in Fig. 30 was taken and the numerous cloud layers make it difficult to determine the lee wavelength in the Fort Collins-Denver area, but it appears to be on the order of 10 km. There is a clear display of lee wave clouds over eastern Utah with wavelengths of about 10 km. This same wavelength dimension is also visible in the cloud structures over southeastern Colorado.

Between 1144Z and 1226Z lee wave clouds to the south southwest of Fort Collins were observed photogrammetrically. The northernmost portions of these clouds were 30 km to the southwest of the camera sites. The clouds were oriented north to south, normal to the flow, with dimensions of 43 km at right angles to the flow and 8 km along the flow. The lenticulars consisted of two stacked layers at approximately 15,000 ft msl and 26,000 ft msl and they remained quasi-stationary.

Several pictures taken during this period were analyzed. Although the dimensions of the lower cloud remained virtually unchanged with time, its overall appearance varied from thin and wispy to very dense, probably indicating an influx of moisture. The upper cloud changed little in appearance but measurements indicated that the altitude of the cloud top varied between 25,000 ft msl and 27,000 ft msl. No lee wavelength calculations were possible since no other lenticulars were observed. There could however, have been other lee wave clouds to the east of those

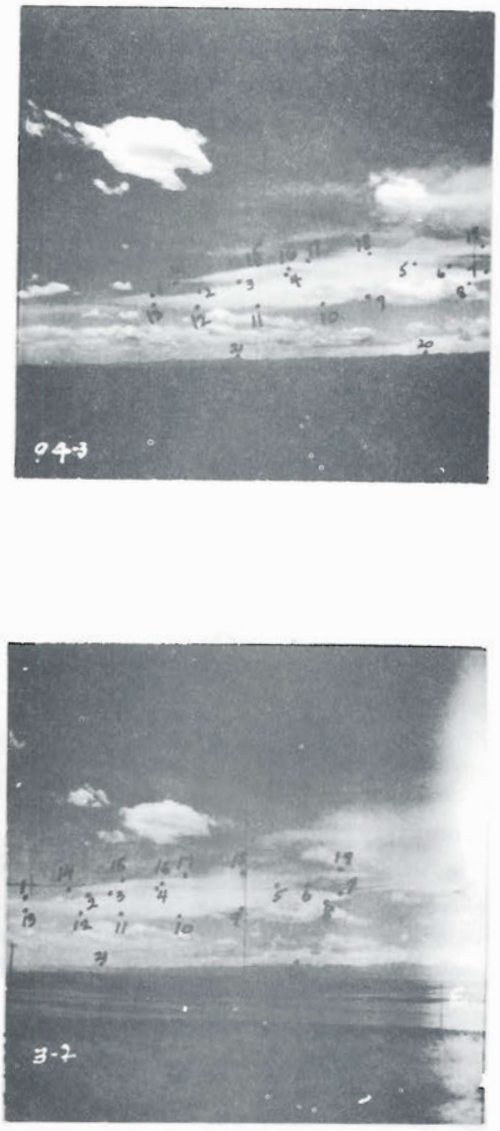

FIG. 33. Cloud photographs taken at 1926Z on May 13, 1966 with a view towards the south southwest. The camera sites were located 12 miles east northeast of Fort Collins, Colorado.

photographed but a cumulus layer prevented their observation. Fig. 33 is a photograph of the lenticulars taken at 1962Z with a view towards the south southwest.

The surface low pressure system over Wyoming and Montana on May 13, 1966, had developed into a deepening cyclone centered over western South Dakota by May 14, 1966. A cold front extending southwestward from this low was pushing into northwestern Colorado. A fairly deep trough of low pressure aloft was over the Pacific States and the flow aloft over eastern Colorado was west to west southwest 25 knots at 700 mb and 45 knots at 500 mb (see Figs. 35 and 36). The surface wind in the Fort Collins area was southerly 10 to 15 knots. There were scattered to broken cloud layers at 12,000 ft msl and 20,000 ft msl with higher cirrus layers above.

There were no photogrammetric cloud measurements taken, but during the day seven constant level balloon releases were made, of which two were terminated due to radar failure, two did not separate from the launch balloons, one was lost in radar ground clutter, one was lost in a cloud, and the other was lost for unknown reasons before reaching altitude.

Release five, made at 2147Z (see appendices), did not reach its programmed altitude of 20,000 ft msl but seemed to level off at about 7500 ft msl. It was tracked about 50 km before it was lost in ground clutter. The track shown in the appendices

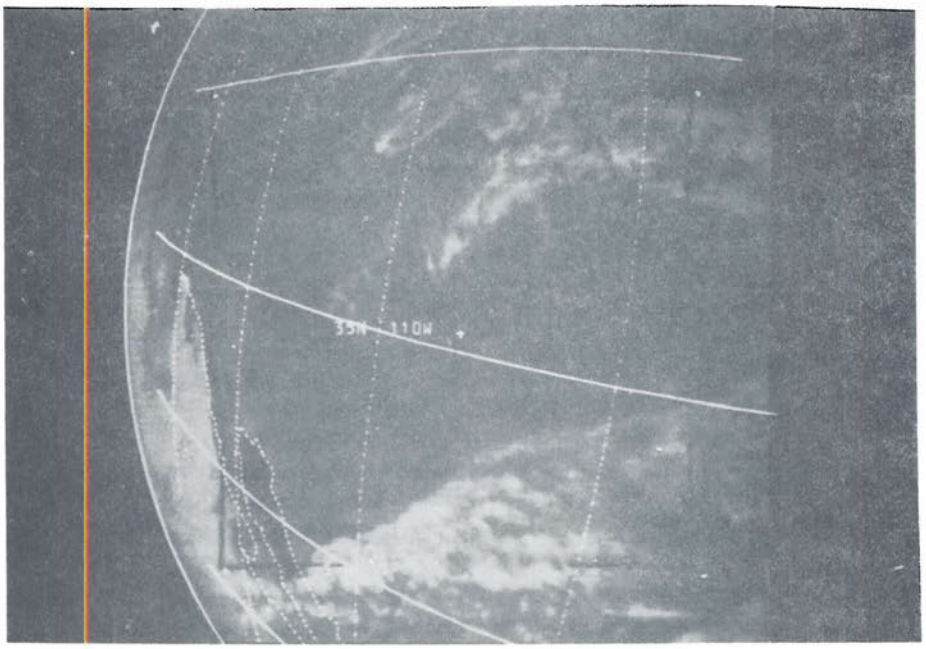

FIG. 34. Satellite photograph taken at 2026Z, May 14, 1966.

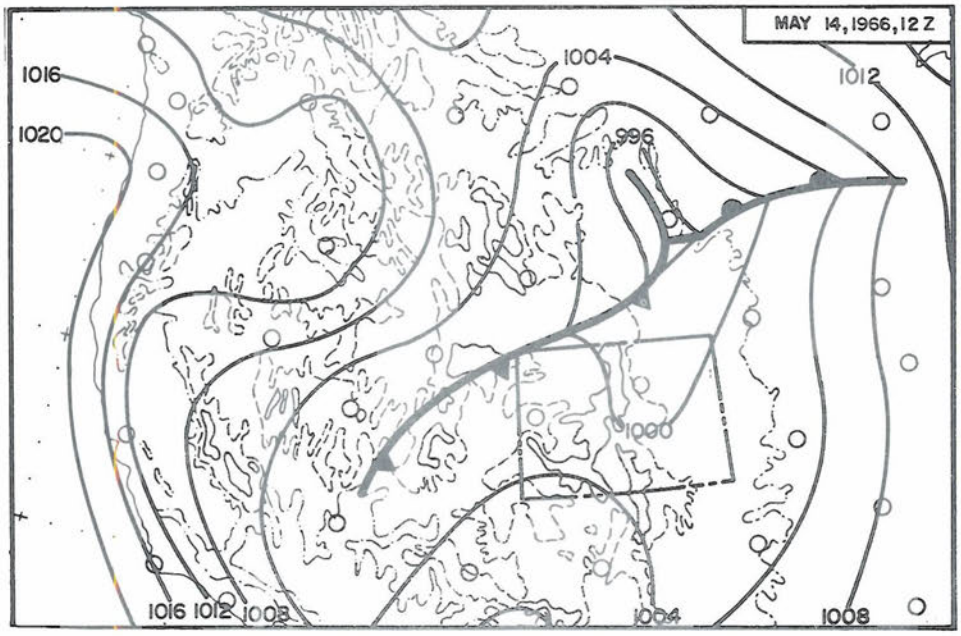

FIG. 35. Surface chart for 12Z, May 14, 1966.

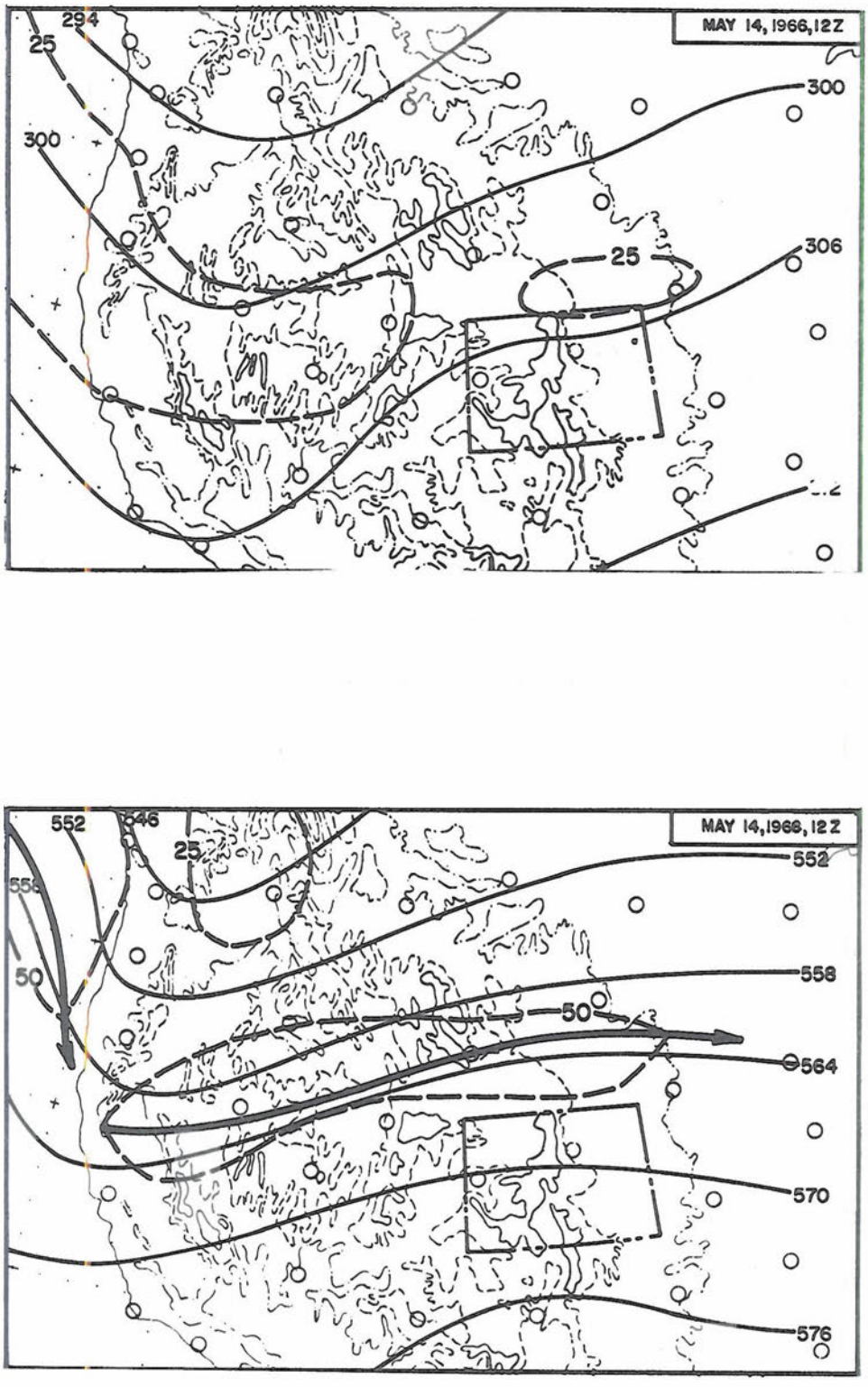

FIG. 36. 700 mb (upper) and 500 mb (lower) charts for 12Z, May 14, 1966.

CHAPTER IV

TECHNIQUES FOR PREDICTING CLEAR AIR TURBULENCE FROM LEE WAVES

Observational Evidence Connecting CAT and Lee Waves

We have seen in Chapter II that CAT has a statistical maximum frequency to the lee of major mountain ridges. In Chapter III evidence is given to lead to the hypothesis that mountain lee waves could be a cause of these CAT maxima. Observations of known lee wave cases will now be presented to show that in these specific instances CAT occurs rather frequently. These cases are identical to those used at the conclusion of Chapter III in connection with lee wave theory. The cloud areas that are depicted by shading in the figures to follow are based upon information contained in pilot reports, rawinsonde data, surface cloud reports, and satellite pictures. Computations [based upon the theoretical work of Scorer (1949) and Wallington (1956)] of lee wavelengths and the maximum vertical velocities in the lee waves are shown at the principal lapse rate discontinuities included in the cross sections. All pilot reports of turbulence occurring within 90 miles of the cross-sectional planes are also entered at their respective altitudes.

Two cross sections (not shown) were chosen for each of the three cases on January 7 and 24, and March 1, 1966; one

across the Appalachians in Pennsylvania, and one across the same mountain range in Virginia. In all three cases the rawinsonde observation showed that there were stable layers present in the atmosphere upon which gravity waves could form. The wavelengths and maximum vertical motions computed on these three dates are given in Tables 12 and 13 (Chapter V) and the special pilot reports collected from these areas are included in Tables 8 and 9. On January 7, 1966, the turbulence reports above the surface friction layer indicated light or no turbulence was experienced, however, there was one light to moderate report of turbulence at 30,000 ft msl. On January 24 and March 1, all pilot reports above the friction layer stated "light" or "no" turbulence.

The cross-sections for 0000Z, February 15, 1966, (Fig. 37) show that there were two very stable layers, one near 700 mb and the other near 500 mb. The topography is entered on the cross-sections (Fig. 37). There were no reports of turbulence greater than light within 90 miles of the cross-sections above the layer where mechanical turbulence was dominant. This layer was quite deep since the wind just above thesurface of the earth was more than 30 knots. Theoretical computations (entered in Fig. 37) of maximum vertical velocities in lee waved indicated that the lee waves, although plainly visible in the photograph shown in Fig. 6, had vertical velocities

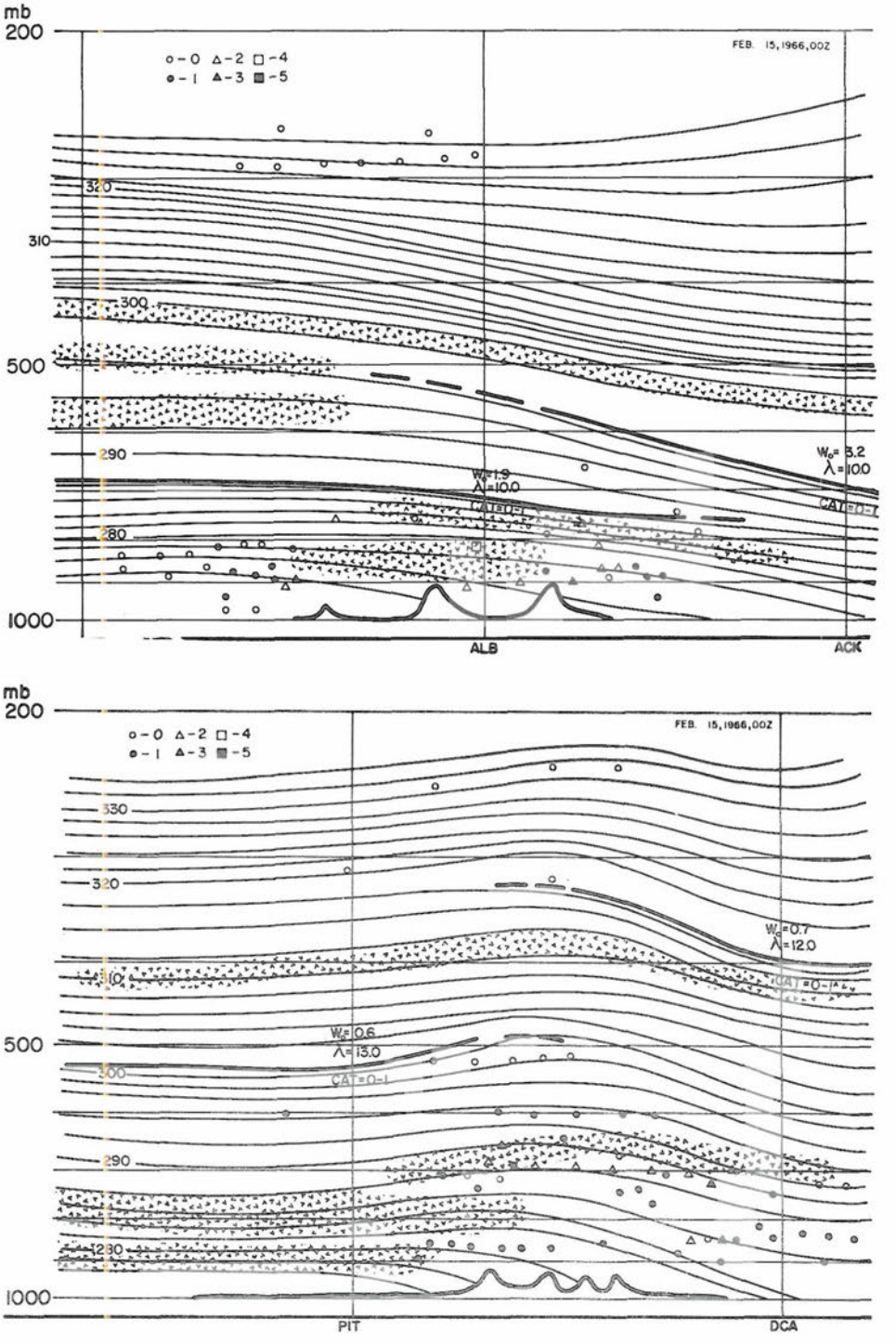

FIG. 37. Cross sections for 00Z, February 15, 1966 through New York and the southern New England States(upper) and through Pennsylvania and Maryland(lower). Cloud zones(shaded), density interfaces(heavy solid), and lines of potential temperature(deg.K) are included. The computed maximum lee wave vertical velocities, lee wavelengths, and resultant CAT forecasts are shown. Pilot reports are entered(N=0, L=1, L-M=2, M=3, M-S=4, S=5).

that were generally less than 1 m sec^{-1} except east of the Appalachian Range in New England where they were about 3 m sec^{-1}.

A cross-section for 0000Z, March 8, 1966, oriented with the 500 mb flow (see Fig. 11), from northern California to the eastern Colorado Rockies is shown in two parts in Fig. 38. In this case it appears that the lee wave clouds formed near the stable layer at about 15,000 ft msl. Cumulus clouds also seemed to form beneath the stable layer at about 10,000 ft msl. Such cloud formations have been noted (Booker 1962) in lee wave cases; however, cumulus formation is enhanced by the positive vertical motions in the lee wave crests and suppressed in the lee wave troughs. The cross-sectional surface projection is depicted on the surface chart in Fig. 10. Note that the Pacific front lies along the cross-section over eastern Nevada and western Utah. The topographical map indicates that the northern Sierras, the Ruby Mountains of eastern Nevada, the northern Wasatch Range, the Uinta Mountains, and the Colorado Rockies have dimensions that might cause lee waves containing significant vertical velocities. Computations, based upon the methods already outlined (see Appendix B) and entered at the lapse rate discontinuity in Fig. 38, reveal that the vertical motions in the lee of Colorado mountains were near 5.0 m sec^{-1}. However,

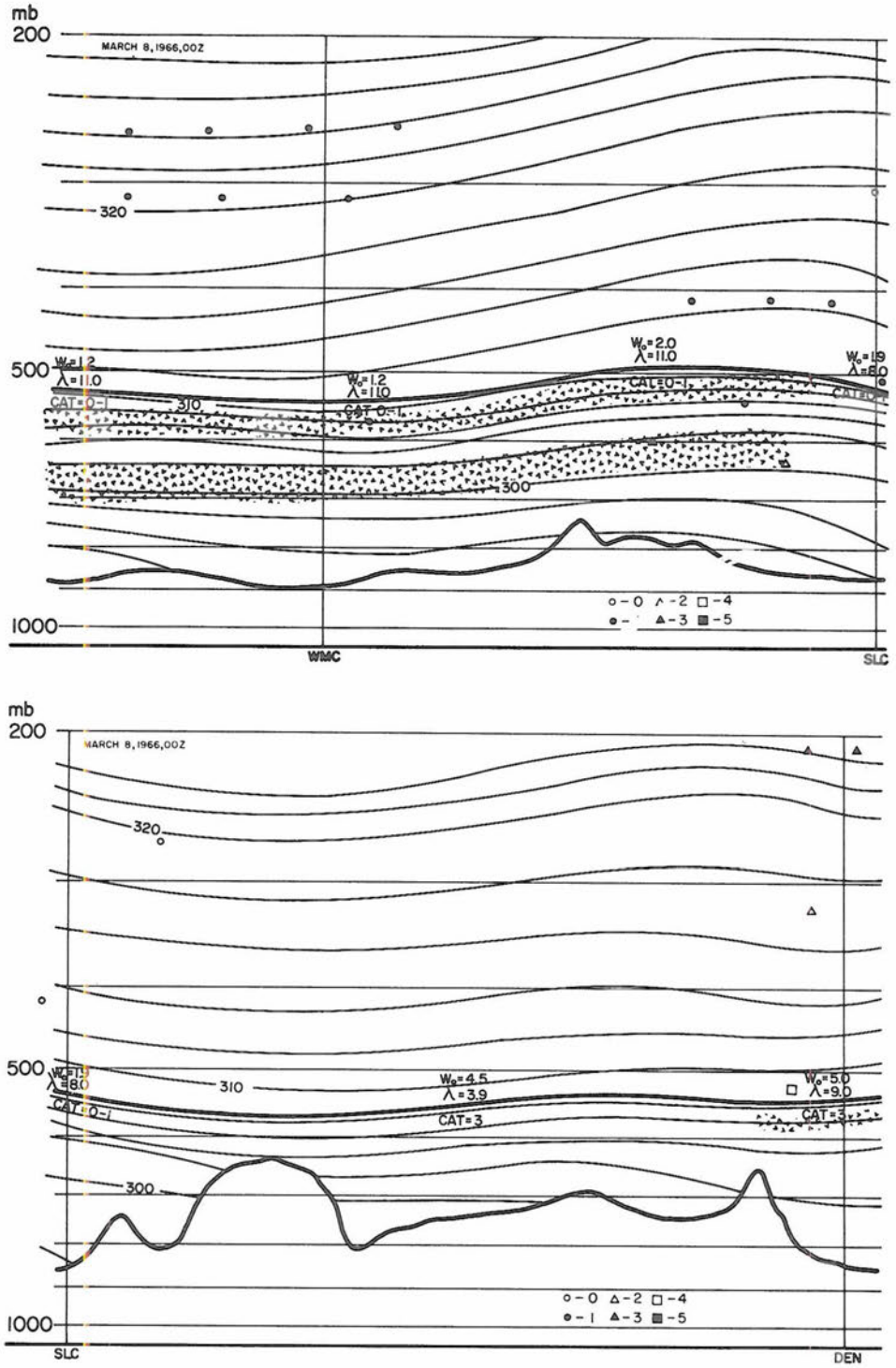

FIG. 38. Cross sections for 00Z, March 8, 1966 through Nevada and Utah(upper) and Utah and Colorado(lower). Cloud zones(shaded), density interfaces(heavy solid), and lines of potential temperature are included. The computed maximum vertical velocities and lee wavelengths of the lee waves and the resultant CAT forecasts are shown. Pilot reports are entered(N=0, L=1, L-M=2, M=3, M-S=4, S=5).

the vertical motions in the lee of the Wasatch, Ruby and Sierra Ranges were less than 2 m sec^{-1}.

Pilot report coverage in this case was quite good in the mountain lee wave area and to the lee of the Colorado Rockies. All planes in the lee wave cloud area over California, Nevada, and western Utah were asked to report clouds and turbulence, but only those experiencing some degree of turbulence greater than light reported over eastern Utah, Wyoming, and Colorado. It is interesting to note that no significant turbulence was reported in the area to the lee of the Sierras or the mountains of eastern Utah. One aircraft at 33,000 ft msl, just to the lee of the Sierras, reported little or no turbulence but had moderate wave action. In other words, the pilot noted the undulation of the long lee waves but experienced no significant bumpiness.

In the lee of the Ruby Mountains there were two reports of light to moderate turbulence near 12,000 ft msl that were not qualified as CAT because they were from an area of cumulus activity. Another aircraft in this area at 15,000 ft msl, just above the cumulus but below the lee wave clouds, experienced light turbulence. Others at higher levels where there were no clouds, so that any turbulence which was reported would qualify as CAT, experienced little or no turbulence. This might indicate the lessening influence of convective motions with height.

There were few clouds in the lee of the Rockies but moderate to severe turbulence was reported at about 16,000 ft msl, light to moderate turbulence was reported at 28,000 ft msl, and two cases of moderate turbulence were reported at 39,000 ft msl.

Cross-sections for 0000Z, March 10, 1966, through the Wyoming and Colorado lee wave cloud areas shown in Fig. 13 are given in Fig. 39, and the cross-sectional surface projections are depicted on the 0000Z, March, 1966, surface chart in Fig. 14. The cross-sections show a very stable layer between 500 and 600 mb on which lee waves could form. Lee waves formed at about 20,000 ft msl and cumulus beneath at about 12,000 ft msl. Special pilot reports of any degree of turbulence, including non-occurrence, were requested over these two routes. The only significant turbulence was reported as light to moderate at 12,000 ft msl in the lee of the Wind River Range in northwestern Wyoming, and a report of moderate turbulence at the same altitude that appears to be on the windward side of the highest Rockies of Colorado (see Fig. 39). This particular report is misleading since it occurred some 70 miles north of the cross-section and to the lee of the Continental Divide. In that area the terrain of the Rockies is greatly different from the mean topography depicted on the cross-section in Fig. 39. Vertical motion computations (entered in the cross-sections in Fig. 39) show that lee wave vertical velocities were 3 to 4 m

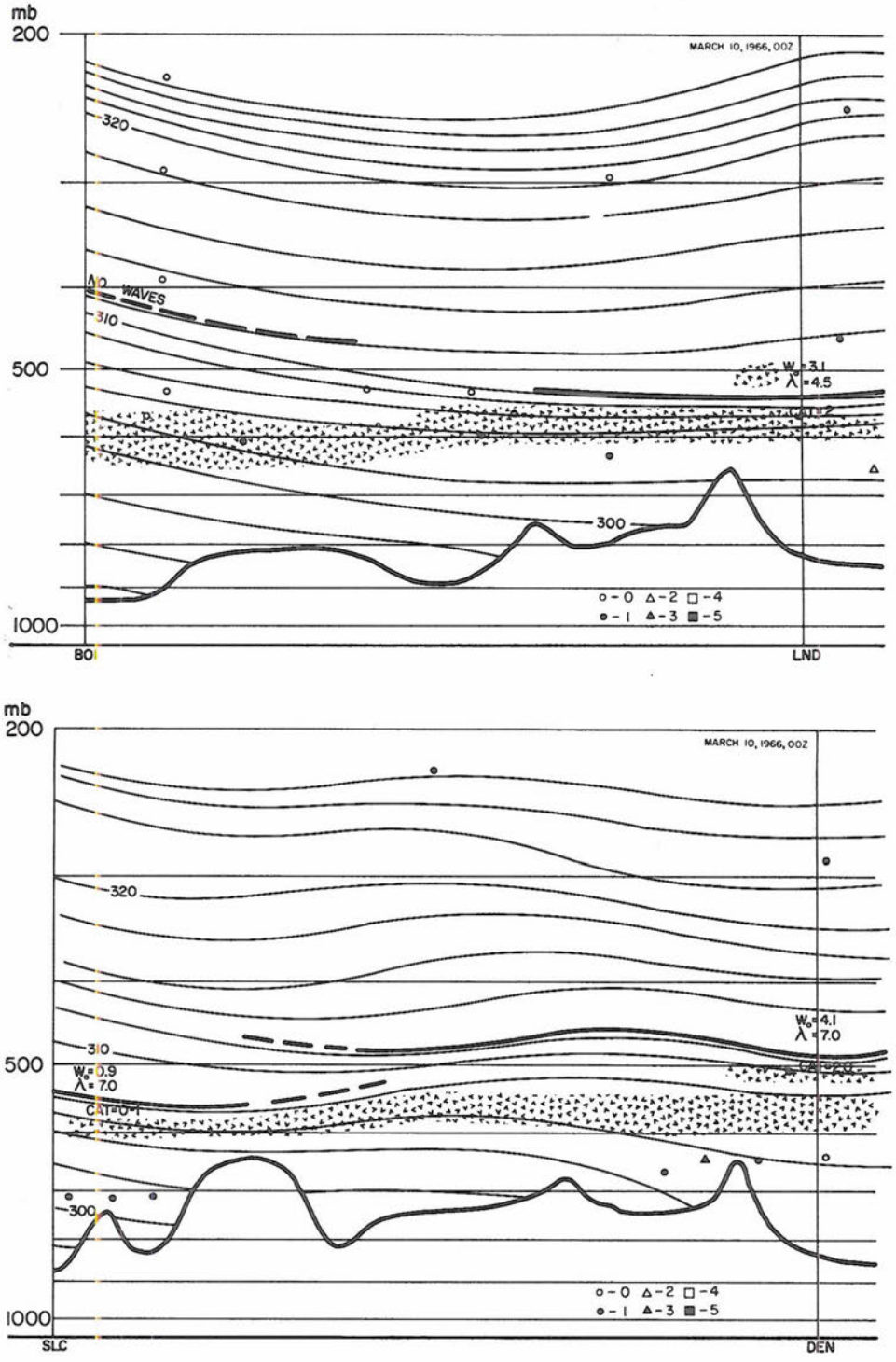

FIG. 39. Cross sections for 00Z, March 10, 1966 through Idaho and Wyoming(upper) and Utah and Colorado(lower. Cloud zones(shaded, density interfaces(heavy solid), and lines of potential temperature are included. Computed maximum lee wave vertical velocities, lee wavelengths, and resultant CAT forecasts are shown. Pilot reports are entered(N=0, L=1, L-M=2, M=3, M-S=4, S=5).

sec^{-1} in the lee of the Colorado Rockies and the Wind River Range, and less than 1 m sec^{-1} in the lee of the northern Wasatch Mountains of eastern Utah.

Vertical motion in the lee waves on April 26, 1966, was computed (see Fig. 40) to be about 4 m sec^{-1} near Salt Lake City and less than 1 m sec^{-1} near Lander and Ely. The pilot reports entered on the cross-sections in Fig. 40 show numerous instances of light to moderate turbulence near Salt Lake City and generally light or no turbulence elsewhere. A few reports of moderate turbulence were made near Ely, but the aircraft were in or near cumulus at the time of the occurrences.

The aircraft turbulence reports and the computed maximum lee wave vertical velocities for the field measurement program cases on April 1 and 16 and May 11, 13, and 14, 1966, are given in Tables 10 and 11. Computations involving the Fort Collins rawinsonde use the mean topographical values for the Colorado Rockies (see Appendix B).

Theoretical Basis for Prediction Techniques

The statistical study in Chapter II and the specific cases discussed above point to a possible connection between CAT and mountain lee waves. We have seen that some of the important parameters which should be considered when investigating either CAT or lee waves are terrain features, the wind velocity and shear, and the thermal stability of the atmosphere. Since a

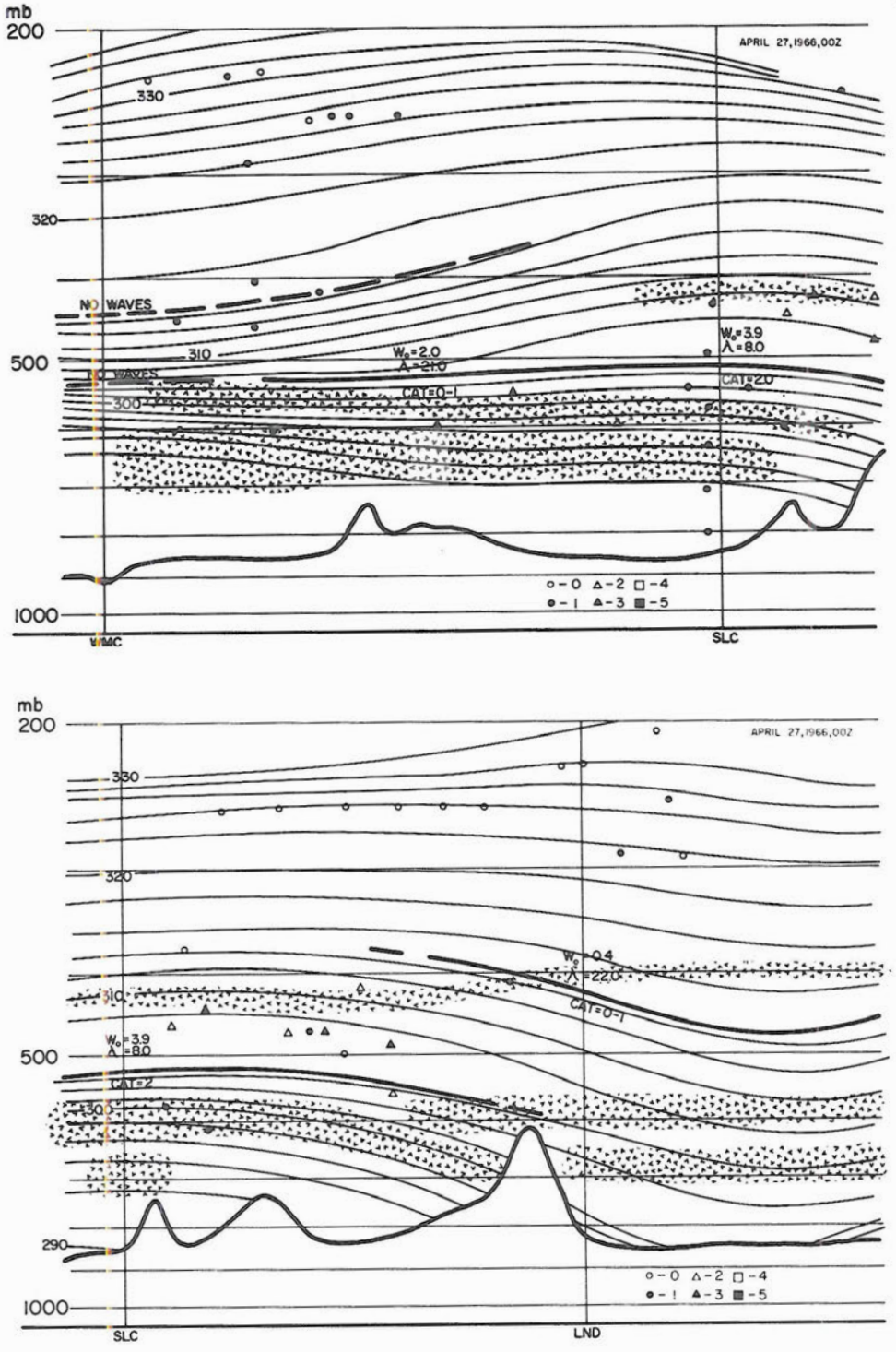

FIG. 40. Cross sections for 00Z, April 27, 1966 through Nevada and Utah(upper) and Utah and Wyoming(lower). Cloud zones(shaded), density interfaces(heavy solid), and lines of potential temperature are included. Computed lee wave maximum vertical velocities, lee wavelengths, and resultant CAT forecasts are shown. Pilot reports are entered(N=0, L=1, L-M=2, M=3, M-S=4, S=5).

mountain lee wave is a special form of gravity wave, this supports the hypothesis made by Reiter (Reiter and Hayman 1962, Reiter 1963b, 1965), who has proposed that CAT has its origin in gravity waves produced by a shearing current on surfaces of temperature lapse rate discontinuity.

The regions of CAT are spotty and of various sizes and shapes (Beckwith 1964, Endlich 1963). They are usually on the order of ten miles in the crosswind direction and much longer along the direction of flow and may vary in vertical dimensions from a very shallow layer to one several thousands of feet thick. The direction of flight and the flight speed have a direct bearing on the duration and degree of turbulence experienced by the aircraft. As a rule, the greater the intensity of turbulence, the larger is the turbulent area and the longer its duration. This pattern might lead one to believe that air parcels, passing through areas where turbulence is generated in the mesoscale, move downstream as the turbulence gradually decays into microscale eddies. The generating regions would move slowly if synoptically controlled or would be stationary in the case of mountain waves.

In this section a procedure for forecasting CAT related to mountain lee waves will be developed. If the major contribution to CAT wavelength energy in and near mountainous regions comes from lee waves, then a reliable forecast method

based upon lee wave mesoscale energies should be applicable to the frequent CAT incidences over rough terrain. These procedures will hold when lee wave clouds are observed, either by ground observer or by a satellite (the seven cases observed principally by satellite are in this category), and in cases where lee waves are present but the air is too dry to allow cloud formation in the wave crests (some of the field measurement program cases are in this category).

Fig. 41 and Table 3 (from Pinus et al. 1965) give instances of spectral measurements made by instrumented aircraft. From these measurements quantitative estimates of the microscale levels of energy required to cause CAT can be made. By use of the "-5/3 law" of turbulence theory an estimate can also be made of the necessary input energy level in the mesoscale that would cause these CAT energy levels in the microscale. These computations are shown in Fig. 42.

The "-5/3 law" has been observed to hold for wavelengths less than one-half kilometer (Reiter et al., 1965, Reiter and Burns 1965, 1966). It holds fairly well for the turbulent energy of $\underline{u}$ and $\underline{v}$ wind components in the one-half to six kilometer wavelength range after energy has been introduced at longer wavelengths. This may be the case with lee waves. Above six kilometer wavelengths we have no evidence to support the use of the -5/3 decay law. However, it is theorized that energy

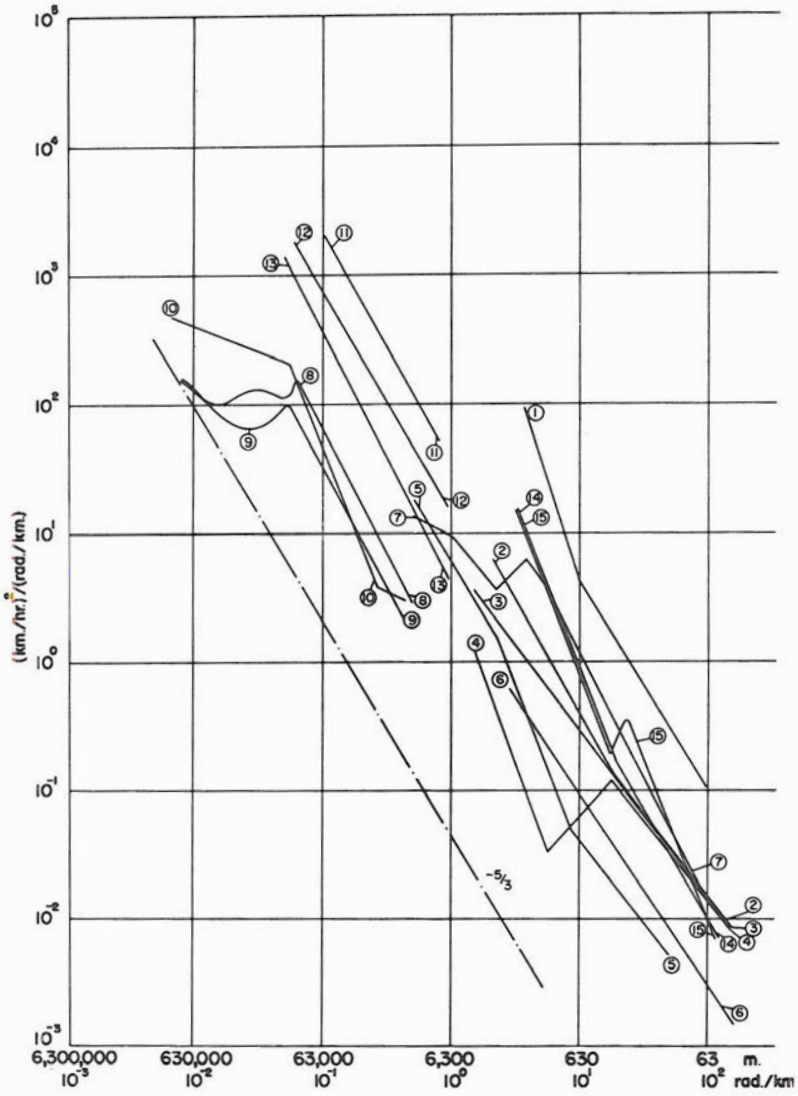

FIG. 41. Schematic presentation of spectral density, $(\frac{km}{hr})^2/\frac{rad}{km}$, as a function of wave number(cycles/km), or wavelength in meters, for turbulence in the free atmosphere. Data sources of spectra are identified in Table 3 (Pinus et al, 1966).

Table 3. Power Spectra of Turbulence in the Free Atmosphere (Pinus, et al., 1966).

Spectrum No.	Source	Characteristics (turbulence components given with respect to course of aricraft)
1	Shur, 1962	w-component, severe CAT, near jet stream level, stable stratification.
2	Reiter and Burns 1965	u, v-components, moderate CAT, jet stream level, stable stratification.
3	Reiter and Burns 1965	w-component, flight parallel to wind, moderate CAT, jet stream level, stable stratification.
4	Reiter and Burns 1965	w-component, flight nearly normal to wind, moderate CAT, jet stream level, stable stratification.
5	Vinnichenko, Pinus Shur, 1965	u-component, no CAT, near jet stream level, stable stratification.
6	Reiter and Burns 1965	u, v, w-components, light turbulence at 100 m altitude, unstable stratification.
7	Vinnichenko, Pinus Shur, 1965	u-component, light turbulence at 1000 m altitude, unstable stratification.
8	Kao and Woods 1964	u-component, at jet stream level, flight parallel to jet stream.
9	Kao and Woods 1964	v-component, at jet stream level, flight parallel to jet stream.
10	Kao and Woods 1964	u, v-components, at jet stream level, flight normal to jet stream.
11	Pinus, 1963	u-component, severe CAT, under core of jet stream, flight normal to jet stream.
12	Pinus, 1963	u-component, moderate CAT, under core of jet stream, flight normal to jet stream.
13	Pinus, 1963	u-component, light CAT, over core of jet stream, flight normal to jet stream.
14	Shur, 1962	w-component, moderate CAT, at jet stream level, stable stratification.
15	Shur, 1962	w-component, moderate CAT, at jet stream level, stable stratification.

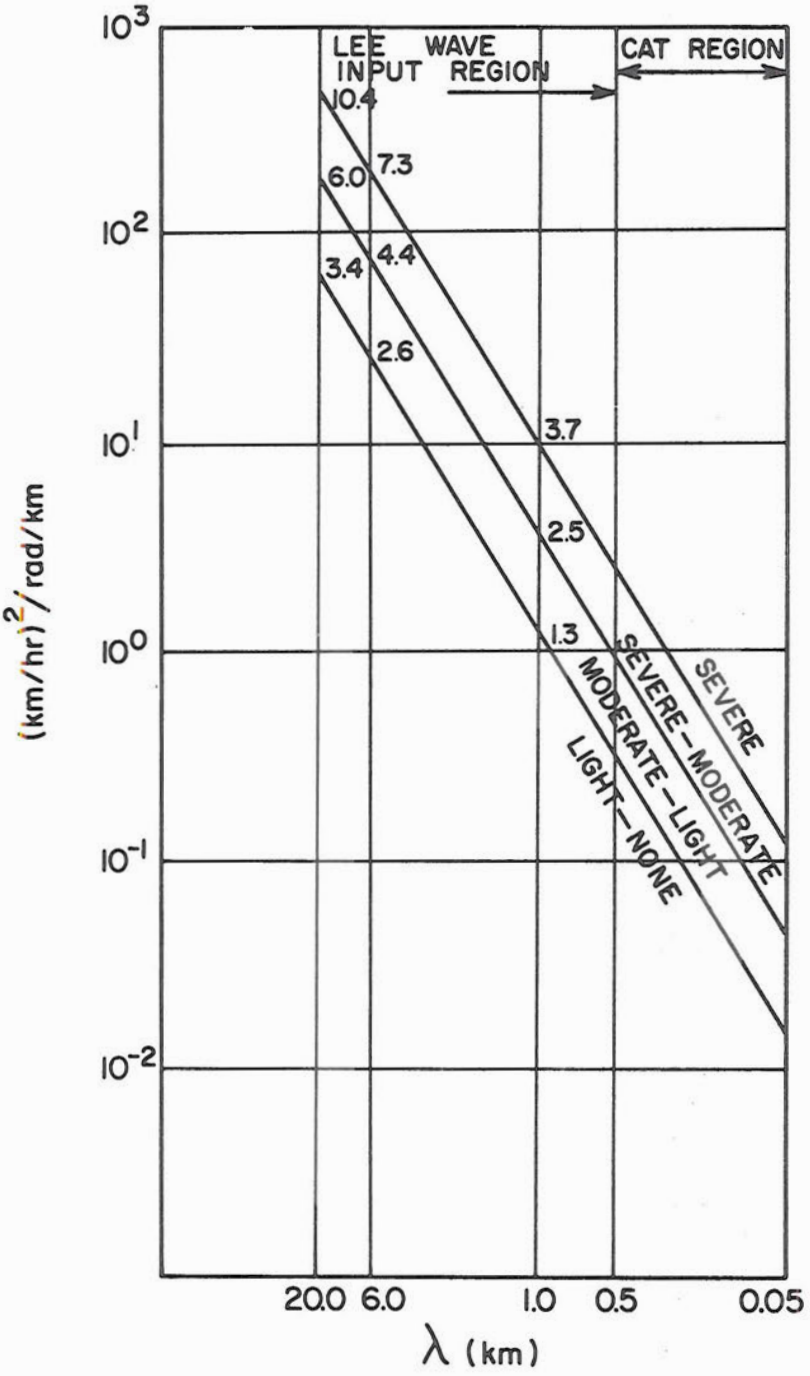

FIG. 42. Spectra of lee wave energy. The values entered on the spectral curves of -5/3 slope are the maximum vertical velocities contained in the lee waves(w_o in Eq. 25) in m sec^{-1} at the lee wavelength necessary to result in the level of energy(w component) in the CAT wavelength region to cause various degrees of CAT.

introduced at longer wavelengths probably decays at a slightly greater rate in the buoyant subrange. This subrange according to Bolgiano (1959, 1962) is just above the inertial subrange and the greater rate of decay is due to buoyant forces acting expecially on the w-component of the larger turbulent eddies.

The computed vertical velocity amplitude of lee waves, w_o, represents an energy input in the mesoscale. The procedures that might be followed in order to compute vertical velocities and the vertical component of kinetic energy in lee waves leading to CAT are outlined in Appendix B.

Assuming that a "-5/3" energy distribution exists in the whole spectrum range under consideration as indicated in Fig. 42, a plot of w_o against λ, the wavelength, would yield a forecast degree of CAT, which would occur when the energy-carrying eddies reach wavelengths of about 100 m. This has been done and Fig. 43 is the resultant forecast diagram. The lines in Fig. 43 separating the forecast categories represent the value of the energy necessary at each wavelength in order to result in various degrees of CAT after the energy provided in the mesoscale has been passed into the microscale (Fig. 42).

As a rough estimate, the vertical component of kinetic energy in lee waves was assumed to be introduced over a very narrow bandwidth in the spectrum and to have decayed following the "-5/3 law". Any forecast criterion developed on the basis

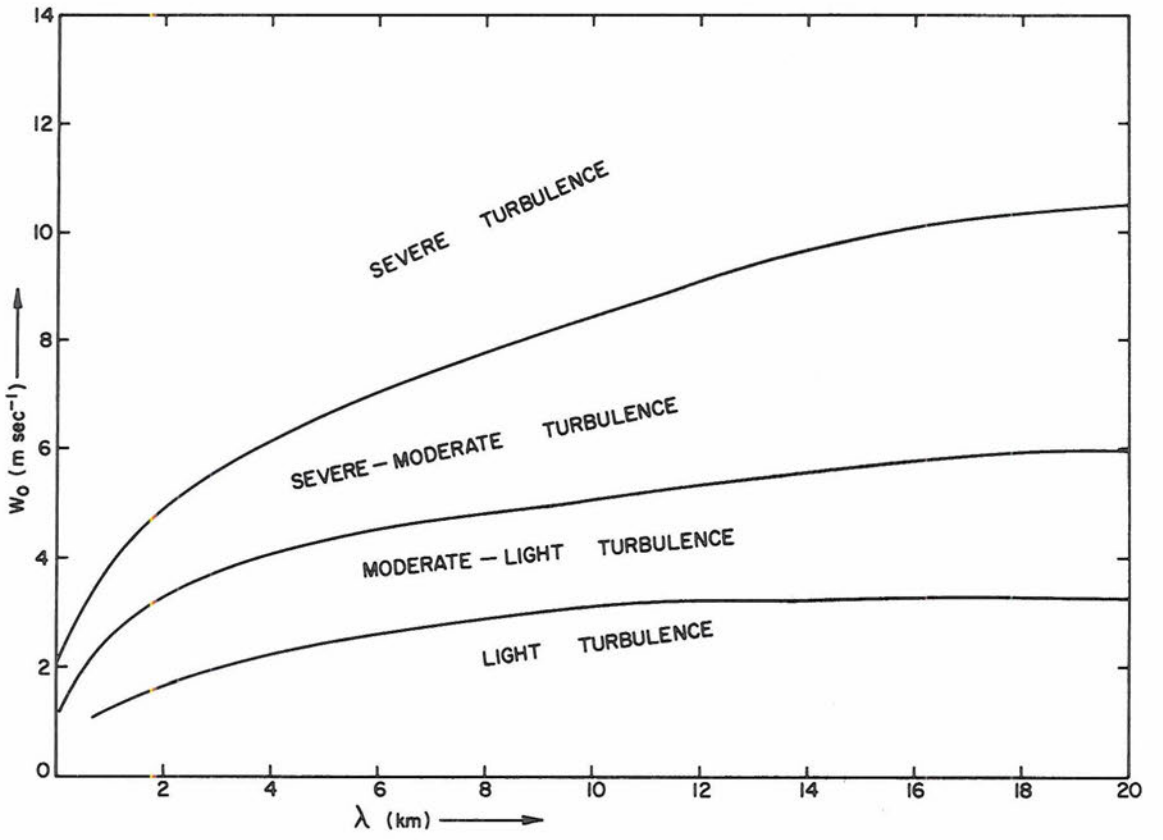

FIG. 43. Forecast degree of CAT. When the maximum vertical velocity in the lee wave is determined from Eq. 25 and the lee wavelength is determined from $\lambda = 2\pi/k$, the degree of CAT can be determined from this graph.

of the -5/3 law will probably overestimate microscale energy levels. In other words, using these assumptions the degree of the resulting turbulence would probably have been slightly over-forecast for longer wavelengths.

If one enters the graph in Fig. 43 at the wavelength determined in step (6) of Appendix B and at the w_o determined in step (7) in Appendix B one finds the degree of turbulence predicted. The results of all CAT forecasts in the case studies using these methods and the actual reports of CAT in the forecast area are included in the cross-sections discussed earlier and in Tables 7 through 9, in the last chapter.

Since the CAT forecasting procedures described in Appendix B are quite complicated for operational use, a "short cut" forecast method which uses the lee wavelength observed by satellite has been developed. It is possible to simplify the expression for the wave number by considering only the second of the two terms on the right hand side of Eq. (22). This term was much larger than the first term in every case studied in this paper. By substituting this term into Eq. (25), we have an expression for the maximum vertical velocity depending on only two unknown quantities, α and λ. If all terms involving α are combined into one expression and maximized by assuming α is 65 degrees (see Fig. B-2) and if λ is determined from

satellite photography, the maximum possible lee wave vertical velocity is known. This method is fully described in Appendix C. Table 12 (Chapter V) contains verification of forecasts using this "short cut" technique.

Supporting Theoretical and Observational Evidence

It must now be established that the patterns of CAT occurrences in the statistical study are consistent with the theory and the methods being used.

If, as a first approximation, a gravity wave of lee wave dimensions is considered to introduce kinetic energy over a very narrow bandwidth in the spectrum, the decay of this energy can be treated analytically (Atlas, Hardy, and Naito 1966) by use of Eq. (3):

$$E(k) = a\,\epsilon^{2/3}\,k^{-5/3} \quad . \qquad 3)$$

This would hold strictly only in the inertial subrange of isotropic turbulence and decay would be at a faster rate at wavelengths above approximately 500 m due to the added energy dissipational effects of buoyant forces.

The spectral densities in the 1 and 6 km wavelength range required to produce the various degrees of CAT can be found from Fig. 42. The spectral densities in the wavelength regions of CAT (500 to 100 m) can be determined also for each category of turbulence from Fig. 42. Since E(k), a,

and k are known at each wavelength, the dissipation rate can be computed by use of Eq. (3) for each wavelength and for all degrees of CAT. Using this method, we may see from Fig. 44 the rates of decay at each wavelength for various degrees of turbulence.

If, from Fig. 44 a mean decay rate for each turbulent category is computed by taking the average value of ϵ over the range of wavelengths between energy input wavelengths of the lee waves and the CAT wavelength near 100 m, --typical for jet aircraft of present design--, the time of decay for turbulent energy at various lee wavelengths to result in CAT can be determined in the following manner. The mean dissipation rate, ϵ, has the dimensions of energy per time; the difference in energy between lee wavelength and 100 m wavelength (using the -5/3 law) is known from Fig. 42; the mean dissipation rate is known from Fig. 44; therefore, the time for this change in energy to take place is also known, as shown in Table 4.

The decay time of turbulent energy contained in lee waves measuring 6 km or less would result in the statistical patterns of frequency of turbulence maxima observed downwind from the ridgelines, observed in Chapter II if the perturbation energy moves with the flow as it passes to smaller scale eddies and if the mean wind values are consistent with the argument.

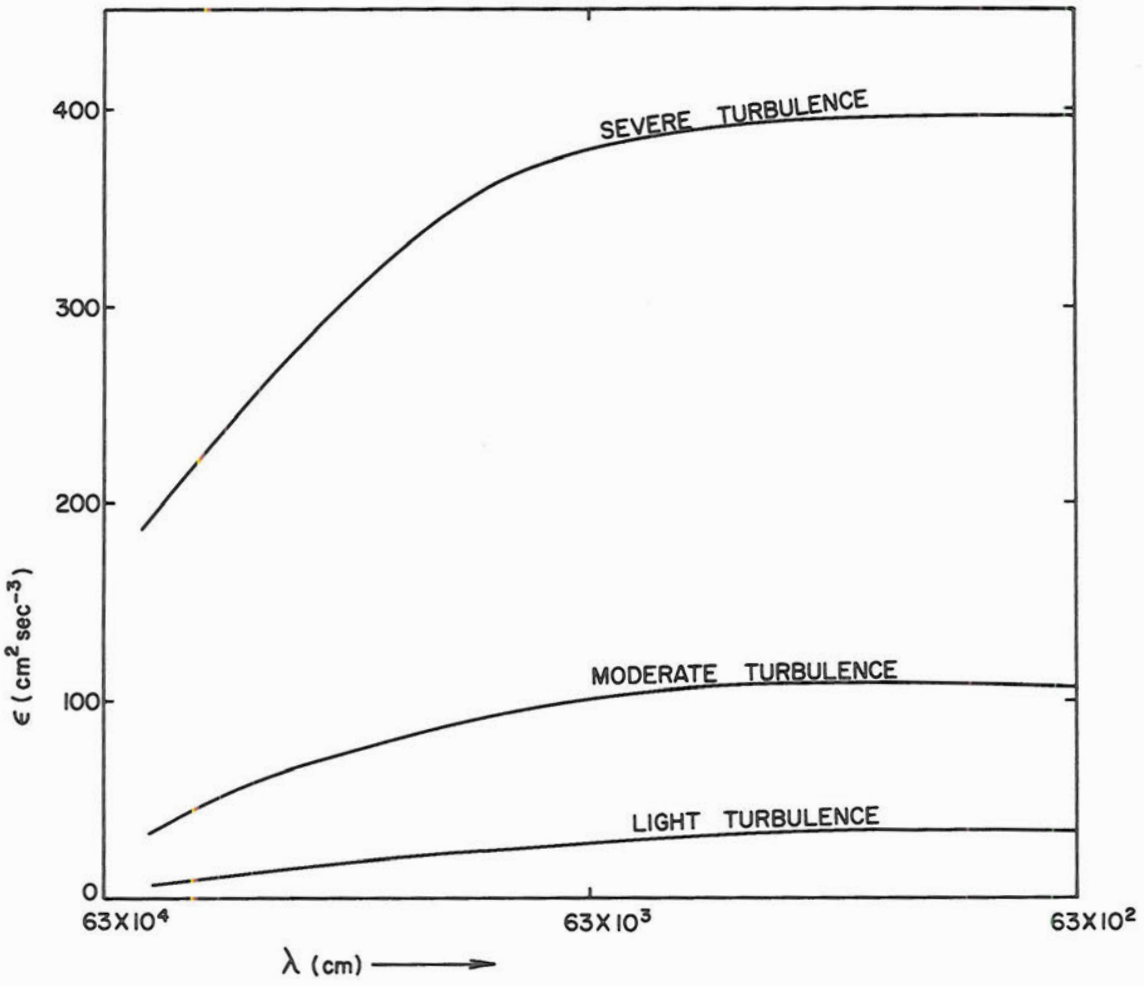

FIG. 44. Dissipation rate, ϵ, in $cm^2 sec^{-3}$, for various wavelengths, λ, in cm.

Table 4. Decay Time of Energy (hours).

Time to decay to CAT wavelengths of cir. 100 m.

Wavelength of Energy Input / Degree of CAT	6 km	1 km
S	2.5	0.7
M	3.2	1.0
L	3.5	1.3

It takes less time for a unit of energy to decay when the level of energy is sufficient to cause severe CAT than for a unit of energy when energy levels leading to lesser degrees of CAT occur. The decay time increases with a decrease in CAT intensity, hence the CAT maxima would tend to be found downstream from mountain ridges in decreasing order of severity, as is evidenced from Figs. 1 through 5.

Table 5 contains climatological information of the jet stream (Serebreny et al. 1958) and upper level winds (Lahey et al. 1960).

Table 5. Jet Stream and Mean Upper Wind Data

Mountain Range	Jet Stream Crossings (Relative Frequency)		Mean Westerly Wind Component (knots)			
	Winter	Spring	Winter		Spring	
			500	300	500	300
Sierras	8	16	27	45	23	35
Washington Cascades	17	16	30	45	23	35
Montana Rockies	35	26	34	50	24	40
Colorado Rockies	40	42	34	55	25	45

The statistical study in Chapter II shows that the regions of CAT maxima over the western United States are also regions of high jet stream incidence and that the mean upper level winds have a large cross mountain component (Table 5). These upper wind velocities and the decay times (Table 4) are consistent with the observed frequency of turbulence patterns. The jet stream is often accompanied by thermally stable layers (Reiter 1963a), strong wind shear and strong cross mountain flow. These properties are conducive to lee wave formation.

CHAPTER V

RESULTS AND CONCLUSIONS

Discussion and Verification of Predictive Methods

The climatological study in Chapter II suggested a relationship between CAT and lee waves, since CAT maxima were located in the lee of all major mountain ridges of the western United States. The frequency maxima of various degrees of CAT displayed a well-organized pattern wherein the highest degree of turbulence occurred closest to the ridge and each succeeding lesser degree of turbulence fell further to the lee of the mountains. This pattern could be explained by the fact that the decay time for energy introduced at lee wavelengths to reach eddies of CAT dimensions decreases with an increase in turbulence severity (see Table 4 in Chapter IV).

This possible connection leads us in Chapter III to the investigation of mountain lee waves and in Chapter IV to the development of CAT-predictive procedures by means of methods described in Appendix B. In the present chapter we will discuss the effectiveness of these CAT forecasting techniques based upon lee wave theory and will present substantiating evidence.

Table 6 contains two summaries of the special pilot reports collected during the seven lee wave cases observed principally by satellite. The upper part of the table is a summary of all special pilot reports taken in the seven cases. The lower part of the table

includes only the reports in the cases where there was probably no mechanical turbulence due to rough terrain.

The vertical velocities in mountain lee waves and their wavelengths obtained from rawinsonde data using the theoretical results of Scorer (1949), Corby, and Wallington (1956) give energy input into the mesoscale which seems to be reasonably close to that found in nature (see Figs. 42 and 43). This is indicated by the fact that this theoretical energy, when passed into the microscale, assuming that it obeys the"-5/3 law", results in a forecast degree of CAT very close to CAT reported in numerous known cases of lee waves.

Verification of some of the forecasts of turbulence made by use of computed lee wavelengths, computed maximum vertical velocities, and Fig. 43 is given in Tables 7, 8, and 9. In addition, Table 7 includes all of the turbulence reports within 90 miles of the cross-sections mentioned in Chapter IV for the western United States lee wave cases observed by satellite regardless of altitude or the location of the report with respect to clouds. Of the 87 pilot reports entered on the cross-sections in Chapter IV, fifty-nine per cent fell in the correct forecast category and thirty-nine per cent in the adjacent forecast category (twenty-nine per cent too low and ten per cent too high). Only two per cent of the cases missed by two categories. Of the eleven occurrences that were reported in higher categories than were forecast, six were from aircraft flying in and near cumulus.

TABLE 6. Pilot Report Summaries (AC-above clouds, BC-below clouds, IC-in clouds, I&O-in and out of clouds, and NC-no clouds).

All Pilot Reports

Turbulence Degree	AC No.	AC %	BC No.	BC %	IC No.	IC %	I&O No.	I&O %	NC No.	NC %	Total No.	Total %	% in each Turbulence Category
N	102	43	48	20	7	3	13	6	65	28	235	100	51
L	35	27	41	31	14	11	15	12	25	19	130	100	28
L/M	6	15	17	41	4	10	5	12	9	22	41	100	9
M	4	10	14	36	6	16	4	10	11	28	40	100	9
M/S	0	0	0	0	0	0	2	25	6	75	8	100	2
S	1	33	2	67	0	0	0	0	0	0	3	100	1
											457		100

Pilot Reports Above 15,000 ft.
Over the West and Above 10,000 ft. Over the East

N	60	55	6	5	4	4	9	8	33	28	112	100	59
L	29	42	8	12	6	9	10	15	15	22	68	100	35
L/M	2	40	0	0	1	20	1	20	1	20	5	100	3
M	1	20	0	0	2	40	1	20	1	20	5	100	3
M/S	0	0	0	0	0	0	0	0	0	0	0	100	0
S	0	0	0	0	0	0	0	0	0	0	0	100	0
											190		100

TABLE 7. Verification of turbulence forecasts for all western United States.

	Observed				
Forecast	L&N	L/M	M	M/S	S
L&N	42	3	2	0	0
L/M	24	7	5	0	0
M	0	1	2	1	0
M/S	0	0	0	0	0
S	0	0	0	0	0

It is not to be expected that this method will correctly forecast all CAT occurrences due to lee waves. It has been pointed out earlier that the use of the "-5/3 law" well into the mesoscale will lead to overforecasting of CAT because the added energy dissipational effects of buoyancy are not considered. The results in Table 7 and in Tables 8 and 9 are consistent with this.

In the western area of our study the mean altitude of occurrence of light or no turbulence (66 cases) was 9300 ft above the stable layer. The mean altitude of light to moderate turbulence (11 cases) was 4000 ft above the stable layer while moderate (9 cases) occurred 2600 ft above it. The only case of moderate to severe turbulence occurred in the stable layer, which could indicate that, on the average, the degree of turbulence decreases quite rapidly with altitude above the stable layer. This is in agreement with the fact that the maximum wave amplitudes and vertical wave velocities are to be expected near the stable layer.

TABLE 8. Verification of eastern United States turbulence forecasts.

All Cases

Forecast	Observed L&N	L/M	M	M/S	S
L&N	158	29	19	8	1
L/M	7	0	1	3	0
M	0	0	0	0	0
M/S	0	0	0	0	0
S	0	0	0	0	0

All Cases Above 10,000 Ft Above Terrain

L&N	64	1	0	0	0
L/M	6	0	0	0	0
M	0	0	0	0	0
M/S	0	0	0	0	0
S	0	0	0	0	0

TABLE 9. Verification of all western United States turbulence forecasts and the eastern United States cases above 10,000 ft msl.

Forecast	Observed L&N	L/M	M	M/S	S
L&N	106	4	2	0	0
L/M	30	7	5	0	0
M	0	1	2	1	0
M/S	0	0	0	0	0
S	0	0	0	0	0

Table 8 (upper half) contains all reports of turbulence within 90 miles of the cross-sections mentioned in Chapter IV for the eastern United States lee wave cases observed by satellite, regardless of altitude. Table 8 (lower half) includes only those cases higher than 10,000 ft above the terrain. This modification is necessary because the wind near the ground reached 50 knots in

many cases of eastern United States lee waves. Table 8 (lower half) should give a reasonable indication of the turbulence due to gravity waves. The precaution of eliminating low level cases was not taken in the western United States cases because the wind speeds were relatively lower.

When all eastern United States cases were considered, there were 226 occurrences of which 70 per cent were correctly forecast, 16 per cent near misses (off by one forecast category) and 14 per cent off by two or more categories. Table 8 also shows that if only the reports above 10,000 ft were considered, there were 71 cases of which 90 per cent were forecast correctly and 10 per cent were near misses. The turbulence was somewhat overforecast as explained before. The mean altitude of the "none to light" category of turbulence above the stable layer was 15,000 ft. However, this figure is not comparable to that found in the western United States cases since all eastern United States cases below 10,000 ft were not included. There was not a large enough sample to compute significant statistics for the other categories of turbulence.

The mean horizontal positions of moderate to severe, moderate, and light to moderate turbulence in all eastern and western United States lee wave cases observed by satellite followed a pattern similar to that shown in the climatological study in Chapter II. The moderate to severe cases occurred, on the average, 70 km downwind from the nearest mountain ridge. Moderate turbulence occurred

120 km downwind while light to moderate usually occurred 160 km downwind from the ridge. It is interesting that in all of the lee wave cases observed by satellite, there were no reports of light to moderate or greater turbulence upwind from any mountain ridge at any altitude above the layer where mechanical turbulence might exist. There were 70 reports of no turbulence and 36 cases of light turbulence from the areas upwind from the mountain in all seven periods under consideration.

Table 9 includes the verification of all eastern and western United States turbulence forecasts regardless of location with respect to clouds, except that the eastern United States turbulence cases below 10,000 ft have been excluded. Of the 158 reports considered, 73 per cent fell into the correct forecast category of turbulence, 26 per cent were near misses (20 per cent too high and 6 per cent too low), and only one per cent was off by two categories.

Table 10 contains the pressure altitude in millibars of all interfaces found in the Denver and Fort Collins rawinsonde observations on designated "lee wave" days during the field measurement program outlined in Chapter III. The computed lee wavelengths and maximum vertical velocities for each of these interfaces are given in kilometers and meters per second. The degree of clear air turbulence (using methods outlined in Chapters III and IV and Appendix B) that should be forecast as a result of lee waves on these interfaces is also entered.

Even though there is a time difference between the soundings taken at Denver and Fort Collins, at times the interfaces have spatial continuity between the two locations. The unsmoothed rawinsondes at Fort Collins indicated more interfaces than the smoothed soundings at Denver on two occasions, but there were the same number on one occasion and even less another time.

The additional interfaces gained by using the unsmoothed sounding data usually could produce lee waves with little predicted energy. An exception was the 523 mb interface at 1400Z on May 13, 1966. Lee waves on this interface could lead to moderate turbulence.

Most of the computed energies contained in lee waves over Fort Collins were greater than those contained in lee waves over Denver on

TABLE 10. Computed Lee Wave Data.

Date 1966	Denver 1200Z				Fort Collins 14Z				Fort Collins 19Z			
	p	w_o	λ	CAT	p	w_o	λ	CAT	p	w_o	λ	CAT
4-1	703	0.7	2.7	L-N	784	1.8	1.4	L-N	731	0.2	1.2	L-N
	700	1.8	5.0	L-N	680	0.3	1.3	L-N	709	3.0	5.2	L-M
	540	1.1	7.0	L-N	541	0.5	10.0	L-N	541	0.6	9.5	L-N
					489	0.7	34.0	L-N				
4-16	516	3.0	5.6	L-M								
	361	1.1	7.1	L-N	None				None			
	300	1.0	10.8	L-N								
5-11	775	0.1	1.5	L-N	554	4.6	8.4	M				
	686	0.3	3.5	L-N								
	540	0.6	5.0	L-N					None			
	352	0.6	5.4	L-N								
	300	1.5	9.2	L-N								

TABLE 10. Continued.

Date 1966	Denver 1200Z				Fort Collins 14Z				Fort Collins 19Z
	p	w_o	λ	CAT	p	w_o	λ	CAT	
5-13	593	1.1	5.5	L-N	790	0.7	1.1	L-N	
	500	2.1	7.5	L-N	543	1.9	5.3	L-N	
	462	1.0	5.2	L-N	523	4.7	4.8	M	
	450	2.2	10.1	L-N	505	1.7	7.8	L-N	None
					434	0.9	5.7	L-N	
					418	1.0	9.0	L-N	
					290	0.6	17.0	L-N	
					279	1.7	19.0	L-N	
5-14	770	4.8	4.6	M	625	2.9	4.6	L-M	
	629	0.4	3.2	L-N	543	1.3	6.7	L-N	
	497	3.2	8.1	L-M	520	2.3	9.4	L-N	None
	300	0.8	10.0	L-N	250	0.5	14.5	L-N	

common interfaces. This probably is due to the fact that the unsmoothed soundings and more specific topography measurements were used in the computations for the Fort Collins lee waves.

On May 14, the smoothed Denver soundings indicated an interface at 770 mb, which did not show up in the Fort Collins detailed sounding. This interface, using mean topographical values for the Colorado Rockies, could produce lee waves with enough energy to cause moderate turbulence, while the maximum possible turbulence computed for the Fort Collins lee waves on this date was light to moderate. These lee waves would have been on an interface at 625 mb. Interfaces such as the one at 770 mb over Denver are sometimes not continuous in space over all of northeastern Colorado. This could partially explain the patchiness of any CAT resulting from mesoscale gravity waves.

It is interesting to note that the unsmoothed soundings at Fort Collins taken at 1400Z and 1900Z on April 1, 1966, were not as similar with respect to lee wave computations as the 1200Z Denver and the 1900Z Fort Collins rawinsondes on that date. This could mean that a smoothed sounding depicts the dominant interfaces and that in time the atmosphere tends to eliminate all but these dominant interfaces.

Table 11 contains all turbulence occurrences reported by aircraft over eastern Colorado during the 12-hour period beginning at 1200Z on the "lee wave" days during the field measurement program. The maximum degree of turbulence that could have been forecast by use of either the Denver or Fort Collins rawinsonde data is also shown. The topography of the Colorado mountains is very complex. Since lee wave energy is strongly dependent on mountain range dimensions (see Appendix B), it can be expected that there will be areas which will experience more or less turbulence than forecast when using either the average mountain dimensions around Fort Collins or the overall mean topographical values for the entire mountain range.

In addition, these pilot reports came from various levels and may or may not have been in or near cumulus clouds. We might then expect that the degree of turbulence reported would be greater than turbulence strictly reported by CAT rules (above 18,000 ft msl and not near clouds). Nevertheless, of the 27 turbulence reports, all but 3 fell into the correct or adjacent forecast category.

TABLE 11. Eastern Colorado Turbulence Reports and Forecasts.

Date 1966	Time (Z)	Reported Degree of Turbulence	Position of Report		Altitude of Turbulence (In thsds ft)	Forecast Degree of Turbulence
4-1	1320	L	38.9N	103.6W	11.5	L-N
	1520	L	37.7	105.3	14.5	L-N
	1520	L	37.3	105.6	13.0	L-N
	1620	L-M	41.5	103.5	6.5	L-N
	1820	L	39.8	104.8	21.0	L-N
	1820	L	39.5	105.5	25.0-26.0	L-N
	1920	M-S	39.8	104.9	10.5-11.5	L-M
	1920	L-M	37.4	103.3	13.0	L-M
	2020	L-M	39.2	106.0	13.5-11.5	L-M
4-16	1720	L	39.8	104.8	35.0	L-M
	1920	M	39.6	105.3	17.0	L-M
	1925	L	39.8	104.8	9.0	L-M
	2120	M	39.7	105.2	39.0	L-M
5-11	1720	M	38.3	106.5	17.0	M
	2149	M	39.0	104.7	10.0	M
	2149	M	39.1	104.7	U	M
	2300	M-S	39.0	104.5	9.0	M
5-13	1520	L	39.6	106.8	11.0-14.0	M
	1820	M-S	41.1	104.8	8.5	M
	1920	S	40.5	104.0	8.0-9.5	M
	2120	L-M	39.3	104.8	15.0-8.0	M
	2220	M	38.3	106.6	13.5	M

TABLE 11. Continued.

Date 1966	Time (Z)	Reported Degree of Turbulence	Position of Report		Altitude of Turbulence (In thsds ft)	Forecast Degree of Turbulence
5-14	1830	L	39.7	105.3	U	M
	2020	L-M	37.7	105.6	12.5	M
	2120	M	38.5	104.7	10.0	M
	2220	M	37.7	104.7	13.5	M
	2220	M-S	39.8	105.3	13.5-14.0	M

The lee wave energy computed from radar observations of the constant level balloon that reached altitude and separated properly (run 2, on April 1, 1966) and the theoretically computed lee wave energy from rawinsonde data on the same day were both of very low magnitude and could result in no appreciable aircraft turbulence.

The energy computed theoretically in this lee wave (run 2, on April 1, 1966) is shown in Table 11. The mean vertical motion in the half wavelength computed from radar tracking measurements was -0.7 m sec^{-1}, thus, the energy in the lee wave, using the relationship $\overline{KE} = 1/2\overline{w^2}$, was 0.25 $m^2 sec^{-2}$. This value would lead to no significant turbulence.

We have seen that the use of the "-5/3 law" up to lee wavelengths of 20 km (see Fig. 43) seems to give reasonable results since the forecast degree of CAT, based upon lee wavelength energy input levels and this decay law, agrees very well with reported CAT. The lee wavelength as observed by the satellites also compares favorably with computed wavelengths based upon atmospheric parameters measured by rawinsondes.

Table 12 refers to those cases observed principally by satellite and contains information concerning lee wavelengths, based upon satellite photo measurements, and theoretical computation using

$$\lambda_\ell = 2\pi/(\ell_2^2 + L^2 \cos^2\alpha)^{\frac{1}{2}} \qquad 27)$$

$$\lambda_b = 2\pi U \sqrt{\theta/g \ \frac{\partial\theta}{\partial z}} \qquad 9)$$

where λ_s is the wavelength in the satellite photo, λ_ℓ is the wavelength using Scorer's theoretical development, and λ_b is the wavelength based upon the Brunt-Väisälä frequency equation. The mean wavelengths of the lee wave clouds measured from satellite photos are very close to the theoretical wavelengths computed by

TABLE 12. Lee Wavelength Values (km)

Date	λ_ℓ	λ_s	λ_b
1-7-66	28.0	28	15.0
	3.3	28	2.6
	31.0	28	10.0
	22.0	28	8.6
2-14-66	10.0	10	12.0
	10.0	10	8.8
	12.0	14	10.0
	13.0	14	9.5
3-1-66	19.0	24	11.0
	13.5	24	7.5
	18.0	24	10.0
	17.0	24	10.3
3-7-66	11.0	13	10.0
	8.0	13	4.1
	11.0	13	11.0
	9.0	13	9.4
	11.5	13	11.0
3-9-66	14.0	10	9.0
	4.5	9	7.0
	13.0	14	10.0
4-26-66	21.0	18	23.0
	8.0	11	5.7
	22.0	18	15.0
Mean Values	14.3	17.4	10.0

using Scorer's work. The wavelengths using the Brunt-Väisälä relationship are relatively close to those observed by satellite for

the western cases, but they are off by more than a factor of two for the eastern United States cases. It should be expected that the results using Eq. 9 would not be as accurate as those using Eq. 27, since the model used to develop Eq. 9 is more sophisticated.

During the field program the lee wavelength on April 1, 1966, observed by radar tracking of constant level balloons (run 2), agreed with the lee wavelength computed from rawinsonde data. Some wavelengths found in the vertical velocity profiles observed by radar tracking of constant level balloons also were in agreement with computed lee wavelengths.

Clouds were so thick on April 16, 1966, and May 13, 1966, two of the lee wave days, that lee wave clouds were not discernible in satellite photographs. On April 1, 1966, there was some indication of cirrus with lee wavelengths of 30 km, which agreed well with theoretical computations of 34 km wavelengths at 489 mb and with the constant level balloon wavelength of 33 km at 20,000 ft msl. On May 14, 1966, the satellite photo measurements indicated a lee wavelength of about 30 km over northeastern Colorado, which compared poorly with a computed theoretical wavelength of 14.5 km at 250 mb. The lee wavelength was computed from rawinsonde data to be 8.4 km on May 11, 1966, and the wavelength over the Fort Collins area was 10 km when measured by satellite.

The photogrammetric measurements taken on April 16, 1966, showed a lee wavelength of 4.5 km, which was reasonably close to the 5.6 km computed theoretical lee wavelength on that date at the very strong interface located at 516 mb over Denver. Lee wave clouds were observed by satellite and photogrammetry on May 13, 1966, but no wavelength comparison was possible since only isolated lenticular clouds were photographed from the ground. No comparison was possible on April 16, 1966, because thick cloud cover precluded discerning any lee wave pattern in the satellite photographs.

Inspection of the upper air sounding during known lee wave situations has shown that there are usually more levels than one where gravity waves could form. The theoretically computed wavelengths of the gravity waves are not normally the same at each level where waves are possible, but they are often very close to each other. It has been found that the lee wavelengths observed by the satellites were close to the wavelengths computed at the level where lee wave vertical motions would be a maximum. Booker (1962) discovered that the lee wavelength and amplitude remain very nearly constant throughout a deep layer of the atmosphere and this seems to show that the dominant interface (the interface with the greatest computed vertical motion) controls the wave motions throughout deep layers adjacent to this interface. Hence the generation of lee wave energy is not only accomplished at the interface but

throughout a deep layer of the atmosphere and, therefore, any resulting CAT should be experienced over a wide range of altitudes.

Various computational aids have been developed in this study which can be used operationally to forecast CAT due to lee waves, but, even with these aids, this procedure is long and tedious. It would be better accomplished by programming the entire operation for a computer. Twice daily CAT forecasts over mountainous terrain using these techniques would be desirable.

Previous research has shown CAT to be correlated with various atmospheric parameters. CAT might be correlated with vertical wind shear because strong shears can lead to unstable gravity waves. Shear also contributes to gravity wave formation since wind speed increase with height contributes to a decrease with height of the Lyra parameter, ℓ, a necessary condition according to theory (Scorer 1949). CAT might be much more frequent over land than over oceans because forcing functions such as convection, differential heating, and terrain features are found more frequently there. CAT is found frequently near the tropopause and the jet stream, probably because of the existence of stable layers in these regions on which gravity waves can form. It might also be correlated with the jet stream because stronger gradient level winds and strong vertical wind shears necessary for high energy levels in the gravity waves usually are found to accompany it [see Eqs. (19) and (25)]. Since the forecast method for computing wave energies is quite tedious, a "short-cut"

method utilizing the lee wavelength measured in satellite photos is described in Appendix C.

Table 13 shows the vertical velocities and the resulting degree of turbulence associated with lee waves computed by means of Scorer's theoretical development and by the "short-cut" method using satellite measurements of the lee wavelength. Seventy-three per cent fell into the same category and twenty-seven per cent fell into a higher category using the maximized value determined from satellite information.

TABLE 13. CAT Forecast Comparisons.

Date	CAT Forecasts Using Rawinsonde Data		CAT Forecasts Using Satellite Data	
	w_o(m sec^{-1})	Forecast CAT	w_o(m sec^{-1})	Forecast CAT
3-7-66	1.2	N-L	1.6	N-L
3-7-66	2.0	N-L	3.6	N-L
3-7-66	1.9	N-L	3.6	N-L
3-7-66	5.0	M	6.5	M
3-9-66	4.1	L-M	4.1	L-M
3-9-66	3.1	L-M	4.1	L-M
3-9-66	4.1	L-M	8.0	M
4-26-66	2.0	N-L	4.0	N-L
4-26-66	3.9	L-M	6.4	M
4-26-66	0.4	N-L	2.7	N-L
2-14-66	1.9	N-L	2.7	N-L
2-14-66	3.2	N-L	7.5	M
2-14-66	0.7	N-L	2.8	N-L
2-14-66	0.6	N-L	7.3	M

The mountains of the eastern United States have dimensions that tend to make the first term in Eq. (B-1) (Appendix B) small compared with the same term for the mountains of the western United States.

On the other hand, term number 3 in Eq. (B-1) is usually much larger over the eastern United States because gradient level winds are stronger in the east, at least in the cases studied. The net result has been that the CAT wavelength energies resulting from Appalachian lee waves were less than those connected with most western ranges. This is also due to stronger winds aloft over the east which resulted in longer lee waves, both theoretically and as observed by the satellite. The longer waves need greater vertical motions to result in CAT (see Fig. 43).

Outlook for Future Research

Although the results of several aspects of the Colorado pilot field measurement program were not as fruitful as might have been anticipated, the overall program, when carried out over an extended period of time with proper instrumentation, offers a means of intensive mountain lee wave investigation. The K-24 camera system should be replaced with lightweight, rapid-firing (with remote control capabilities) 70 mm wide-angle cameras. Also, a radio communication system between operators is a necessity. In this study there was a loss of much film footage because sometimes one of the two cameras malfunctioned and cumulus clouds obscured the lee wave clouds at one camera site while lee waves were still visible at the other camera location.

The radar set used in any future study must be capable of locating transponder-carrying constant-level balloons far upwind from the radar site. It would be best to position two radar sets along the prevailing wind direction in order to insure tracks up to 300 km in length. In this way numerous wavelengths could be observed. Additionally, the radar should have automatic readout capabilities so that a continuous record of the balloon trajectory would be available for spectral analysis. The fuse rope separation system should be replaced by a pressure switch mechanism to insure separation at the programmed altitude. The installation of a GMD-1 apparatus would be desirable in making rawinsonde observations so that the radar sets would be free at all times to track constant-level balloons.

Frequent rawinsonde releases at both radar and GMD-1 sites would allow for a study of interfaces both in time and space. Arrangements should be made to have FAA Traffic Control Centers elicit pilot reports of turbulence (including reports of no turbulence) from all aircraft in the study area. It would be desirable to utilize a small aircraft to fly into the lee waves and the surrounding areas. This aircraft could be used to release constant-level balloons at assigned altitudes in order to get the longest tracking possible.

Future research should be based in large part upon measurements taken by sophisticated instrumentation carried aloft by several aircraft used only as inertial reference frames. The aircraft should

probe the areas of CAT as well as the surrounding airspace. In particular, energy-spectral measurements should be made in the airstream upwind from lee waves, in lee waves, in areas immediately downwind from lee waves and in any resulting CAT areas. By this means one could determine if lee waves do provide the input energies which eventually cause CAT in the mountainous West.

More complete coverage of any lee wave area may be accomplished with the availability of more continuous satellite surveillence. With all of the methods that were used in the field measurement program properly instrumented and the innovations mentioned above, a comprehensive study of lee waves should produce a collection of data that will lead to the understanding of lee wave formation, energy transfer in the turbulence spectrum, and subsequently, to the processes whereby this energy will be finally dissipated in the atmosphere.

LITERATURE CITED

Alaka, M. A. (Ed.), 1960: The Airflow over Mountains. Technical Note No. 34, World Meteorological Organization, Geneva, 135 pp.

Angell, J.K. and D.H. Pack, 1960: An analysis of some preliminary low-level constant level balloon (tetroon) flights. U.S. Department of Commerce, Weather Bureau Manuscript, March 1960, 37 pp.

Atlas, D., K.R. Hardy, and K. Naito, 1966: Optimizing the radar detection of clear air turbulence. Paper presented at National Air Meeting of Clear Air Turbulence, Washington, D.C., February 23-24, 1966, 10 pp.

Bannon, J.K., 1952: Weather systems associated with some occasions of severe turbulence at high altitude. Meteorological Magazine, London, 81, 97-101.

Batchelor, G.K., 1953: The Theory of Homogeneous Turbulence. Cambridge University Press, London, 197 pp.

Beckwith, W.B., 1963: Sampling of clear air turbulence incidents by aircraft gust recorders. Paper presented at Third Conference on Severe Local Storms, Urbana, Illinois, November 12-14, 1963, 18 pp.

Blackman, R.B. and J.W. Tukey, 1958: The Measurement of Power Spectra. Dover Publications, New York, 190 pp.

Bolgiano, R., Jr., 1959: Turbulent spectra in a stably stratified atmosphere. Journal of Geophysical Research, 64, 2226-2236.

_____, 1962: Structure of turbulence in stratified media. Journal of Geophysical Research, 67, 3015-3028.

Booker, D.R., 1963: Modification of convective storms by lee waves. Meteorological Monographs, 5, 129-140.

Clodman, J., G.M. Morgan, Jr., and J.T. Ball, 1960: High level turbulence. Air Weather Service Technical Report 158, under Contract No. AF19 (604)-5208. New York University, New York, 83 pp.

Colson, D., 1963: Analysis of clear air turbulence data for March 1962. Monthly Weather Review, 91, 73-82.

Colson, D., 1966: Nature and intensity of clear air turbulence. Paper presented at National Air Meeting on Clear Air Turbulence, Washington, D.C., February 23-24, 1966, 5 pp.

_____ and H.A. Panofsky, 1965: An index of clear air turbulence. Quarterly Journal of the Royal Meteorological Society, 91, 507-513.

Conover, J.H., 1964: Lee wave clouds photographed from an aircraft and a satellite. Weather, 19, 79-92.

Corby, G.A. and C.E. Wallington, 1956: Airflow over mountains: The lee wave amplitude. Quarterly Journal of the Royal Meteorological Society, 82, 266-274.

Crooks, W., 1965: High altitude clear air turbulence. Technical Report No. AFFDL-TR-65-144, 114 pp.

Danielsen, E.F., 1959: The laminar structure of the atmosphere and its relation to the concept of the tropopause. Archiv fur Meteorologie, Geophysik und Bioklimatologie, A11, 293-332.

Döös, B.R., 1962: A theoretical analysis of lee wave clouds observed by TIROS I. Tellus, 14, 301-309.

Endlich, R.M., 1963: The detailed structure of the atmosphere in regions of clear-air turbulence. Final Report, Contract Cwb-10324, Stanford Research Institute, Menlo Park, California, 62 pp.

_____ and R.L. Mancuso, 1964: Clear-air turbulence and its analysis by use of rawinsonde data. Final Report, Contract Cwb-10624, Stanford Research Institute, Menlo Park, California, 55 pp.

_____ and G.S. McLean, 1957: The structure of the jet stream core. Journal of Meteorology, 14, 543-552.

_____, S.M. Serebreny and M.G. Ligda, 1966: Clear air turbulence research programs of the Aerophysics Laboratory. Paper presented at National Air Meeting on Clear Air Turbulence, Washington, D.C., February 23-24, 1966, 8 pp.

Fritz, S., 1965: The significance of mountain lee waves as seen from satellite pictures. Journal of Applied Meteorology, 14, 31-37.

_____ and C. V. Lindsay, 1964: Lee wave clouds photographed over the Appalachians by TIROS V and VI. Soaring, 28, 14-17.

Gerbier, N. and M. Bérenger, 1958: Ondes de ressant dans les Alpes francaises. 3e campagne d'études, janvierfévrier 1958. Direction de la Météorologie Nationale.

Hardy, K.R., D. Atlas, and K.M. Glover, 1966: Microwave backscatter from the clear atmosphere. Journal of Geophysical Research, 71, 1537-1552.

Harrison, H.T. and D.F. Sowa, 1966: Mountain wave exposure on jet routes. United Air Lines Meteorology Circular No. 60, 66 pp.

Haurwitz, B., 1941: Dynamic Meteorology. McGraw-Hill, New York, 365 pp.

Hayman, R.W. and J.A. Peterka, 1963: Feasibility of balloon trajectory analysis utilizing analytical photogrammetry. Technical Paper No. 45, Part II, Department of Atmospheric Science, Colorado State University, Fort Collins, Colorado, 8 pp.

Hinze, J.O., 1959: Turbulence. McGraw-Hill, New York, 568 pp.

Holmboe, J. and H. Klieforth, 1957: Investigation of mountain lee waves and the air flow over the Sierra Nevada. Final Report, Contract No. AF19(604)-728, 290 pp.

Kadlec, P.W., 1963: An in-flight study of the relation between jet stream, cirrus, and wind shear turbulence. Final Report, Contract Cwb-10356, Eastern Air Lines, Inc., Miami, Florida, 48 pp.

_____, 1964: A study of flight conditions associated with jet stream cirrus, atmospheric temperature change, and wind shear turbulence. Final Report, Contract Cwb-10674, Eastern Air Lines, Inc., Miami, Florida, 45 pp.

Kao, S.-K. and H.D. Wood, 1964: Energy spectra of mesoscale turbulence along and across the jet stream. Journal of Atmospheric Science, 21, 513-519.

Kolmogorov, A., 1941: The local structure of turbulence in incompressible viscous fluid for very high Reynolds' number. Doklady ANSSSR, 30, 301 pp.

Kuettner, J., 1939: Moazagotl und Föhnwelle. Beitrage zur Physik der Atmosphäre, 25, 79-114.

Lahey, J.F., R.A. Bryson, H.A. Corzine, and C.W. Hutchins, 1960: Atlas of 300 mb and 500 mb wind characteristics for the Northern Hemisphere. Final Report-Part I, U.S. Air Force Contract AF19(604)-2278. University of Wisconsin Press, Madison, Wisconsin, 128 pp.

Loving, N.V., 1966: High altitude clear air turbulence (HICAT), a menace to the aerial highway. Air Force Flight Dynamics Laboratory, Wright-Patterson AFB, 18 pp.

Lumley, J.L. and H.A. Panofsky, 1964: Structure of Atmospheric Turbulence. Wiley, New York, 239 pp.

Lyra, G., 1940: Uber den Einfluss von Bodenerhebiengen auf die Stroemung einer stabil geschicheten Atmosphaere. Beitrage zur Physik der Atmosphäre, 26, 197-206.

MacCready, P.B., Jr., 1953: Structure of atmospheric turbulence. Journal of Meteorology, 10, 434-449.

_____, 1962: The inertial subrange of atmospheric turbulence. Journal of Geophysical Research, 67, 1051-1059.

Makjanić, B., 1962: A contribution to the mathematical theory of air flow over mountains including the effects of turbulent viscosity. Report under NSF Grant NSF6-22557, Department of Meteorology, University of California, Los Angeles, California, 20 pp.

Manley, G., 1945: The helm wind of Crossfell, 1937-1939. Quarterly Journal of the Royal Meteorological Society, 71, 197-219.

Musaelyan, Sh.A., 1964: Barrier Waves in the Atmosphere. Israel Program for Scientific Translation, Jerusalem, 111 pp.

Panofsky, H.A. and J.C. McLean, Jr., 1964: Physical mechanism of clear-air turbulence. Final Report, Contract Cwb-1039, Pennsylvania State University, University Park, Pennsylvania, 22 pp.

Petterssen, S., 1956: Weather Analysis and Forecasting, Volume I. McGraw-Hill, New York, Toronto, London, 267 pp.

_____ and W.C. Swinbank, 1947: On the application of the Richardson's criterion to large scale turbulence in the free atmosphere. Quarterly Journal Royal Meteorological Society, 73, 335-345.

Pinus, N.Z., E.R. Reiter, G.N. Shur, and N.K. Vinnichenko, 1966: Power spectra of turbulence in the free atmosphere. Tellus, 18, 97-104.

Queney, P., 1947: Theory of perturbations in stratified currents with applications to air flow over mountain barriers. University of Chicago, Department of Meteorology, Miscellaneous Report No. 23, 81 pp.

Reiter, E.R., 1960: Turbulenz im Wolkenfreien Raum (Clear Air Turbulence). Berichte des Deutschen Wetterdienstes, 61, 42 pp.

_____, 1961 a: The detailed structure of the wind field near the jet stream. Journal of Meteorology, 18, 9-30.

Reiter, E.R., 1961 b: Project jet stream research flight number 30 April 1957. Quarterly Journal of the Royal Meteorological Society, 87, 332-345.

_____, 1962: The atmosphere micro-structure and its on clear air turbulence (CAT). Technical Paper No. 39, Department of Atmospheric Science, Colorado State University, Fort Collins, 12 pp.

_____, 1963 a: Jet-Stream Meteorology. Chicago and London, The University of Chicago Press, 191-220, 431-433.

_____, 1963 b: Nature and observation of high-level turbulence especially in clear air. Technical Report No. 41, Atmospheric Science Department, Colorado State University, Fort Collins, 28 pp.

_____, 1963 c: Exploratory study on the physical nature of certain mesostructural details in vertical wind profiles. Technical Paper No. 47, Atmospheric Science Department, Colorado State University, Fort Collins, 17 pp.

_____, 1963 d: Occurrences and causes of high-level turbulence. Technical Paper No. 45, Department of Atmospheric Science Colorado State University, Fort Collins, 7 pp.

_____, 1965: The fine-scale structure of the atmosphere. Colorado State University Miscellaneous Report, Fort Collins, 17 pp.

_____, D.W. Beran, J.D. Mahlman, and G. Wooldridge, 1965: Effect of large mountain ranges on atmospheric flow patterns as seen from TIROS satellites. Technical Paper No. 69, Atmospheric Science Department, Colorado State University, Fort Collins, 110 pp.

_____, and A. Burns, 1965: Atmospheric structure and clear air turbulence. Technical Paper No. 65, Atmospheric Science Department, Colorado State University, Fort Collins, 17 pp.

_____, and A. Burns, 1966: The structure of clear-air turbulence derived from TOPCAT aircraft measurements. Journal of the Atmospheric Sciences, 23, 206-212.

_____, and R.W. Hayman, 1962: On the nature of clear air turbulence (CAT). Technical Paper No. 28, Atmospheric Science Department, Colorado State University, Fort Collins, 33 pp.

Reiter, E.R., and A. Nania, 1964: Jet-stream structure and clear air turbulence. Journal of Applied Meteorology, 3, 247-260.

Scorer, R.S., 1949: Theory of waves in the lee of mountains. Quarterly Journal of the Royal Meteorological Society, 75, 41-56.

_____, 1954: Theory of airflow over mountains: III-airstream characteristics. Quarterly Journal of the Royal Meteorological Society, 80, 417-428.

_____, 1958: Natural Aerodynamics. New York, London, Paris, Los Angeles, Pergamon Press, 229-254.

Serebreny, S.M. and E.J. Wiegman, 1964: The distribution of clear air turbulence reports and cloud patterns as seen in satellite photographs. Final Report under Contract No. Cwb-10481, Stanford Research Institute, Menlo Park, California, 43 pp.

_____, E.J. Wiegman and R.G. Hadfield, 1958: A study of jet stream conditions in the Northern Hemisphere during spring and winter. Technical Reports Nos. 5 and 7, Pan American World Airways, Inc., Meteorology Department, 218 pp.

Shur, G.N., 1962: Experimental investigations of the energy spectrum of atmospheric turbulence. Tsentral'naya aerologicheskaya observatoriya. Trudy, No. 43, 79-90.

Stinson, R., A.I. Weinstein, and E.R. Reiter, 1964: Details of wind structure from high resolution balloon soundings. NASA Technical Memorandum NASA-TM-53115, George C. Marshall Space Flight Center, Huntsville, Alabama, 28 pp.

Wallington, C.E., 1961: Meteorology for Glider Pilots. London, John Murray, 203-232.

Weinstein, A.I. and E.R. Reiter, 1965: Mesoscale structure of 11-20 km winds. NASA Contract Report NASA CR-61080, George C. Marshall Space Flight Center, Huntsville, Alabama, 47 pp.

Wiegman, E.J., 1965: The distribution of clear air turbulence and cloud patterns as seen in satellite photographs. Final Report, under Contract No. Cwb-10791, Stanford Research Institute, Menlo Park, California, 50 pp.

APPENDIX A

List of Symbols

a = a universal constant

a_n = amplitude factor

b = mountain half-width

c = wave speed

c_s = speed of sound

D = structure function

$E(k)$ = twice the energy, per unit mass, per unit wave number

$\tilde{F}$ = force vector

$g, \tilde{g}$ = acceleration of gravity

h = mountain height

h_1 = height of the density interface above the earth's surface

k = wave number, the wavelength per unit length

K_m = exchange coefficient of momentum

K_t = exchange coefficient of heat

$(\ell^*)^2$ = Scorer's parameter $g\beta/U^2 - 1/U \quad \partial^2 U/\partial z^2$

$(\ell)^2$ = Lyra's parameter $g\beta/U^2$

L^2 = $\ell_1^2 - \ell_2^2$

p = atmospheric pressure

Q = absolute vorticity (normal component)

R = universal meteorological gas constant

R_i = Richardson number

$R(\tau)$ = autocorrelation function of the vertical gust velocity

s, n, z = right angle coordinate system oriented with s along the streamline, n normal to the streamline, and z along the vertical.

t = time

T = temperature in degrees absolute

$T(\omega)$ = aircraft frequency response function

u, v, w = velocity components of the perturbed flow

U, V, W = velocity components of the undistrubed flow

U_1 = horizontal wind component normal to the mountains at the gradient wind level

V_b = volume of balloon

$\tilde{V}$ = three dimensional velocity vector

W_b = weight of balloon and attachments

w_o = maximum vertical velocity (its amplitude) in a lee wave where the lee wave has maximum amplitude

x, y, z = Cartesian coordinates

α = an angle satisfying $n\pi - \alpha / \alpha = Lh$, and $0 \leq \alpha \leq \pi/2$, where n is the solution that gives the maximum w_o and λ

β = static stability $1/\theta \ \partial\theta/\partial z$

ϵ = dissipation rate of energy, per unit mass, per unit time

δ = $z - z_b$, the vertical displacement of a particle from its original level

ρ = density

θ = potential temperature

ψ = stream function

λ = wavelength

$\tilde{\Omega}$ = the earth's angular rotation (velocity) vector

APPENDIX B

Application of the Theory - Determination of Lee Wave Energy Leading to CAT

The following steps, some of which will be enlarged upon below, must be taken in order to compute vertical velocities and energies in lee waves:

1) Determine $(\ell)^2 = g\beta/U^2$ for each layer from the rawinsonde data collected nearest to the suspected lee wave area.

2) Compute $L^2 = (\ell_1)^2 - (\ell_2)^2$ from the $(\ell)^2$ values obtained in step (1).

3) Determine if $L^2 > \pi^2/4h_1^2$ where h_1 is the height above the surface of the earth of the surface separating the two layers wherein ℓ^2 is constant. If this condition is not satisfied there can be no lee waves.

4) Use the equation $Lh_1 = n\pi - \alpha / \sin\alpha$ for various values n to find various values of α (see step (a) below).

5) Use the relationship $k^2 = (\ell_2)^2 + L^2 \cos^2\alpha$ to find k, the wave number.

6) Use $\lambda = 2\pi/k$ to determine the lee wavelength.

7) Use the equation

$$w_o = \left(\frac{2\pi hb}{e^{kb}}\right)\left(\frac{\sin^2\alpha}{n\pi - \alpha + \tan\alpha}\right)(U_1 L^2) \qquad \text{B-1)}$$

to determine vertical velocities in the wave (see step (b), (c), and (d) below).

8) The vertical velocity amplitude expressed by the equation in step (7) above is used to compute the mean kinetic energy (vertical component) per unit mass contained in the lee waves in the following manner.

$$w = w_o \sin 2\pi \frac{x}{\lambda} \qquad \text{B-2)}$$

$$w^2 = w_o^2 \sin^2 2\pi\frac{x}{\lambda} \qquad \text{B-3)}$$

$$\overline{KE} = \frac{1}{2}\,\overline{w^2} = \frac{1}{2}\,\frac{1}{\lambda}\int_o^\lambda w_o^2 \sin^2\frac{2\pi x}{\lambda}\,dx = \frac{w_o^2}{4} \qquad \text{B-4)}$$

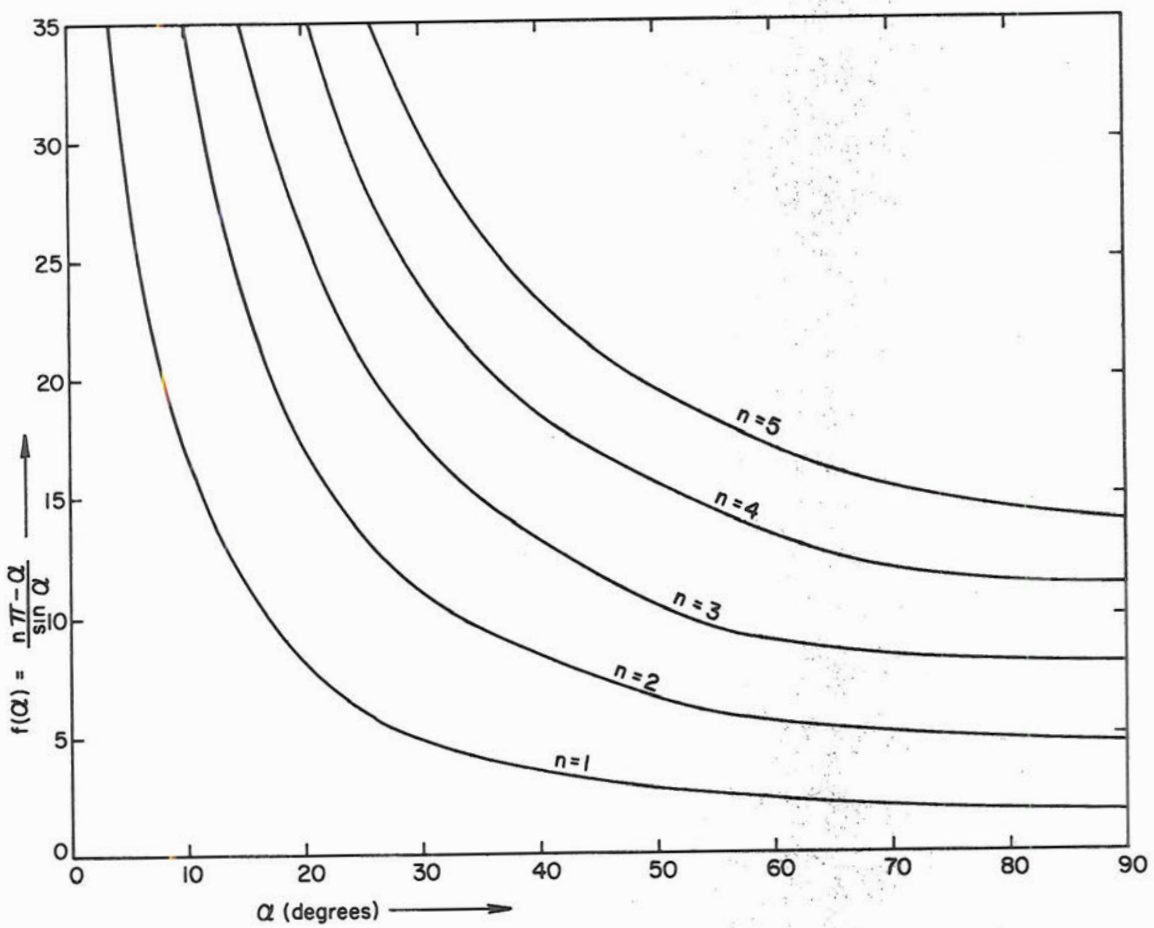

FIG. B-1. Determination of α. Enter graph at f (α) and read off α values for values of n that are pertinent.

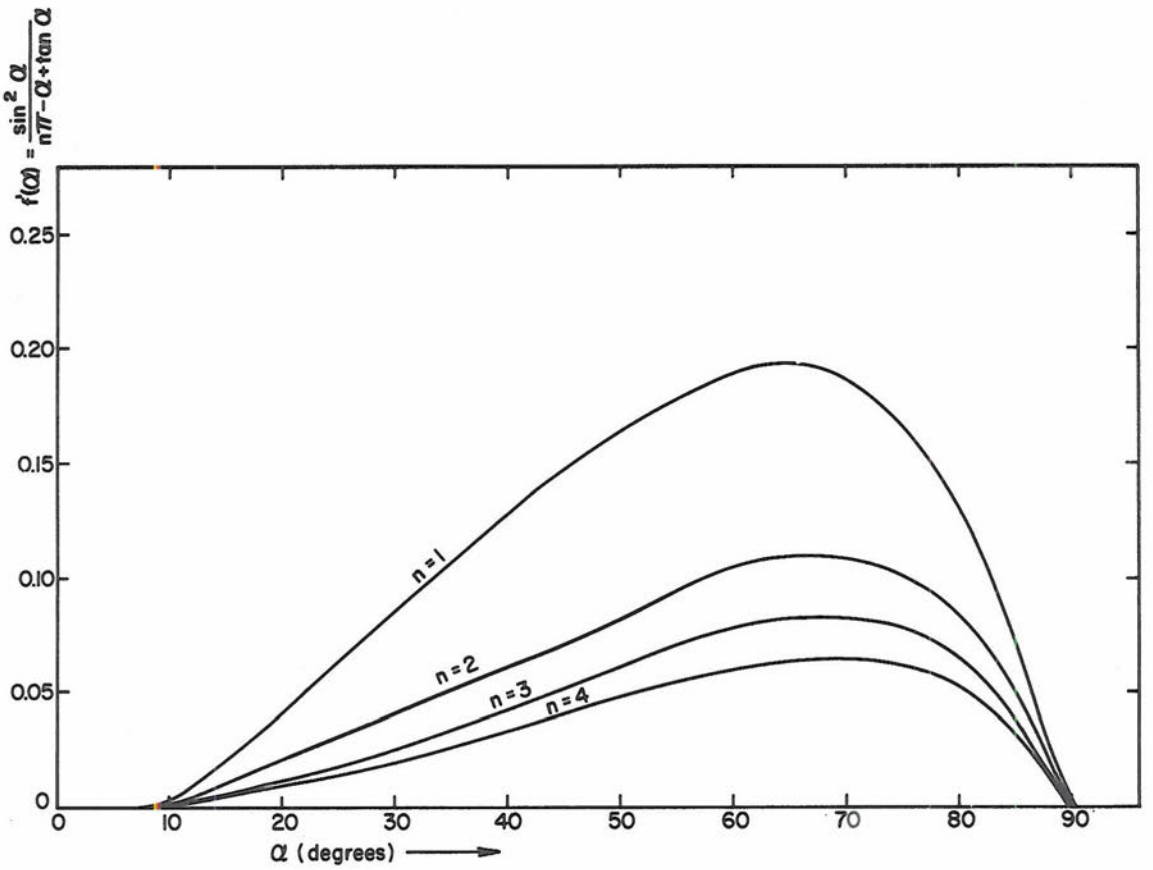

FIG. B-2. When α and n are known from Fig. B-1, enter graph to determine f' (α). Only the n that accompanies the largest λ should be used as this is the dominant wave.

The following aids have been developed in order to simplify some of the above steps:

a) Fig. B-1 shows the relationship between $f(\alpha) = n\pi - \alpha / \sin \alpha$ and α. Since $f(\alpha)$ is known from the rawinsonde data (Lh_1) enter the graph at $f(\alpha) = Lh_1$ to determine valid values of α to be used in step (5) above (for various values of n).

b) In step (7) above the expression for w_o has been divided into three terms. The first term is $(2\pi hb/e^{kb})$ and is a function of k only, provided h and b are known. The measurements of mean values of h and b for an entire mountain range were taken with respect to an altitude where the mountain range became the main obstruction to air flow above any low level ridges and foothills in the area. We are studying a phenomenon which is more responsive to relatively high and narrow ridges. If the mean values for the entire ridge are used, it must be realized that some area in the lee of the range will develop much more vigorous waves than predicted by the use of the mean values of h and b, while on the other hand, some area will show less active waves than forecast. Close inspection of aeronautical charts produced the topography values listed in Table B-1 for several well known mountain ranges.

c) Table B-2 shows the value of the term $(2\pi hb/e^{kb})$, assuming h is equal to one kilimeter. λ in Table B-2 is obtained from step (6) above and b from Table B-1. If h differs from one kilometer

in Table B-1, multiply the value in Table B-2 by the mountain range height (h in kilometers).

d) Fig. B-2 shows the relationship of the second term in step (7) above, $f'(\alpha) = \sin^2 \alpha / n\pi - \alpha + \tan \alpha$ to α for various values of n. In step (4) above (notice a above) we determined valid values of n and α by use of Fig. B-1. Enter Figure B-2 at the largest α and read off the value of $f'(\alpha)$ from the n curve (n=1, 2, . . .) that accompanies the largest α. This n and α lead to the longest lee wavelength, which will dominate the flow (see step (5)).

e) Multiply the terms obtained in c and d by the third term in step (7), $(U_1 L^2)$, to determine w_o. The term $(U_1 L^2)$ is obtained from rawinsonde data.

Table B-1. The Height and Half Width (in km) of Important Mountain Ranges

Mountain Range	Height (h) (km)	Half Width (b) (km)
Sangre de Cristo	1.1	2.5
Colorado Rockies	0.9	2.5
Southern Wasatch	0.3	2.2
Southern Sierras	1.1	8.0
Ruby Hills	0.8	2.0
Northern Sierras	0.5	2.5
Northern Wasatch (SLC-DEN)	0.8	4.0
Montana Rockies	0.8	3.0
Big Horn Mountains	0.6	2.0
Black Hills	0.3	4.0
Wind River Range	1.0	2.0

Table B-2. Value of $(2\pi hb/e^{kb})$ for various dimensions of b and λ, assuming h=1 km (Units are km).

λ (km) / b (km)	1	2	3	4	5	6	7	8	9	10	15	20
1	0.01	0.30	0.80	1.30	1.80	2.30	2.60	2.90	3.10	3.40	4.20	4.50
2	0.00	0.03	0.19	0.50	0.97	1.70	1.90	2.50	3.10	3.80	5.50	7.00
3	----	0.02	0.04	0.15	0.39	0.89	1.30	1.70	2.30	3.10	5.60	7.60
4	----	0.00	0.01	0.04	0.14	0.46	0.68	1.00	1.50	2.30	5.00	7.50
5	----	----	0.00	0.01	0.05	0.21	0.35	0.57	0.95	1.50	4.20	7.00
6	----	----	----	0.00	0.02	0.09	0.17	0.31	0.57	1.00	3.10	6.20
7	----	----	----	----	0.01	0.04	0.08	0.16	0.33	0.65	2.60	5.30
8	----	----	----	----	0.00	0.02	0.04	0.08	0.18	0.41	2.00	4.20
12	----	----	----	----	----	0.00	0.00	0.01	0.02	0.05	0.41	1.40
15	----	----	----	----	----	----	----	0.00	0.00	0.01	0.24	1.10
19	----	----	----	----	----	----	----	----	----	0.00	0.06	0.39

APPENDIX C

Shortcut CAT Forecast Method Using Satellite Data

1) Measure the lee wavelength, λ, from a satellite photo to compute the value of the term $(2\pi hb/e^{kb})$ in Eq. (25), (see Table B-2 in Appendix B).

2) Since $k^2 = L^2 \cos^2 \alpha + (\ell_2)^2$ [Eq. (22)] and since $(\ell_2)^2$ is usually much smaller than $L^2 \cos^2 \alpha$,

$$4\pi^2/\lambda^2 = L^2 \cos^2 \alpha \qquad \text{C-1)}$$

3) Eq. (25) now becomes,

$$w_o = \left(\frac{2\pi hb}{e^{kb}}\right)\left(\frac{\sin^2 \alpha}{n\pi - \alpha + \tan \alpha}\right)\left(U_1 \quad \frac{4\pi^2}{\lambda^2 \cos^2 \alpha}\right) \qquad \text{C-2)}$$

$$w_o = \left(\frac{2\pi hb}{e^{kb}}\right)\left(\frac{\tan^2 \alpha}{n\pi - \alpha + \tan \alpha}\right)\left(U_1 \frac{4\pi^2}{\lambda^2}\right) \qquad \text{C-3)}$$

4) Since h (mountain height), b (mountain half-width), U_1 (gradient wind), k (wave number = $2\pi/\lambda$) and λ (lee wavelength) are all known from the satellite photo, the topography map, and the wind sounding data, α is the only unknown. Fig. B-2 shows that $f'(\alpha)$ is a maximum at α equal 65 degrees and n=1. The middle term in Eq. (C-3) (right hand side) equals unity under these conditions. If α becomes much greater than 65 degrees, $L^2 \cos^2 \alpha$ is no longer much larger than ℓ_2^2. This condition will only permit relatively long lee waves containing little perturbation kinetic energy.

The value of w_o is maximized with α at 65 degrees and thus the highest possible degree of turbulence can be determined by use of Fig. 9.

APPENDIX D

Constant Level Balloon Data Discussed in Chapter IV

The following diagrams show various data for the constant level balloon releases made during the Lee Wave Field Program in the spring of 1966. The abscissa in all diagrams is the xy distance (in ft) of the balloon from the radar site. The heavy dark line is the track of the balloon (ordinate is z in ft), the solid light line is the horizontal direction of the balloon (ordinate is direction in degrees), the dotted line is the uv wind component (ordinate is m sec^{-1}) and the dashed line is the w wind component (ordinate is m sec^{-1}).

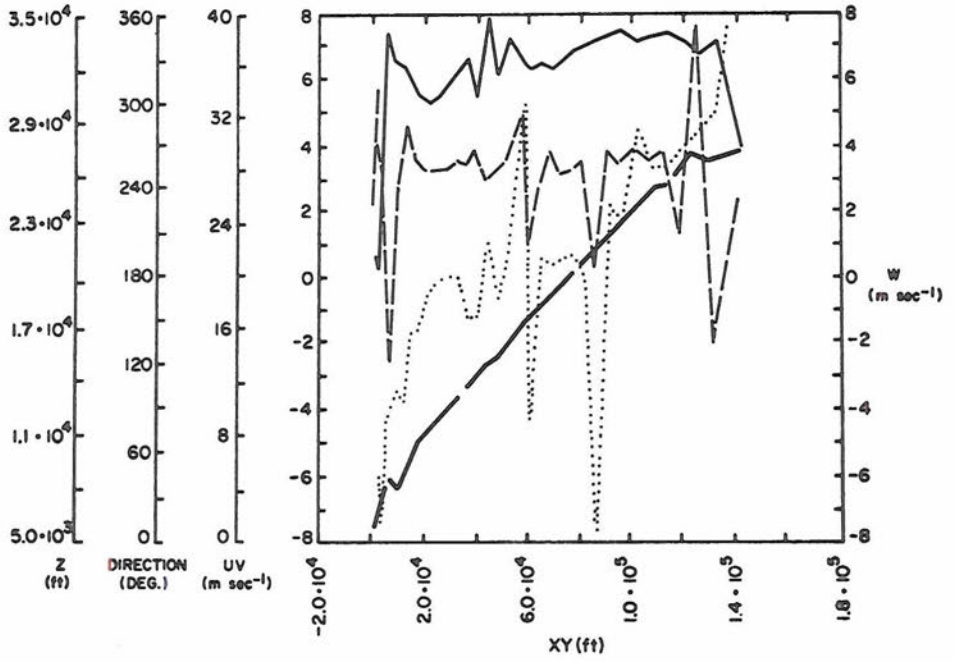

FIG. D-1. April 1, 1966, run 1 at 1732Z. No separation.

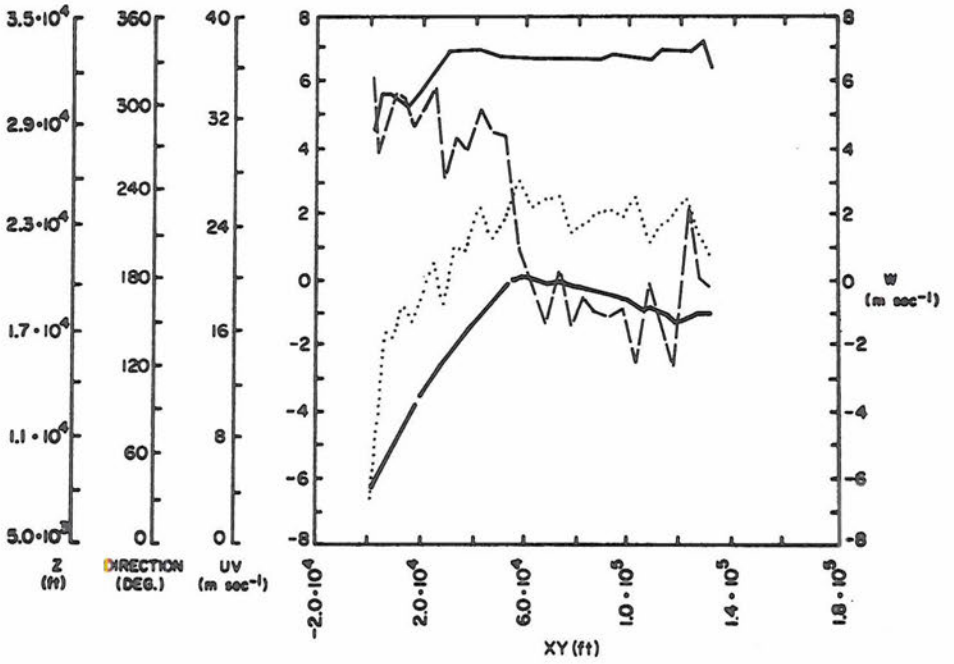

FIG. D-2. April 1, 1966, run 2 at 2025Z.

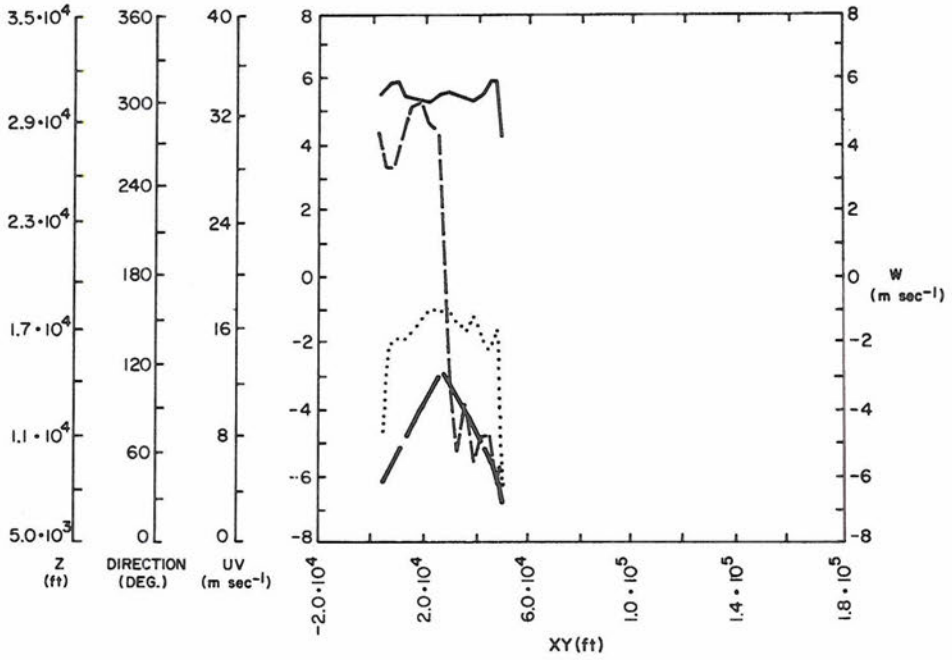

FIG. D-3. April 1, 1966, run 3 at 2238Z. Balloon tore.

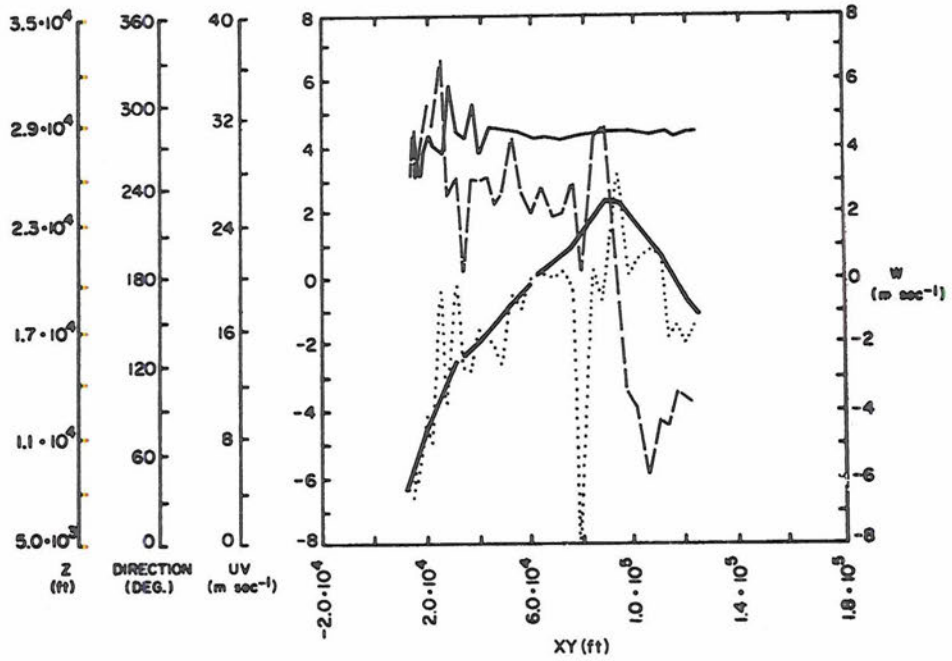

FIG. D-4. May 13, 1966, run 1 at 1533Z. Late separation.

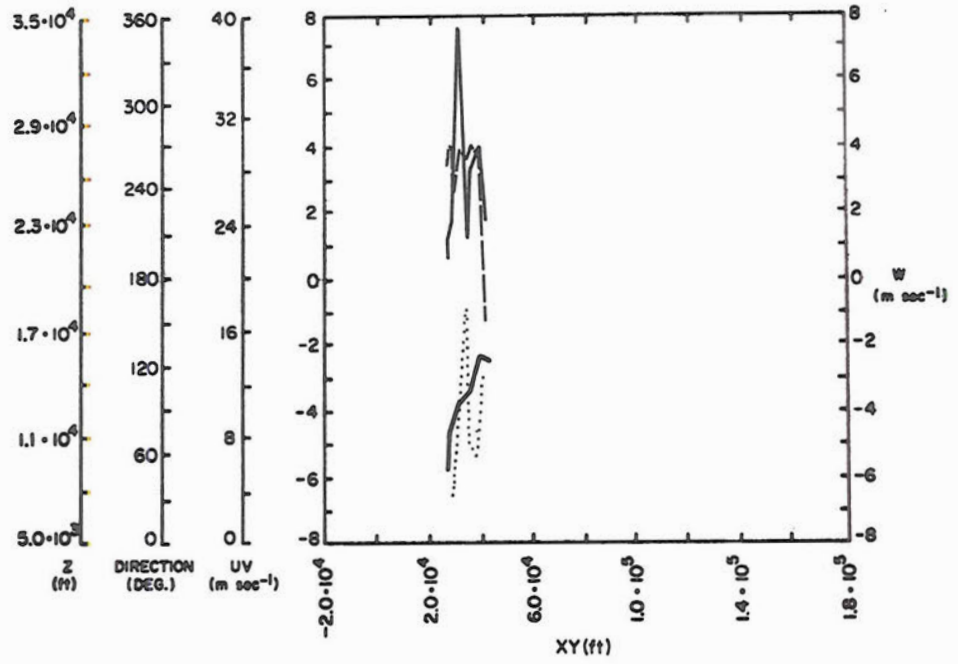

FIG. D-5. May 13, 1966, run 2 at 1625Z. Balloon went into clouds.

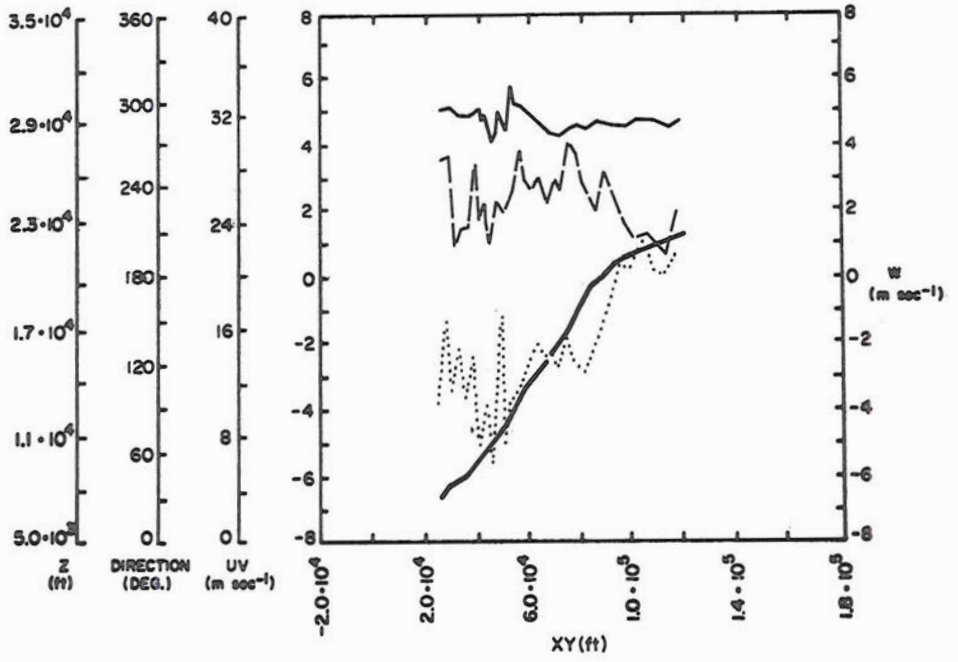

FIG. D-6. May 13, 1966, run 3 at 1725Z. Balloon went into clouds.

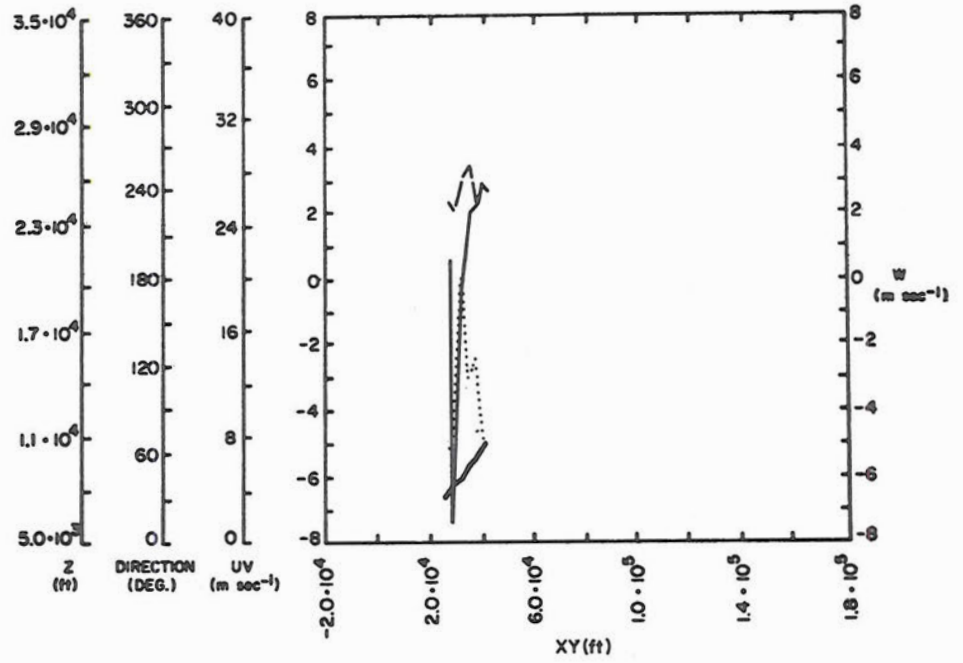

FIG. D-7. May 14, 1966, run 1 at 1740Z. Radar malfunction.

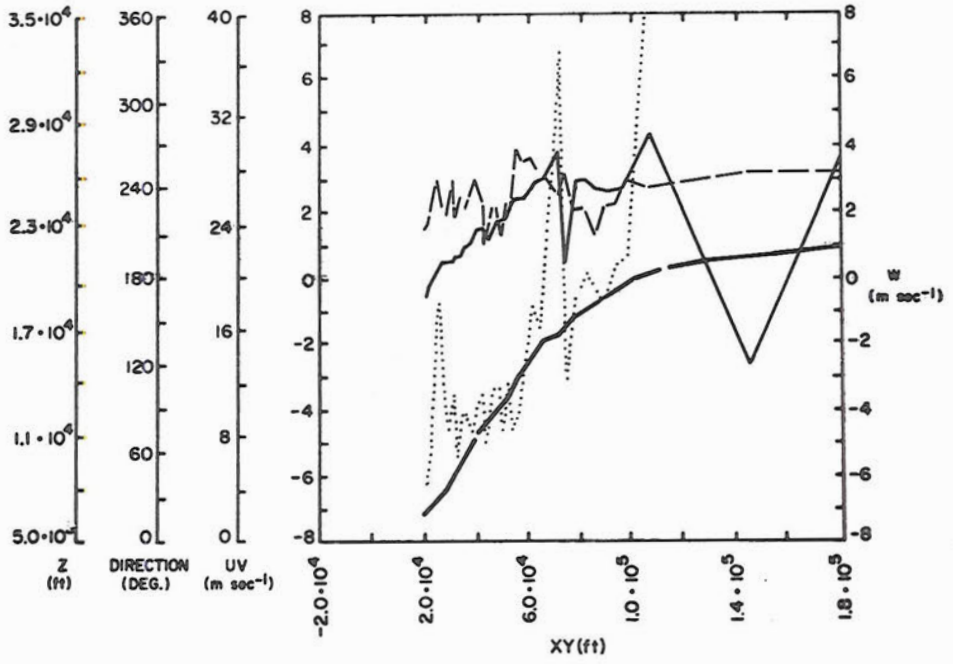

FIG. D-8. May 14, 1966, run 2 at 1812Z. No separation.

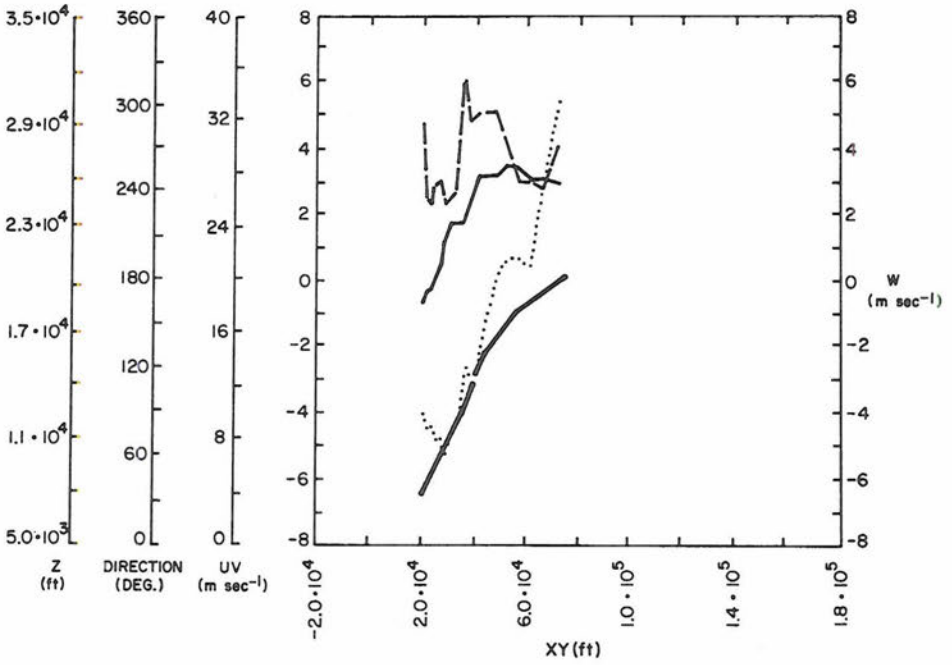

FIG. D-9. May 14, 1966, run 3 at 1925Z.

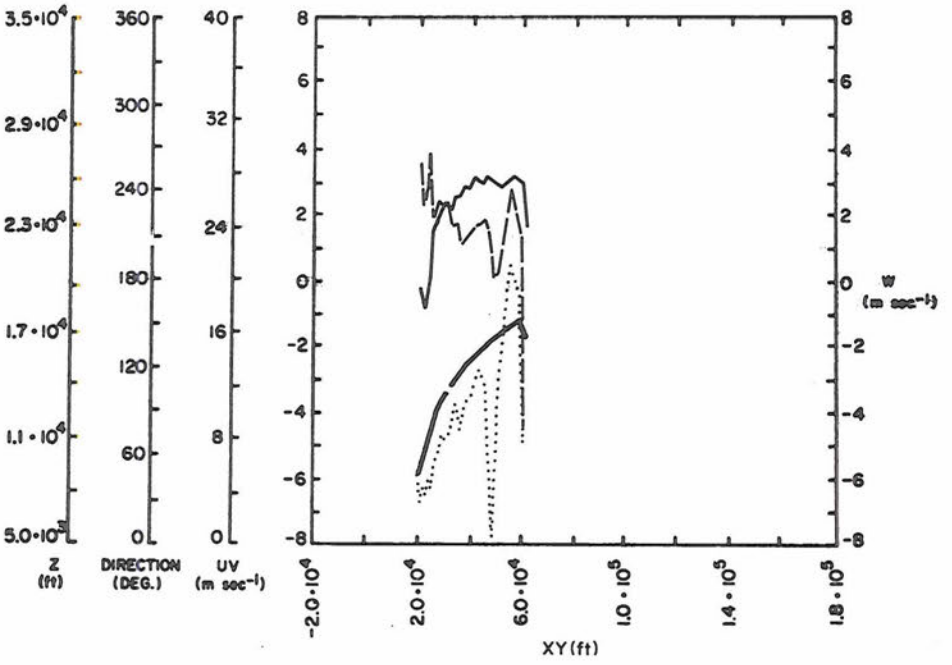

FIG. D-10. May 14, 1966, run 4 at 2037Z. Balloon went into clouds.

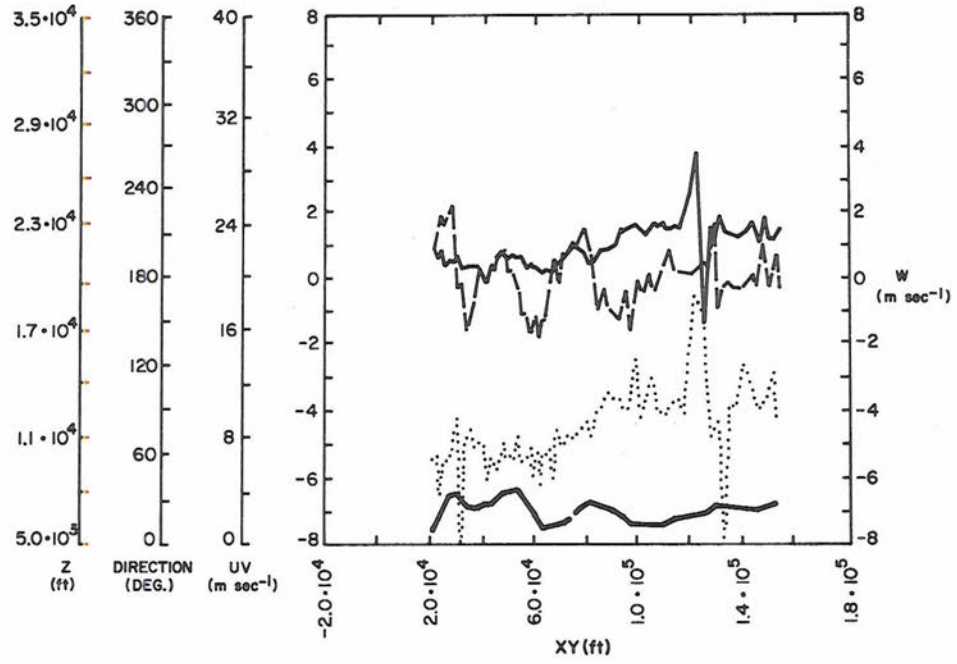

FIG. D-11. May 14, 1966, run 5 at 2147Z. Lost in ground clutter.

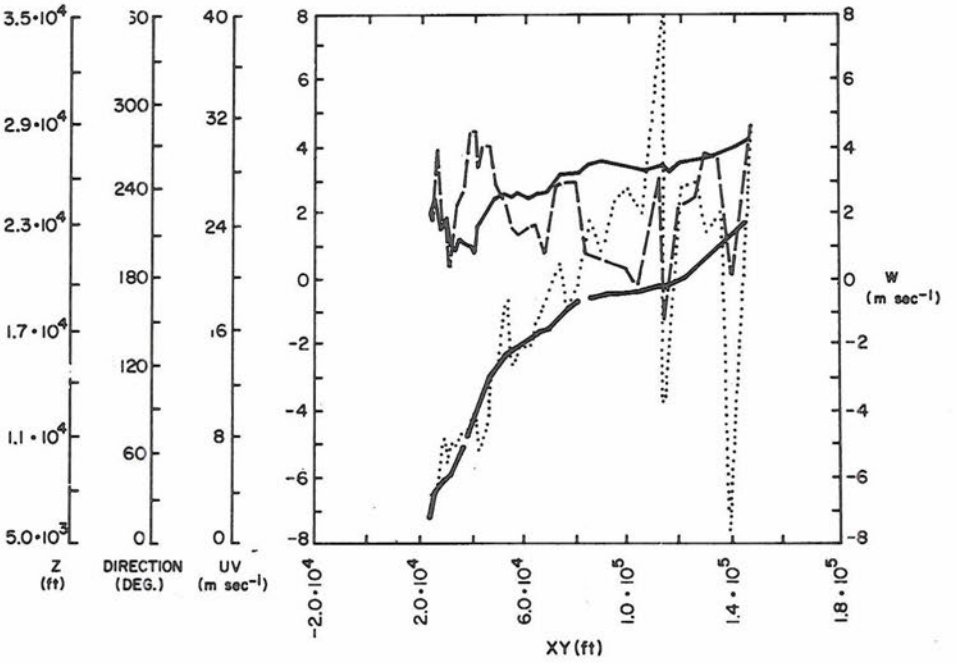

FIG. D-12. May 14, 1966, run 6 at 2319Z. No separation.

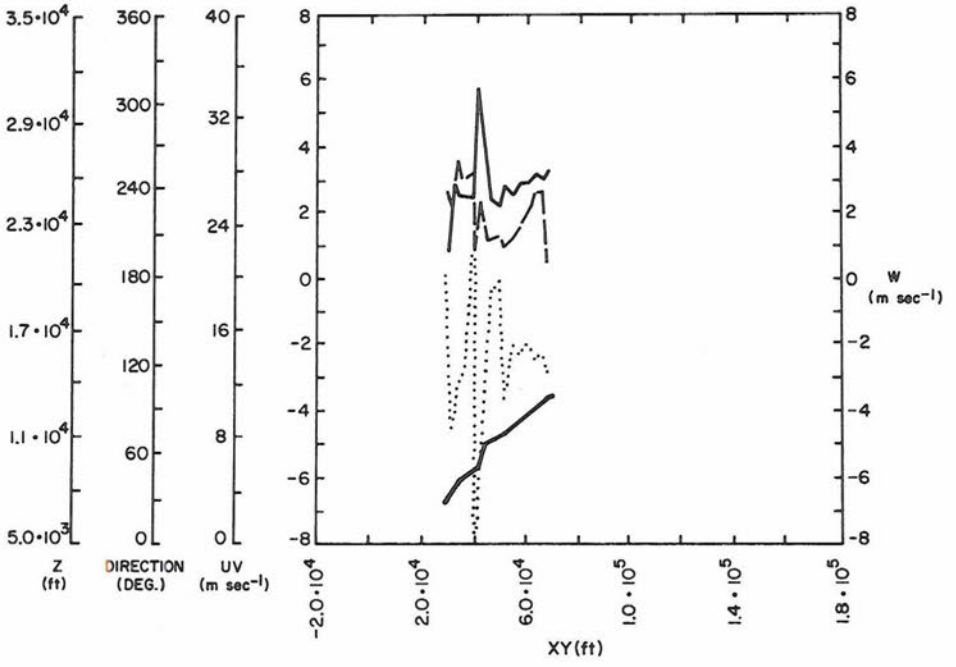

FIG. D-13. May 15, 1966, run 7 at 0031Z. Radar malfunction.

Author: H. P. Foltz

PREDICTION OF CLEAR AIR TURBULENCE

Colorado State University
Atmospheric Science Paper No. 106

Prepared under Grant No. WBG-59 from the National Environmental Satellite Center, ESSA.

551.551.5
551.558.21

Subject Headings:
Clear Air Turbulence Forecasting
Lee Waves
Mountain Waves

A statistical study of 9000 subjective aircraft turbulence reports shows a connection between mountain lee waves and such turbulence. A physical model based upon lee wave energies computed by using the theoretical work of Scorer and Corby and Wallington and energy decay according to the "-5/3" spectral density slope leads to energy levels in the microscale, which can be related by recent aircraft measurements to clear air turbulence. The intensity of predicted turbulence using this method agrees quite well with reported aircraft turbulence near lee wave regions.

Author: H. P. Foltz

PREDICTION OF CLEAR AIR TURBULENCE

Colorado State University
Atmospheric Science Paper No. 106

Prepared under Grant No. WBG-59 from the National Environmental Satellite Center, ESSA.

551.551.5
551.558.21

Subject Headings:
Clear Air Turbulence Forecasting
Lee Waves
Mountain Waves

A statistical study of 9000 subjective aircraft turbulence reports shows a connection between mountain lee waves and such turbulence. A physical model based upon lee wave energies computed by using the theoretical work of Scorer and Corby and Wallington and energy decay according to the "-5/3" spectral density slope leads to energy levels in the microscale, which can be related by recent aircraft measurements to clear air turbulence. The intensity of predicted turbulence using this method agrees quite well with reported aircraft turbulence near lee wave regions.

Author: H. P. Foltz

PREDICTION OF CLEAR AIR TURBULENCE

Colorado State University
Atmospheric Science Paper No. 106

Prepared under Grant No. WBG-59 from the National Environmental Satellite Center, ESSA.

551.551.5
551.558.21

Subject Headings:
Clear Air Turbulence Forecasting
Lee Waves
Mountain Waves

A statistical study of 9000 subjective aircraft turbulence reports shows a connection between mountain lee waves and such turbulence. A physical model based upon lee wave energies computed by using the theoretical work of Scorer and Corby and Wallington and energy decay according to the "-5/3" spectral density slope leads to energy levels in the microscale, which can be related by recent aircraft measurements to clear air turbulence. The intensity of predicted turbulence using this method agrees quite well with reported aircraft turbulence near lee wave regions.

Author: H. P. Foltz

PREDICTION OF CLEAR AIR TURBULENCE

Colorado State University
Atmospheric Science Paper No. 106

Prepared under Grant No. WBG-59 from the National Environmental Satellite Center, ESSA.

551.551.5
551.558.21

Subject Headings:
Clear Air Turbulence Forecasting
Lee Waves
Mountain Waves

A statistical study of 9000 subjective aircraft turbulence reports shows a connection between mountain lee waves and such turbulence. A physical model based upon lee wave energies computed by using the theoretical work of Scorer and Corby and Wallington and energy decay according to the "-5/3" spectral density slope leads to energy levels in the microscale, which can be related by recent aircraft measurements to clear air turbulence. The intensity of predicted turbulence using this method agrees quite well with reported aircraft turbulence near lee wave regions.

ATMOSPHERIC SCIENCE PAPERS

(Beginning May 1966)

(Previous Numbers Refer to "Atmospheric Science Technical Papers")

101. On the Mechanics and Thermodynamics of a Low-Level Wave on the Easterlies by Russell Elsberry. Report prepared with support under Grant No. WBG-61, Environmental Science Services Administration. May 1966.

102. An Appraisal of TIROS III Radiation Data for Southeast Asia by U. Radok. Report prepared with support under Grant No. WBG-61, Environmental Science Services Administration. August 1966.

103. Atmospheric General Circulation and Transport of Radioactive Debris by J. D. Mahlman. Report prepared with support under Contract No. AT(11-1)-1340, U. S. Atomic Energy Commission. September 1966.

104. The Mutual Variation of Wind, Shear and Baroclinicity in the Cumulus Convective Atmosphere of the Hurricane by Wm. M. Gray. Report prepared with support under Grant No. GF-177, National Science Foundation. October 1966.

105. Further Studies of Denver Air Pollution by N. Djordjevic, W. Ehrman, and G. Swanson. Report prepared with support under Grant 5 ROI AP 00216-03, Department of Health, Education and Welfare. December 1966.

The "Atmospheric Science Papers" are intended to communicate without delay current research results to the scientific community. They usually contain more background information on data, methodology, and results than would normally be feasible to include in a professional journal. Shorter versions of these papers are usually published in standard scientific literature.

Editorial Office: Head, Department of Atmospheric Science
Colorado State University
Fort Collins, Colorado 80521